

Benchmark interest rates when the government is risky*

Patrick Augustin,[†] Mikhail Chernov,[‡] Lukas Schmid,[§] and Dongho Song[¶]

First draft: May 2017

This draft: September 21, 2019

Abstract

Future interbank uncollateralized borrowing costs can be locked in using interest rate swap instruments tied to the effective federal funds rate (OIS) or LIBOR (IRS). Since the Global Financial Crisis, OIS and IRS rates have fallen below maturity-matched U.S. Treasury rates across different maturities. That is surprising, because Treasuries are deemed to have superior liquidity and safety associated with the safe haven status of the U.S. government. This should make Treasuries expensive and produce yields that are lower than those of maturity-matched swap rates. We suggest that U.S. sovereign default risk explains the negative difference between the OIS and Treasury rates. This explanation is supported using a quantitative equilibrium model that jointly accounts for macroeconomic fundamentals, as well as the term structures of OIS, IRS, and credit default swap (CDS) rates. In our model, we account for interbank credit risk, liquidity effects, and cost of collateralization. Thus, the sovereign risk channel complements existing explanations based on frictions such as balance sheet constraints, convenience yield, and hedging demand.

JEL Classification Codes: C1, E43, E44, G12, H60.

Keywords: sovereign credit risk, negative swap rates, recursive preferences, term structure.

*We thank Vadim di Pietro, Valentin Haddad, Michael Johannes, Arvind Krishnamurthy, Lars Lochstoer, Francis Longstaff, Renate Marold, Guillaume Roussellet, and Suresh Sundaresan for comments on earlier drafts, and participants in seminars sponsored by Canadian Derivatives Institute, McGill, UCLA, and the HEC-McGill 2019 Summer Finance Workshop. The authors acknowledge financial support from the Canadian Derivatives Institute. The latest version is available at

https://sites.google.com/site/mbchernov/ACSS_NSS_latest.pdf.

[†] Desautels Faculty of Management, McGill University; patrick.augustin@mcgill.ca.

[‡] Anderson School of Management, UCLA, NBER, and CEPR; mikhail.chernov@anderson.ucla.edu.

[§] Fuqua School of Business, Duke University, and CEPR; lukas.schmid@duke.edu.

[¶] Carey Business School, Johns Hopkins University; dongho.song@jhu.edu.

1 Introduction

The financial crisis of 2008 marked the beginning of a number of disruptions in financial markets that have persisted to date. In fixed-income markets, three phenomena stand out: (i) long-term swap rates linked to LIBOR fell below maturity-matched U.S. Treasury yields (Klingler and Sundaresan, 2018; Jermann, 2019), (ii) short- to intermediate-term maturity swap rates linked to the Effective Federal Funds Rate (EFFR) also fell below maturity-matched U.S. Treasury yields (Klingler and Sundaresan, 2019), and (iii) premiums on CDS contracts on the U.S. government have risen to at least 100 times their pre-crisis levels (Chernov, Schmid, and Schneider, 2019).

Observations (i) and (ii) appear puzzling from the viewpoint of standard asset pricing theory. They imply that swap spreads (i.e., the difference between swap and Treasury rates) linked to LIBOR and EFFR are negative, an irregularity often referred to as ‘negative swap spread puzzle’. While these puzzles did receive a fair amount of attention in the literature, they are typically studied in isolation. The third phenomenon is perceived as puzzling by many observers because of the sheer magnitude of U.S. CDS premiums.

In this paper, we argue that all these phenomena are interrelated and can be understood jointly by accounting for a change in the perceived credit quality of the United States, a truly new development since the crisis. In contrast, the factors behind extant explanations of (i) and (ii), while absolutely valid, were also at work before the crisis, when swap spreads were positive.

The puzzles stem from the no-arbitrage argument for the relative magnitude of interest rates. Consider a strategy that sells short a par Treasury bond borrowed via a reverse repo transaction, together with a position in a swap contract that receives a fixed rate of interest. The total cash flows are equal to the difference between the swap rate and the Treasury yield (coupon in the case of par), net of the difference between the floating payments in the swap and the reverse repo. Because we expect uncollateralized interest rates to be greater than collateralized ones, the present value of the floating payments (one-period interest rates) is positive. Therefore, it must be that the difference between the swap rate and the Treasury yield is positive as well. We analyze violations of this condition in three steps.

First, we provide additional evidence on various interest rate spreads. The swap linked to the EFFR is known as the overnight indexed swap (OIS), and the one linked to LIBOR is the interest rate swap (IRS). The difference between OIS and Treasury rates continues to be negative at longer maturities. The difference between IRS and Treasury rates is negative between maturities of 7 years and up to 30 years. Finally, the spread between IRS and OIS rates is positive across all maturities for the entire sample, just as someone in 2007 would have expected. As a consequence, the negative swap spread puzzles must have a common source that lies with the relation between OIS and Treasury rates. Moreover, empirically, we provide suggestive evidence that OIS swap spreads and CDS premiums exhibit significant comovement.

Second, we argue that the negative difference between swap and Treasury rates is driven by the credit riskiness of the U.S. government. If the U.S. can default, one can restore a credit-risk-free position by combining a short Treasury bond and Treasury protection sold via a CDS contract. Thus, the original no-arbitrage argument reviewed above should be modified by introducing a CDS position. As a result, the difference between the swap rate and the Treasury yield minus the CDS premium should be positive, implying that negative swap spreads can persist even in the absence of arbitrage. The key insight is that Treasury bonds can default, but benchmark indices like LIBOR or EFRR cannot because they are not investable. This feature can make swap contracts more valuable than Treasuries, thereby lowering swap rates relative to those of bonds.

Third, we propose a realistic quantitative model that captures the evidence. That endeavor necessitates accounting for the sovereign credit risk of the U.S. government. As observed by [Chernov, Schmid, and Schneider \(2019\)](#), an equilibrium model is required to measure the credit risk premium in the absence of an observed risk-free reference rate. We follow their modeling strategy, but depart in two dimensions. Because the nature of our exercise demands high quantitative realism, we specify a more realistic model of the joint behavior of macroeconomic fundamentals. Furthermore, we simplify the modeling of the default trigger and switch from the structural approach to the intensity-based approach. The default intensity is driven by macroeconomic variables whose choice is inspired by the analysis of [Augustin \(2018\)](#) and [Chernov, Schmid, and Schneider \(2019\)](#).

To provide plausible quantitative guidance on swap spreads, our model has to account for other factors beyond sovereign credit risk that likely affect differences between interest rates in current markets. We focus on the most relevant factors such as a convenience yield on Treasuries, bank risk (credit and funding liquidity), and the opportunity cost of collateral associated with swap transactions. The first factor lowers Treasury yields. The second factor increases swap rates. The third factor increases swap rates if the short interest rate and the cost of collateral are positively correlated ([Johannes and Sundaresan, 2007](#)). An important objective of our work is to evaluate the contributions of these different channels along with sovereign credit risk to the overall swap spreads.

Empirically, we identify the convenience yield and bank risk using observable interest rate spreads, and the unobserved collateral factor by matching one-year IRS and the term structure of CDS. Thus, we obtain all the ingredients needed for the valuation of OIS and IRS without using the data on their respective rates. As a result of this approach, the OIS and IRS valuation is truly a relative value exercise whereby we determine the theoretical value of the swap rates using the market values of other instruments. We estimate our model via Bayesian MCMC methods and thereby recover the model-implied time series for the relevant variables in our sample.

We find that our quantitative model provides an accurate account of the dynamics in both OIS and IRS markets. In particular, the model generates swap spread series that were positive before the crisis, and turned negative after the onset of the financial crisis in 2008. In counterfactual experiments, we can assess the role of the U.S. credit risk in the behavior

of swap spreads. Critically, we find that they are uniformly positive in the absence of that risk. This result establishes the quantitative relevance of the sovereign risk channel in the pricing of Treasuries and swaps. Conceptually, this relative-value-based view differs from existing explanations of negative swap spread puzzles, all of which are based on limits to arbitrage.

Related literature

First, we contribute to a small but growing literature on the puzzling observation that the difference between interest rate swaps denominated in USD and U.S. Treasury rates, a.k.a. swap spreads, turned negative for multiple maturities, effectively suggesting that the U.S. government is riskier than a presumably safe AA-rated bank. Several explanations have been proposed for the apparent pricing anomaly in financial markets, including demand for duration by underfunded pension plans (Klingler and Sundaresan, 2018), dealer funding costs (Lou, 2009), or increases in regulatory leverage ratios (Boyarchenko, Gupta, Steele, and Yen, 2018). Klingler and Sundaresan (2019) consider fading demand for U.S. Treasury bonds as a leading explanation for negative OIS-Treasury spreads. Jermann (2019) proposes a theoretical equilibrium explanation for negative swap spreads by considering regulatory leverage constraints for dealer balance sheets. Table 1 summarizes the main differences between our and the existing contributions.

While explanations based on frictions have their merits, we argue that they fail to provide a unified explanation of Treasury spreads that exceed maturity-matched spreads of short-term and long-term funding instruments in interbank markets. Demand for duration by underfunded pension plans is a plausible explanation for 30-year negative swap spreads, but less so for shorter maturities, even though these have also been persistently negative for many years. Second, limits-to-arbitrage arguments speak to the persistence of negative swap spreads, but they do not explain why they turned negative in the first place. Third, a focus on individual segments of the maturity structure or selective instruments ignores the inherent equilibrium relationships that must exist between benchmark interest rates. Importantly, we propose a model that explains both positive swap spreads before and negative swap spreads after the crisis.

We suggest that negative swap spreads can be obtained without frictions (even though frictions may amplify the phenomenon). By incorporating sovereign default risk into the modeling of benchmark interest rates, we hope to provide a unified explanation of the price dynamics of various fixed income instruments during the financial crisis, which poses a challenge to existing partial equilibrium pricing models to date. Dittmar, Hsu, Roussellet, and Simasek (2019) propose sovereign default risk as an explanation for the pricing anomalies observed among inflation-indexed securities (Fleckenstein, Longstaff, and Lustig, 2013; Hilscher, Raviv, and Reis, 2014).

More generally, our study builds on the vast literature on no-arbitrage affine term structure modeling and credit-sensitive instruments, prominently summarized in Duffie and Singleton

(2003). In addition, we relate to studies on the modeling of the term structure of overnight index swaps, interest rate swaps, or LIBOR rates (Duffie and Huang, 1996; Duffie and Singleton, 1997; Collin-Dufresne and Solnik, 2001; Grinblatt, 2001; He, 2001; Liu, Longstaff, and Mandell, 2006; Johannes and Sundareshan, 2007; Feldhutter and Lando, 2008; Filipovic and Trolle, 2013; Monfort, Renne, and Roussellet, 2016) and their empirical examinations (Litzenberger, 1992; Sun, Sundareshan, and Wang, 1993; Gupta and Subrahmanyam, 2000; Wang and Yang, 2018). Finally, we also relate to the literature that examines the convenience yield embedded in Treasury bonds (Krishnamurthy, 2002; Longstaff, 2004; Gurkaynak, Sack, and Wright, 2007; Goyenko, Subrahmanyam, and Ukhov, 2011; Krishnamurthy and Vissing-Jorgensen, 2012; Nagel, 2016; Du, Im, and Schreger, 2018).

2 Preliminary evidence

2.1 Benchmark interest rates in the U.S.

Our analysis is focused on four types of U.S. interest rates and their interaction: (i) Treasury yields; (ii) OIS premiums; (iii) IRS premiums; (iv) and CDS premiums. The U.S. Treasury borrows money on behalf of the government by issuing debt securities of different maturities. The effective annual interest that can be earned along the maturity spectrum characterizes the Treasury yield curve. The Treasury yield curve can be characterized using zero coupon, coupon, par, or forward rates. The most convenient way is to work with zero-coupon yields that are bootstrapped from coupon bonds (e.g., Gurkaynak, Sack, and Wright, 2007, henceforth GSW). Another popular indicator of the U.S. government’s borrowing costs is the constant maturity Treasury (CMT) yield curve, or par rates, which are bootstrapped from coupon bonds as well. CMT_t^n denotes the coupon at time t of a bond maturing in n periods.

Overnight indexed swaps (OIS) are fully collateralized contracts in which a fixed rate payer exchanges a constant cash flow, i.e., the OIS rate, against a floating payment that is computed as the geometric average of the daily EFFR. The Federal Funds Target Rate is determined by the Federal Open Market Committee in order to conduct monetary policy. The EFFR is the actual interest rate at which banks lend reserve balances to other banks overnight without collateral. Since March 1, 2016, it is measured as the volume-weighted median of the bilaterally negotiated transactions. Before that, it was measured as the volume-weighted average. OIS contracts with maturities up to one year have only one settlement (the geometric average is computed over the lifetime of the contract), while cash payments for contracts with maturities above one year arise quarterly (the geometric average is re-computed every quarter). Hull and White (2013) and Wang and Yang (2018) discuss the institutional details of OIS contracts. OIS_t^n denotes the rate at time t of a swap maturing in n periods.

Interest rate swaps (IRS) have arrangements similar to those of OIS but with a different reference floating rate, which is the 3-month London interbank offered rate (LIBOR) that

is fixed at the previous settlement date of an IRS. LIBOR is the interest rate at which banks in the Eurodollar area are willing to lend to each other on an uncollateralized basis. See [Duffie and Singleton \(1997\)](#), [Collin-Dufresne and Solnik \(2001\)](#), and [Johannes and Sundaresan \(2007\)](#) for discussions on the institutional details of LIBOR swap contracts. IRS_t^n denotes the rate at time t of a swap maturing in n periods.

The definitions of LIBOR and EFFR are conceptually similar as they both relate to uncollateralized interbank lending. So, one should expect overnight LIBOR to be similar to EFFR. The rates should not be literally the same, however. The banks in the LIBOR panel are not identical to the banks in the Fed system, and logistics of lending within the Fed system are different from that in the Eurodollar area. [Figure 1](#) compares the two rates.

They are sitting right on top of each other with one exception: the onset of the banking crisis of 2008. The difference between the instruments linked to LIBOR and EFFR arises because of the term effect. The floating legs are linked to three-month LIBOR and daily EFFR compounded over three months. In the presence of banks' credit risk, lending to banks without collateral for three months outright (at LIBOR) is more risky than lending overnight (at EFFR) and rolling that over daily for three months.

Another closely related rate is the interest earned on collateralized borrowing through a repurchase agreement contract, henceforth repo. We do not study repo in this paper as it has its own host of issues and puzzles. In the context of our analysis, one could be concerned about two issues. First, general collateral (GC) repo rates seem like a natural proxy for the risk-free rate. As [Duffie and Stein \(2015\)](#) point out, GC rates exhibit similar flight-to-quality spikes as Treasury bills and excess volatility due to the very short-term maturity of one day. Also, the GC repo market is not active at maturities beyond three months, and so there is no readily available term structure information. Finally, the post 2008 quantitative easing program that involved the purchase of Treasury bonds affected the supply of collateral in repo transactions, leading to distortions in rates. A second concern is whether the repo rate should play some role in our analysis. We use repo rates only qualitatively without relying on the specific values or their dynamics.

The last rate we focus on is the premium on credit default swaps (CDS) associated with the U.S. government. CDS are effectively insurance contracts, in which the protection seller has to make payments in case of a credit event, which may include failure to pay, repudiation/moratorium, and restructuring. CDS_t^n denotes the rate at time t of a swap maturing in n periods.

If the U.S. government has no credit risk, one would expect these premiums to be approximately zero, which was the case prior to October 2007. The subsequent elevation in the CDS premiums is a prima facie evidence of U.S. credit risk, as argued by [Chernov, Schmid, and Schneider \(2019\)](#). In fact, there is a debate in the industry and in academia whether CDS premiums reflect compensation for credit risk at all. We argue that, on balance, both theory and evidence are favorable of the U.S. credit risk view.

First, existing theories imply the presence of credit risk, even in cases when it is not the main driving force behind CDS premiums. [Chernov, Schmid, and Schneider \(2019\)](#) attribute most of the CDS premium to credit risk in a model with a version of a [Bansal and Yaron \(2004\)](#) pricing kernel, an intertemporal government budget constraint, and a decline in government revenues when taxes are too high, also known as the Laffer curve. [Lando and Klingler \(2018\)](#) take a different view and attribute most of the CDS premium to regulatory frictions. The underlying reason is that uncollateralized counterparty risk exposures demand capital charges, which can be offset by purchasing CDS protection against that counterparty. That action artificially inflates the CDS premium. This argument crucially depends on the presence of non-zero credit risk, otherwise there is no charge.

Second, from an empirical perspective, the United States defaulted before, both on external and domestic debt ([Zivney and Marcus, 1989](#); [English, 1996](#); [Reinhart and Rogoff, 2008](#)). Most recently, Standard & Poor’s stripped the U.S. off the highest AAA credit rating in 2011, suggesting the presence of some credit risk. In the modern times, we have also experienced effective defaults by high-quality sovereigns despite relatively low CDS premiums. Indeed Ireland, which still benefitted from a AAA credit rating going into the global financial crisis, saw its CDS premiums rise from about 2 bps in 2007 to north of 400 bps when it was bailed out by the Eurozone countries in 2010 (see discussions around Figure 1 in [Acharya, Drechsler, and Schnabl, 2014](#)). Similarly, Spain received a AAA credit rating in 2003 when its CDS premiums fluctuated around 3 to 4 bps. Yet, it was at the cusp of junk status in 2012 when it received financial support from the Eurozone, and CDS premiums reached levels close to 600 bps.

2.2 Data

We source data on LIBOR, IRS and OIS rates from Bloomberg, and U.S. CDS premiums from Markit. We start the sample on May 8, 2002, when data for OIS rates start having few missing observations, and end on September 26, 2018. The 30-year OIS rates are often discarded by researchers because of their low liquidity. Further, during the crisis, no OIS data are available for maturities beyond 10 years. Thus, longer-term OIS rates are available only for part of the sample period. Because swap rates are par rates, we use the constant maturity Treasury (CMT) rates published by the U.S. Federal Reserve Bank as a maturity-matched Treasury rate.

We report basic summary statistics for the term structure of all rates in Table 2, summarizing the information for maturities of 3 and 6 months, as well as 3, 5, 7, 10, 20, and 30 years. Panels A, B, and C in Table 2 show that, on average, CMTs are lowest, with an upward sloping term structure ranging from 1.25% at the short end to 3.95% at the 30-year horizon. OIS rates, reported in Panel A, are higher, ranging on average from 1.40% to 2.54% at the 5-year maturity. Average OIS rates with maturities above 5 years are not directly comparable to the CMTs, as there are fewer observations. OIS data for the 7-year and 10-year maturities start in May 2012 and August 2008, respectively, while those for the 20-year and

30-year maturities start in September 2011. LIBOR/swap rates reported in Panel B are the largest, ranging on average from 1.66% to 3.97% at the short and long end of the maturity spectrum. All interest rates exhibit a decreasing term structure of volatility, as the standard deviation for long-term maturities is lower than that for short-term maturities.

In Panel D, we report statistics for the [Gurkaynak, Sack, and Wright \(2007\)](#) zero coupon Treasury yields, which we use in our estimation. These are available for 1-year to 30-years, and are slightly larger than the CMTs, with an average yield of 1.50% to 4.07%.

In Panels E and F of [Table 2](#), we report both USD and EUR denominated CDS premiums on the U.S. Treasury. We use USD denominated contracts in our empirical analysis. EUR contracts cover a longer span of data (from 2007 instead of 2010), so we use them for qualitative indication of the magnitude of the U.S. credit risk premium during the crisis. The average cost of insurance against a default by the U.S. Treasury ranges from 11 bps to 37 bps for USD contracts, and from 13 bps to 44 bps for EUR denominated contracts. The 5-year contract is the most liquid. At the 99th percentile of the distribution, the 5-year insurance premium is as high as 66 bps during the post-2010 period, but at the height of the global financial crisis (GFC), 5-year spreads jumped to a maximum of 95 bps (unreported in the [Table](#)).

2.3 Swap spreads

[Figure 2](#) visualizes the evidence on swap spreads, i.e., the difference between OIS or IRS rates and maturity-matched Treasury rates. In particular, panel (d) of the figure confirms the negative long-term IRS swap spreads observed in the post-crisis period, as emphasized by [Jermann \(2019\)](#) and [Klingler and Sundaresan \(2018\)](#). According to [Boyarchenko, Gupta, Steele, and Yen \(2018\)](#) and [Jermann \(2019\)](#), long-term swap spreads remain negative because regulatory caps on leverage ratios make it too costly for investors to arbitrage away the difference. Panels (a) and (b) of the same figure confirm the negative short-term OIS spreads observed in the post-crisis period, as emphasized by [Klingler and Sundaresan \(2019\)](#). They associate this inversion with a fading demand for U.S. Treasury notes and a corresponding decline in the convenience yield.

All the panels put together additional evidence. Specifically, OIS swap spreads continue to be negative at longer maturities. The liquidity of OIS with maturities over 5 years declines. Nevertheless, the prices convey qualitative information about the relative magnitudes of OIS and Treasury rates. The difference is so large that it is hard to imagine that it could be explained away by liquidity effects.¹

¹In fact, the direction of liquidity effects could be ambiguous, ex ante. The reason is that for assets in zero net supply, such as swaps, the liquidity premium is earned by the marginal investor, who is either long or short swaps on average (see, e.g., [Bongaerts, De Jong, and Driessen, 2011](#), [Deuskar, Gupta, and Subrahmanyam, 2011](#), and [Brenner, Eldor, and Hauser, 2001](#)).

2.4 U.S. credit risk and negative swap spreads

In this section, we explain the intuition behind our thesis of the relation between negative swap spreads and U.S. credit risk. We rely on the no-arbitrage bound type of argument. To appreciate the impact of credit risk, it is worth revisiting the case without credit risk first. A negative swap spread suggests that the Treasury is relatively less expensive. As an arbitrageur, one would want to exploit this by buying the Treasury via a repo transaction and take a position that pays the fixed (and receives the floating) rate in a swap contract. The cash flows corresponding to these positions are displayed in Table 4.

We use notation CMS_0^n for a generic swap rate, either OIS_0^n or IRS_0^n . The contractual floating rate in a swap (a LIBOR rate, or EFR compounded over the period in-between tenors) is f_t . The three-month repo rate is r_t . SS_0^n denotes the swap spread and equals $CMS_0^n - CMT_0^n$. The term S_t denotes the difference $f_t - r_t$. For expositional simplicity, we assume that floating and fixed payments are paid each period.

One receives $S_{t-1} - SS_0^n$ at each point t . No-arbitrage implies that $PV(SS_0^n) = PV(S_{t-1})$, where PV denotes the present value computed at time 0 (the swap inception). Because uncollateralized borrowing costs are greater than collateralized borrowing costs, the present value of the floating payments has to be positive. That implies a pure arbitrage opportunity if $SS_0^n < 0$.

If the Treasury is credit risky, the no-arbitrage argument above no longer holds, because, upon default at a random date τ , the Treasury bond terminates, the future interest payments CMT_0^n are no longer received, and the bond pays $1 - L$ instead of the full face value. That, in turn, affects the repayment of the repo loan. The swap contract is unaffected by the Treasury default because it is linked to an index f_t that is not investable. That feature makes a swap more valuable than a credit-risky Treasury bond.

It is possible to hedge the credit risk by complementing a position in the bond with the purchase of default protection via a CDS contract. That affects the cash flows of the overall position. See Table 5. Specifically, in the case of default, the joint bond-CDS position has full recovery of par, which is used to close out the repo loan. In addition, one receives the unwind value of the swap, U_τ . For simplicity, we assume that accruals due upon default are rolled into the unwind value.

On balance, one receives $S_{t-1} - SS_0^n - CDS_0^n$ every period t in which there is no default. If there is a default at time τ , one receives U_τ . By no-arbitrage, the present value of these cash flows has to be equal to zero at the swap inception, implying:

$$PV(SS_0^n) = PV(S_{t-1}) - PV(CDS_0^n) + PV(U_\tau) \geq PV(U_\tau) - PV(CDS_0^n).$$

Thus, for sufficiently large CDS premiums and sufficiently small values of $PV(U_\tau)$, the swap spread can be negative. It is thus fair to conclude that the lower bound for the swap spread

can be negative, and that observing a negative swap spread would not necessarily lead to arbitrage opportunities.

Accounting for the cumulative probability of no default, \mathcal{S}_0^n , the bound can be represented as $SS_0^n \geq PV(U_\tau)/\mathcal{S}_0^n - CDS_0^n$. Figure 2 demonstrates the relation between swap spreads and the negative of the CDS premiums. We see that in the case of IRS, $SS_0^n > -CDS_0^n$, suggesting a small value of $PV_0(U_\tau)$. In the case of OIS, SS_0^n is occasionally less than $-CDS_0^n$, implying a negative value of $PV_0(U_\tau)$.

Figure 2 suggests that, besides serving an approximate lower bound for swap spreads, CDS premiums are co-moving with the spreads. Motivated by this observation, Table 3 provides additional evidence on the relation between OIS spreads and U.S. CDS by regressing monthly changes in the OIS swap spread on changes in the maturity-matched U.S. CDS premiums and various controls.² We run panel regressions by pooling all maturities, and match the 3-month swap spreads with the 6-month CDS premium, because there exists no CDS contract with a lower maturity. We add maturity-specific fixed effects to absorb time-invariant cross-maturity differences due to possible clienteles.

The finding in column (1) is consistent with a negative relation between OIS swap spreads and CDS premiums. In column (2), we show that the economic magnitude is similar for maturities above 5 years, and in column (3), we pool all maturities together. The estimated coefficient suggests that a 10 bps increase in the CDS premium is associated with a 0.7 bps drop in the OIS swap spread. The larger coefficient (-0.13) reported in column (4) suggests that the sensitivity of the changes in OIS-Treasury to changes in CDS premiums has increased in more recent years.

In columns (5) to (10), we successively introduce lagged swap spreads, quarterly fixed effects to absorb the influence of common macroeconomic and financial factors, and controls.³ Even a conservative specification with the interaction of maturity and quarterly fixed effects in column (7) does not alter the significance or economic magnitude of the regression coefficient. Longer-term OIS contracts were less liquid around the crisis and became successively more liquid, as the discounting using OIS rates became more common practice over time. Thus, the negative relation between swap spreads and CDS premiums manifests itself in later years, as demonstrated by the larger magnitude of the regression coefficient in columns (4), (8), and (12), in which we restrict the regression to the time period post 2014. This finding also suggests that our result is not merely driven by the U.S. debt ceiling episodes in August 2011 and in October 2013.

²We examine the relation between swap spreads and U.S. credit risk at the monthly frequency, because the decision interval in our model is monthly. Results at the weekly frequency, which are stronger, are available upon request.

³Control variables include the CBOE VIX index, the exchange rate of the USD against a basket of a broad group of major U.S. trading partners, the West Texas Intermediate oil price index, the economic policy uncertainty index, the high-yield and investment-grade bond indices, inflation, the TED spread, the 3-month LIBOR-OIS spread, the 3-month T-bill rate, the U.S. Treasury total cash balances, and CDS depth defined as the number of dealer quotes used to compute the mid-market spread.

3 A realistic model

As we have established, a negative swap spread can obtain even in absence of arbitrage opportunities, and may in fact be plausible in the context of current market data. In order to flesh out precisely and quantify what is happening in reality, we have to explicitly model the forces that drive the magnitude of swap spreads. Furthermore, an important implication of perceived credit risk of the U.S. government is that we do not get to observe a risk-free rate. Thus, an equilibrium model is required to identify a risk-free rate. We rely on a model of a representative agent with recursive preferences for this purpose.

Another, more subtle, advantage of using the equilibrium framework pertains to the change in how the industry approaches the discounting of cash flows associated with collateralized swap agreements. Because of full collateralization, market participants started using the OIS rates instead of the LIBOR ones at the end of 2007, and the whole industry has switched to OIS by the end of 2008 (e.g., [Cameron, 2013](#), [Spears, 2019](#)). Thus, a no-arbitrage model would have to address the choice of reference interest rate.⁴

Under the null of our model, we obtain an equilibrium pricing kernel that we use to discount cash flows of a given financial instrument. The reference interest rate is the theoretical real risk-free rate in this case. All other interest rates appear as derived quantities in this framework on an internally consistent basis.

3.1 Joint dynamics of macroeconomic fundamentals

As is well-known from the long-run risk literature, accounting for variation in conditional expectation and volatility of consumption growth is central for a quantitative success of the framework. That motivates us to identify these quantities from a rich model of the joint dynamics of consumption growth, inflation, output growth, and government expenditures.

This strategy has the following three attractive features. First, we identify risk-free rates (both real and nominal) without relying on asset price data. Second, we can exploit the rich joint interactions between the macro fundamentals to identify conditional moments of consumption growth ([Schorfheide, Song, and Yaron, 2018](#), [Zviadadze, 2016](#)). Third, we identify the dynamics of macro variables other than consumption that we would need in our model: inflation to value nominal assets; output growth and government expenditures to model the default probability of the U.S. government (as in [Chernov, Schmid, and Schneider, 2019](#)); macroeconomic uncertainty as an important driver of sovereign credit risk in developed economies (as in [Augustin, 2018](#)).

⁴For example, [Chernov and Creal \(2016\)](#) reflect this change, by using OIS rates as a measure of reference rates starting in 2009, and by using a weighted average of LIBOR and OIS in 2008, with weights gradually shifting towards OIS by the end of 2008.

Consistent with the description above, we introduce a vector z_t of macroeconomic fundamentals:

$$z_t = (\Delta c_t, d_t, g_t, \pi_t)^\top,$$

where $\Delta c_t = \log(C_{t+1}/C_t)$ is log consumption growth, d_t is log output growth, g_t is the government expenditure to output ratio, and π_t is inflation. Dynamics of state variables in many long-run risk models are specified as a VAR(1) process in observable macro and latent states, e.g., [Bansal and Yaron \(2004\)](#), or [Bansal and Shaliastovich \(2012\)](#). They are similar to VARMA(1,1) models in observable macro states only (they are literally the same in homoscedastic cases).

Thus, we assume that z_t follows a VARMA(1,1) process with time-varying variance:

$$z_{t+1} = \mu_z + \Phi_z z_t + \Phi_{zv} v_t + \Sigma_z \cdot V_{z,t}^{1/2} \cdot \varepsilon_{z,t+1} + \Theta_z \cdot \Sigma_z \cdot V_{z,t-1}^{1/2} \cdot \varepsilon_{z,t}, \quad (1)$$

where z_{t+1} denotes a $N \times 1$ vector ($N = 4$ in our case), $\varepsilon_{z,t+1} \sim \mathcal{N}(0, I)$, μ_z is an $N \times 1$ vector, Φ_z is an $N \times N$ matrix, and Σ_z is an $N \times N$ matrix, where the diagonal elements of Σ_z are defined as σ_{z_i} , for $i = 1, 2, \dots, N$. Denote the last term in equation (1) as w_{t+1} ,

$$w_{t+1} = \Theta_z \cdot \Sigma_z \cdot V_{z,t}^{1/2} \cdot \varepsilon_{z,t+1},$$

and stack the elements of z_t and w_t into a new vector $y_t = [z_t^\top, w_t^\top]^\top$.

We treat π_t as being Granger-caused by the other macro variables, but not vice-versa. This is a reduced-form representation of the exogenous and endogenous variables that allows us to be consistent with the setup of [Chernov, Schmid, and Schneider \(2019\)](#). To achieve that, we restrict the off-diagonal elements of the last column of Φ_z and Θ_z to zero.

The vector y_t follows a VAR(1):

$$y_{t+1} = \mu_y + \Phi_y y_t + \Phi_{yv} v_t + \Sigma_y \cdot V_{y,t}^{1/2} \cdot \varepsilon_{y,t+1},$$

where y_{t+1} denotes a $2N \times 1$ vector, $\varepsilon_{y,t+1} \sim \mathcal{N}(0, I)$, μ_y is a $2N \times 1$ vector, Φ_y is a $2N \times 2N$ matrix, and Σ_y is a $2N \times 2N$ matrix, where the diagonal elements of Σ_y are defined as σ_{y_i} , for $i = 1, 2, \dots, 2N$.

We assume that the volatility vector consists of autonomous univariate autoregressive gamma processes characterized by the bivariate vector v_t , such that each element $v_{i,t+1}$ follows an autoregressive gamma process $v_{i,t+1} \sim ARG(\nu_i, \phi_i, c_i)$ ([Gourieroux and Jasiak, 2006](#) and [Le, Singleton, and Dai, 2010](#)), that is,

$$v_{i,t+1} = \nu_i c_i + \phi_i v_{i,t} + \eta_{i,t+1}, \quad \text{var}_t \eta_{i,t+1} = \nu_i c_i^2 + 2c_i \phi_i v_{i,t}.$$

In particular, the unconditional mean is $E v_{i,t} = \nu_i c_i (1 - \phi_i)^{-1}$, and we select $c_i = (1 - \phi_i) \nu_i^{-1}$ to set it to 1 for identification purposes.

We augment the state vector y_t with the volatility vector to get $x_t = [z_t^\top, w_t^\top, v_t^\top]^\top$. With $K = (2 \times N + 2)$, the $K \times 1$ -dimensional multivariate state vector x_{t+1} follows a VAR(1) process:

$$x_{t+1} = \mu + \Phi x_t + \Sigma \cdot V_t^{1/2} \cdot \varepsilon_{x,t+1},$$

where $\varepsilon_{x,t+1}$ defines a vector of independent shocks, Φ is a $K \times K$ matrix with positive diagonal elements, Σ is a $K \times K$ matrix with strictly positive elements, and V is a $K \times K$ diagonal matrix with elements given by:

$$V_{i,t} = a_i + b_i^\top v_t,$$

where parameter restrictions are required to guarantee non-negativity of the volatility process.

3.2 The pricing kernel

We assume a representative agent with recursive preferences:

$$\begin{aligned} U_t &= [(1 - \beta)C_t^\rho + \beta\mu_t(U_{t+1})^\rho]^{1/\rho}, \\ \mu_t(U_{t+1}) &= E_t(U_{t+1}^\alpha)^{1/\alpha}, \end{aligned}$$

where $\rho < 1$ captures time preferences (intertemporal elasticity of substitution is $(1 - \rho)^{-1}$), and $\alpha < 1$ captures the risk aversion (relative risk aversion is $1 - \alpha$). Aggregate consumption is denoted by C_t . With this utility function, the real pricing kernel is:

$$\widehat{M}_{t+1} = \beta(C_{t+1}/C_t)^{\rho-1}(U_{t+1}/\mu_t(U_{t+1}))^{\alpha-\rho}.$$

We can approximate the (log) pricing kernel using the solution method outlined in [Hansen, Heaton, and Li \(2008\)](#) and [Backus, Chernov, and Zin \(2014\)](#). We log-linearize the scaled time-aggregator:

$$\log(U_t/C_t) \equiv u_t \approx b_0 + b_1 \log \mu_t(e^{\Delta c_{t+1} + u_{t+1}}),$$

where

$$\begin{aligned} b_1 &= \beta e^{\rho \log \mu} ((1 - \beta) + \beta e^{\rho \log \mu})^{-1} \\ b_0 &= \rho^{-1} \log((1 - \beta) + \beta e^{\rho \log \mu}) - b_1 \log \mu, \end{aligned}$$

with $\log \mu = E(\log \mu_t)$. We guess u_t to be a linear function of the state x_t , substitute this guess into the log-linearized expression for u_t , and use the method of undetermined coefficients to solve for u_t . Then the log pricing kernel is:

$$\begin{aligned} \widehat{m}_{t,t+1} &= \log \beta + (\rho - 1) \Delta c_{t+1} + (\alpha - \rho) [\Delta c_{t+1} + u_{t+1} - \log \mu_t (e^{\Delta c_{t+1} + u_{t+1}})] \\ &= \log \beta - (\alpha - \rho) b_0 b_1^{-1} + (\alpha - 1) \Delta c_{t+1} + (\alpha - \rho) [u_{t+1} - b_1^{-1} u_t]. \end{aligned}$$

See Appendix [A](#) for details.

3.3 Equilibrium risk-free rates

The price of a zero-coupon bond paying one unit of consumption n -periods ahead from now must satisfy the Euler equation

$$\widehat{P}_t^n = E_t \left[\widehat{M}_{t,t+n} \right].$$

We show in Appendix B.1 that the term structure of real interest rates is affine in the state vector x_t .

Similarly, the price of an n -period zero-coupon nominal bond is obtained from the nominal stochastic discount factor and must satisfy the Euler equation

$$P_t^n = E_t [M_{t,t+n}],$$

where the nominal (log) stochastic discount factor is defined as $m_{t,t+1} = \widehat{m}_{t,t+1} - \pi_{t+1} = \widehat{m}_{t,t+1} - e_2^\top y_{t+1}$. We show in Appendix B.2 that the term structure of nominal interest rates is affine in the state vector x_t .

3.4 The valuation approach for defaultable interest rates

To capture the credit risk of the U.S. government, we use the [Chernov, Schmid, and Schneider \(2019\)](#) model as a basis. Their model is based on the contingent claims approach (CCA), which delivers a fiscal default via the budget deficit that can no longer be restored by raising taxes or eroding the real value of debt by creating inflation. That model requires a numerical solution even under oversimplified assumptions about the underlying economy. Because we are seeking high degree of realism, we do not model the whole elaborate structure of the default mechanism for tractability. Instead, we exploit the equivalence between the CCA and compound Poisson approaches ([Duffie and Lando, 2001](#)) and model a default hazard rate.

The exogenous variables in [Chernov, Schmid, and Schneider \(2019\)](#) that drive the U.S. credit risk are the aggregate consumption growth rate, output growth, and the government expenditures to output ratio. [Augustin \(2018\)](#) also shows that macroeconomic uncertainty is an important driver of sovereign credit risk in developed economies. Thus, we assume that the government's default risk is driven by a default intensity h_t defined as:

$$h_t = h + h_c \Delta c_t + h_d d_t + h_g g_t + h_{v_1} v_{1,t} + h_{v_2} v_{2,t}. \quad (2)$$

To model default risk, we also need a corresponding loss given default (LGD), denoted by L , which we assume to be constant.

One might think that inflation or the bank credit risk would affect the default probability of the U.S. government. The former may be relevant if one believes that the U.S. government

may attempt to “inflate away” its nominal debt. The latter may be important because of the potential link between banks’ solvency and government default (see, e.g., [Acharya, Drechsler, and Schnabl, 2014](#)). For instance, if the Fed bails out the banks, it could be forced into insolvency. That, in turn, could trigger government default because of the fiscal support provided by the Treasury ([Reis, 2015](#)).

As we discussed earlier in the case of π_t and as we will show later in the case of the factor capturing bank risk, the two variables are being Granger-caused by macro variables, but not vice-versa. Nevertheless, inflation and bank credit risk are related to the default probability of the U.S. government, albeit implicitly.

Given these assumptions, we can follow the approach of [Duffie and Singleton \(1999\)](#) that implies, under the recovery-of-market-value assumption, that one could account for credit risk by augmenting the (log) discount factor with $L \cdot h_t$:

$$\bar{P}_t^n \approx E_t e^{\sum_{j=1}^n m_{t+j-1,t+j} - L \cdot h_{t+j}}.$$

However, \bar{P}_t^n does not correspond to an observable bond price. That is because Treasury prices also reflect the convenience yield.

Thus, to progress further, we have to address the following conceptual challenge. While our focus is on the U.S. credit risk, the swap spreads are affected by other factors. First, Treasury bonds are considered to be expensive and embed a convenience yield relative to other asset classes (e.g., [Longstaff, 2004](#); [Krishnamurthy and Vissing-Jorgensen, 2012](#); [Nagel, 2016](#); [Du, Im, and Schreger, 2018](#)). Second, the swap rates typically reflect the credit and funding risk of financial intermediaries (e.g., [Feldhutter and Lando, 2008](#)). Third, as pointed out by [Johannes and Sundaesan \(2007\)](#), full collateralization of swaps increases the rates because of an opportunity cost of collateral (if the correlation between the short interest rate and the cost of collateral is positive). So, we have to model all these additional drivers of swap spreads.

Furthermore, there is no single asset that is sensitive to only one of these factors. Thus, in order to identify them, we have to use several assets simultaneously. Specifically, both Treasuries and U.S. CDS are informative about the U.S. credit risk. The former also reflects the convenience yield, while the latter does not. Similarly, the latter reflects the opportunity cost of collateral, which is irrelevant for Treasuries, but also impacts swap rates. IRS contracts are exposed to the opportunity cost of collateral as well, and the credit risk of banks in the Eurodollar area. Thus, the combination of these assets will help us identify all the needed factors. Once identified, we use all factors to evaluate the central object of the negative swap spread puzzle, i.e., the OIS-Treasury spread, as an “out-of-sample test” of our model.

3.5 Spread factors

Empirically, we identify the safety factor via the difference between the one-month OIS rate o_t and (risky) Treasury rates \tilde{y}_t^1 , $s_{1,t} = o_t - \tilde{y}_t^1$. As we discussed earlier, this factor reflects

not just the ease of trading in Treasuries, but also the credit risk of banks in the Federal Reserve system. We identify the bank credit factor via the difference between 1-month LIBOR and OIS rates, $s_{2,t} = \ell_t - o_t$. We refer to s_2 as the LIBOR-OIS spread. The cost of collateral $s_{3,t}$ is treated as latent in the absence of an observable measure. We stack them into a vector $s_t = [s_{1,t}, s_{2,t}, s_{3,t}]^\top$.

The quantitative and conceptual evolution of these spreads is a rich topic for discussion. We necessarily limit ourselves to the key takeaways. Roughly speaking, the difference between LIBOR and EFFR would represent the credit risk of banks in the Eurodollar area, while the difference between EFFR and a Treasury bill rate would represent the convenience yield.

The first point is consistent with the view of the LIBOR-OIS spread and its use as an indicator of the health of the banking sector in the wake of the financial crisis of 2008. The use of OIS here is subtle, because it reflects the credit risk of banks in the Federal Reserve system. Thus, the spread $s_{2,t}$, reflects the relative riskiness of the banks in the Eurodollar area. Practically speaking, the U.S. LIBOR is used for transactions between banks and other financial institutions, such as mutual funds, while EFFR is used for transactions between banks in the Fed system.

The second point assumes that the EFFR and the Treasury rate represent the same credit quality. Many researchers and practitioners treat the whole OIS curve as risk-free, because it is used to discount fully collateralized transactions. Full collateralization largely mitigates the counterparty risk, but not the cash flow risk of the underlying asset, the EFFR in this case. The credit risk of the U.S. Treasury is linked to that of the Federal Reserve system because of the fiscal support of the latter by the former (Reis, 2015). That means the Fed will never be insolvent separately from the Treasury. If one were to assume that the EFFR is risk-free while the Treasury is credit-risky, it would be much easier for us to explain the negative swap spread. Because of the aforementioned bank risk embedded in the EFFR, the spread $s_{1,t}$ would reflect that risk in addition to the convenience yield of Treasuries.

We assume that s_t follows a multivariate Gaussian AR(1) process, and it may also be affected by the dynamics of the macro volatility v_t :

$$s_{t+1} = \mu_s + \Phi_{sv}v_t + \Phi_s s_t + \Sigma_s \varepsilon_{s,t+1}, \quad (3)$$

where the innovations $\varepsilon_{s,t+1} \sim \mathcal{N}(0, \mathbb{I})$. By construction, s_t does not Granger cause the macro variables (z_t, v_t) . The conditional covariance of the one-period pricing kernel and the factor is zero, so there is no one-period risk premium associated with s_t .⁵ Their multi-period counterparts covary, thereby generating risk premiums, because of the presence of macro fundamentals in the conditional expectation of s_t . We introduce an extended state vector $\tilde{x}_t^\top = [x_t^\top, s_t^\top]$.

⁵The impact of macro innovations on s_{t+1} was estimated imprecisely so we zeroed that out to save on cumbersome notation.

3.6 Valuation of credit sensitive instruments

Risky Treasury bonds. Following [Duffie and Singleton \(1999\)](#), the resulting risky Treasury price is

$$\tilde{P}_t^n \approx E_t e^{\sum_{j=1}^n m_{t+j-1,t+j} - L \cdot h_{t+j} + s_{1,t+j}},$$

and we show in [Appendix B.3](#) that the term structure of risky interest rates is affine in the extended state vector \tilde{x}_t .

Hypothetical LIBOR bonds. We work with hypothetical zero-coupon LIBOR bonds L_t^n discounted at the continuously compounded yield ℓ_t^n (defined at the monthly frequency), such that:

$$L_t^n = \exp(-\ell_t^n \cdot n), \quad (4)$$

where $n \leq 12$ corresponds to LIBOR rate maturities of up to 12 months.⁶ Using the approach of [Duffie and Singleton \(1999\)](#), the resulting price is:

$$L_t^n \approx E_t e^{\sum_{j=1}^n m_{t+j-1,t+j} - L \cdot h_{t+j} - s_{2,t+j}},$$

and we show in [Appendix B.4](#) with the term structure of LIBOR rates is affine in the extended state vector \tilde{x}_t , with rates ℓ_t^n inferred from Equation (4).

IRS. The fixed rate payer pays the annual interest rate swap premium $IRS_{t,T}$. The floating rate payer pays the LIBOR rate that has been realized at the previous coupon period. We assume monthly time intervals to match the frequency of macroeconomic data. Thus, in case of a quarterly IRS payment frequency, the floating leg would pay each period the 3-month LIBOR rate realized on the previous coupon period, ℓ_{t-1}^3 . The one-month LIBOR rate is equal to $\ell_t \equiv \ell_t^1 = \tilde{y}_t^1 + s_{1,t} + s_{2,t}$.

We have valued the term structure of zero-coupon LIBOR rates in [appendix B.4](#) and can thus directly use the three-month LIBOR rates for the computation of the LIBOR swap contracts.⁷ We discount all cash flows accounting for the cost of collateral $s_{3,t}$ as in [Johannes and Sundaesan \(2007\)](#). Thus, the present value of expected future payments by the fixed leg is given by:

$$\omega_t^{fix} = IRS_t^n \sum_{j=1}^{n\Delta-1} E_t [e^{m_{t,t+j\Delta} + s_{3,t+j\Delta}}],$$

⁶Because actual LIBOR rates $\ell_t^{q,n}$ are periodic and quoted on an annualized basis, we map the data into continuously compounded rates according to the formula $\ell_t^n = n^{-1} \log(1 + \ell_t^{q,n} \cdot n \cdot 30/360)$. The day count convention for LIBOR rates is act/360. We use 30/360 as the daycount convention given that it is numerically close to act/360, and it simplifies the implementation.

⁷For maturities up to one year, zero-coupon rates are equivalent to par rates. For the numerical implementation, we map the continuously compounded LIBOR rates into periodic rates assuming a 30/360 daycount convention for simplicity.

where Δ defines the time interval between two successive coupon periods. The present value of expected future payments by the floating leg is given by:

$$\omega_t^{float} = \sum_{j=1}^{n\Delta-1} E_t \left[e^{m_{t,t+j\Delta} + s_{3,t+j\Delta}} \left(e^{\Delta \cdot \ell_{t+(j-1)\Delta}^3} - 1 \right) \right].$$

where Δ defines the time interval between two successive coupon periods.

A LIBOR swap contract is priced fairly if both the fixed and the floating legs have the same value. The condition yields the formula for the IRS spread IRS_t^n :

$$IRS_t^n = \frac{\sum_{j=1}^{n\Delta-1} E_t \left[e^{m_{t,t+j\Delta} + s_{3,t+j\Delta}} \left(e^{\Delta \cdot \ell_{t+(j-1)\Delta}^3} - 1 \right) \right]}{\sum_{j=1}^{n\Delta-1} E_t \left[e^{m_{t,t+j\Delta} + s_{3,t+j\Delta}} \right]}. \quad (5)$$

See Internet Appendix B.5 for the derivation.

OIS. The fixed rate payer pays the annual OIS premium OIS_t^n . The floating rate payer pays the geometric mean of daily overnight rates. Because of the assumed monthly minimal time interval in our model, there is no distinction between $o_t \equiv OIS_t^1$ and EFR compounded over a month. Thus, the quarterly payment frequency corresponds to the floating leg paying the geometric average of three one-month OIS rates.

As was the case for IRS premiums, we discount all cash flows accounting for the cost of collateral $s_{3,t+1}$. The present value of expected future payments by the fixed leg is given by:

$$\pi_t^{fix} = OIS_t^n \sum_{j=1}^{n\Delta-1} E_t \left[e^{m_{t,t+j\Delta} + s_{3,t+j\Delta}} \right],$$

where Δ defines the time interval between two successive coupon periods. The present value of expected future payments by the floating leg is given by:

$$\pi_t^{float} = \sum_{j=1}^{n\Delta-1} E_t \left[e^{m_{t,t+j\Delta} + s_{3,t+j\Delta}} \left[\exp \left(\sum_{i=1}^{\Delta} o_{t+j\Delta-i} \right) - 1 \right] \right].$$

OIS swaps of maturity less than one year are subject to only one payment settlement, while those of maturities equal to and greater than one year are subject to quarterly payments.

An OIS contract is priced fairly if both the fixed and the floating legs have the same value. This condition yields the formula for the OIS spread OIS_t^n :

$$OIS_t^n = \frac{\sum_{j=1}^{n\Delta-1} E_t \left[e^{m_{t,t+j\Delta} + s_{3,t+j\Delta}} \left[\exp \left(\sum_{i=1}^{\Delta} o_{t+j\Delta-i} \right) - 1 \right] \right]}{\sum_{j=1}^{n\Delta-1} E_t \left[e^{m_{t,t+j\Delta} + s_{3,t+j\Delta}} \right]}. \quad (6)$$

See Internet Appendix [B.6](#) for the derivation.

CDS. To value CDS contracts, we need to model both the premium leg that pays the annual CDS premium CDS_t^n , and the protection leg that pays the loss given default L . We note the distinction between CDS contracts, which contractually recover a fraction of face value, and risky Treasuries, which are usually modeled as recovering a fraction of market value. [Duffie and Singleton \(1999\)](#) find little difference across different modeling assumptions of recovery on the term structure of defaultable interest rates (see Figure 2 on p. 703).

A CDS contract with time to maturity n pays the annual premium until the earlier of default or the contract's termination date. As is the case with other swap contracts, we account for the cost of collateral. Accordingly, the present value of the premium payments of a USD-denominated CDS contract is equal to:

$$\pi_t^{pb} = CDS_t^n \sum_{j=1}^{n\Delta^{-1}} E_t [e^{m_{t,t+j\Delta} + s_{3,t+j\Delta}} I(\tau > t + j\Delta)],$$

where Δ defines the time interval between two successive coupon periods, and $I(\cdot)$ is an indicator function that is equal to one if the condition inside the brackets is met, and zero otherwise. For simplicity, we omit accrual payments in the notation, but account for them in the formal implementation of the model. The present value of expected future payments by the protection seller is given by:

$$\pi_t^{ps} = L \cdot E_t [e^{m_{t,\tau} + s_{3,\tau}} I(\tau \leq n)].$$

A CDS contract is priced fairly if both the premium and the protection legs have the same value. This condition yields the formula for the CDS premium CDS_t^n :

$$CDS_t^n = L \cdot \frac{E_t [e^{m_{t,\tau} + s_{3,\tau}} I(\tau \leq n)]}{\sum_{j=1}^{n\Delta^{-1}} E_t [e^{m_{t,t+j\Delta} + s_{3,t+j\Delta}} I(\tau > t + j\Delta)]}. \quad (7)$$

See Internet Appendix [B.7](#) for the derivation of the CDS premiums.

4 Results

4.1 Estimation

We use macroeconomic fundamentals and financial asset data to estimate the model via Bayesian MCMC with diffuse priors. The outputs of the procedure are the state variables and parameter estimates. Posterior estimates are provided in [Table 6](#) and [Table 7](#).

The key feature of our approach is that we conduct a two-stage estimation. In the first stage, we estimate the macro dynamics described by the autonomous VARMA for z_t . In the second stage, we use asset market data for the identification of the financial factors s_t .

There are two advantages to doing so. First, we have a much shorter time interval with available data on CDS and interest rate swap premiums, which start in 2002 (USD-denominated U.S. CDS start even later in 2010). Thus, the first stage allows for using a longer history of macroeconomic fundamentals to learn about z_t . Second, we can identify the dynamics of the macroeconomic factors and, therefore, of the pricing kernel, without relying on asset market data. Thereby, we are avoiding the “dark matter” critique of [Chen, Dou, and Kogan \(2017\)](#).

We provide a brief outline of our two-stage estimation procedure. See [Appendix C](#) for details. In the first stage, we use consumption growth, output growth, log government expenditure-to-output ratio, and inflation from 1982 to 2018. Except for inflation data, which are monthly, the other macro variables are quarterly.⁸ Because the decision interval is one month in our model, we estimate the monthly counterparts of the respective quarterly series. We adjust the state-space representation to address the mixed frequency of the observables. Posterior estimates from the first stage estimation are provided in [Table 6](#).

The estimated AR matrix Φ_z and MA matrix Θ_z imply that consumption and output growth rates do not affect inflation and government expenditures. The latter affects all macro fundamentals (consumption is affected indirectly via output and the MA term). The two variance factors affect the conditional mean of inflation only. The other elements of the matrix Φ_{zv} are set to zero because they were poorly identified in our sample.

Having filtered out the estimates for z_t and v_t at the monthly frequency, we use data on the term structure of Treasury GSW zero-coupon rates (maturity of 1, 3, 5, 7, 10, 20, 30 years), the term structure of CDS premiums (maturity of 1, 3, 5, 7, 10, 20, 30 years), and the empirical measures of $s_{1,t}$ and $s_{2,t}$ to learn about the joint dynamics of s_t . We do not use the IRS and OIS data in the estimation so that we can evaluate the implied swap spreads as an out-of-sample test of our model. The one-year IRS is the only exception to the strategy, because it is helpful in identifying the latent cost of collateral, s_3 .⁹ We use the bootstrap particle filter to estimate $s_{3,t}$.

To estimate the dynamics of the financial variables in the second stage, we condition on the filtered macroeconomic fundamentals from the corresponding period. Furthermore, these fundamentals exhibit visible shifts in level in this later part of our sample. Thus, we re-estimate the constant term μ_z to accommodate possible structural breaks in the level of macroeconomic fundamentals z_t . Relatedly, we impose a one-time structural break in the

⁸In particular, our choice of using quarterly consumption growth avoids modeling measurement errors in monthly consumption growth (see [Schorfheide, Song, and Yaron, 2018](#) for a detailed discussion). That significantly reduces the dimension of the state vector leading to a much more tractable estimation problem.

⁹Using the one-year IRS data for estimation is innocuous, because it is the shortest maturity and does not exhibit any puzzles.

default intensity h_t by assuming that it switched from zero to a positive value in December 2007 to reflect nearly zero U.S. CDS premiums prior to that date. Posterior estimates from the second stage estimation are provided in Table 7.

With the exception of the variance factors, other macro variables do not affect the financial ones (the matrix Φ_{sy} was poorly identified). The variances have a significant impact on the convenience yield s_1 , perhaps reflecting the flight-to-safety effect, and the cost of collateral s_3 , reflecting lenders' collateral demand. With the exception of output growth, all other macro variables play an important role in the default intensity. Output growth affects forecasts of future h_t via its impact on consumption growth (matrix Φ_z).

Most studies on no-arbitrage modeling of credit-sensitive assets do not estimate the LGD separately from the default intensity because of a joint identification problem. We need the separation between the two for the sole purpose of simplifying the interpretation of the magnitude of the default rate. Thus, following [Chernov, Schmid, and Schneider \(2019\)](#), we calibrate the LGD to a specific value of $L = 0.3$.

Estimated risk aversion is $1 - \alpha \approx 5$. This value is clearly insufficient to match the equity premium, which is natural in a bond pricing model. Elasticity of intertemporal substitution $(1 - \rho)^{-1} \approx 1.33$ is in line with standard calibrations in the long-run risk literature.

4.2 Factors

Figures 3 and 4 display the factors that we use in our model. The first figure shows the macro variables z_t . We note a downward trend in inflation throughout the sample. While that can be attributed to the great moderation in the early part of our sample period, it may appear puzzling in the post-crisis sample when monetary policy was particularly accommodating. Our series are consistent, however, with the observation, sometimes labeled the 'missing inflation puzzle', that inflation is low in spite of expansionary monetary policies conducted by central banks around the globe ([Arias, Erceg, and Trabandt, 2016](#)).

We also note a gradual elevation in government expenditures (as a fraction of output) throughout the sample, consistent with stabilization policies put in place after the onset of the financial crisis. Log consumption and output growth are standard series. In particular, the latter part of the sample period exhibits lower consumption growth volatility, consistent with the period of great moderation, except for a bump in anticipation of a potential turmoil in 2008.

The second figure shows the observable finance variables, s_1 and s_2 , together with the latent finance variable s_3 . The convenience yield and the LIBOR-OIS factors exhibit familiar patterns with substantial spikes during the period surrounding the financial crisis of 2008, reflecting a flight to quality on the one hand, and rising perceptions of bank risk in the

aftermath of Lehman’s collapse, on the other hand. The cost of posting collateral gradually rises during the overheating credit markets heading into the crisis, when investment opportunities were abundant.

Both s_1 and s_3 collapse after the crisis. This pattern is important as a decline in both of these factors diminishes their effects on swap spreads. Quantitatively, that leaves credit risk of the U.S. Treasury as the main force affecting the spreads.

The post-crisis pattern in s_1 and s_3 is natural. The decline in convenience is associated with an increase in the riskiness of Treasuries. In fact, our estimated parameters imply that both variance factors are associated with an increase in the default intensity and a decline in s_1 . The cost-of-collateral is influenced by the cost of holding cash and lending out Treasuries in rehypothecation. Indeed, interest rates have been at historical lows since the financial crisis.

4.3 Fit

Figures 5 - 6 demonstrate the model fit to the financial data used in the estimation. We have an unusual setup in that our model is a hybrid of an endowment economy and a reduced-form no-arbitrage valuation. Formally, it belongs to the class of affine models, but we impose a host of additional economic restrictions not typically present in a traditional no-arbitrage model. So we do not expect as pristine of a fit as a regular affine no-arbitrage model would deliver. Nevertheless, a high degree of realism would be welcome. Otherwise, the implications for the IRS-Treasury and OIS-Treasury spreads would not be very plausible and relevant.

Figure 5 compares model-implied credit-risky and observed zero-coupon Treasury yields of different maturities, up to a 30-year horizon. The model is having some difficulty in matching the one-year rate, but performs well at longer horizons. That is not surprising. Our model does not explicitly account for the prolonged near-zero-bound interest rate experience after the crisis. The short end of the curve is much more sensitive to that than the long end.

Figure 6 shows observed and model-implied U.S. CDS rates. CDS premiums are stripped of the level of benchmark interest rates, so they naturally do not have a first-order sensitivity to the aforementioned misspecification of the short interest rates. The fit of the model is good throughout all maturities.

4.4 The U.S. “credit spread”

Having verified a reasonable fit of the model, we proceed with exploring its implications. Figure 7 displays nominal credit-risk-free interest rates (without convenience yield) against

the risky nominal Treasury benchmark. Before the financial crisis, there is little difference between the riskless and the risky nominal rates. This is expected because the U.S. CDS premium was literally zero before the crisis. They are not identical because of the presence of the convenience yield.

U.S. CDS premiums jumped in the financial crisis and stayed elevated ever since. As we show in Figure 6, CDS premiums fluctuated between 20 and 60 bps at different maturities between 2011 and 2018. Accordingly, the ignition of U.S. credit risk is reflected in the difference between risky and riskless nominal Treasury interest rates. The difference between these rates is small at short horizons, but becomes progressively more visible at longer horizons. For example, the difference averages around 44 bps (70 bps) at the 5-year (10-year) maturity during the post-crisis period, and reaches maximum levels of 74 bps (91 bps).

Focusing on the variation in the quantitative magnitude of credit risk, we plot the U.S. default intensity in Figure 8(A). The likelihood of a U.S. default spikes to 0.2% during the global financial crisis (GFC), and then flares up again in times of elevated fiscal stress. Over the last decade, the threats of government shutdowns have risen as anticipations of U.S. debt ceiling breaches are increasingly common. On August 5, 2011, the rating agency Standard & Poor’s stripped the U.S. off its AAA credit rating and lowered it by one notch to AA+. During the post-GFC period the average intensity is about 0.05%.

Figure 8(B) quantifies the impact of the credit risk premium on the CDS valuation. Specifically, we characterize the “distress” risk premium associated with unpredictable variation in the arrival rate h_t . To this end, we follow Longstaff, Mithal, and Neis (2005) and Pan and Singleton (2008), and report the difference between the model-based five-year CDS premium and a hypothetical premium for the case of a risk-neutral investor (denoted CDS^\dagger). We omit the cost of collateral s_3 to focus on the pure effect of credit risk premium.

The difference between CDS and CDS^\dagger is stable throughout the sample averaging 14 bps. The relative difference measuring the fraction of the CDS premium due to distress risk ranges between 20 and 80 percent. In contrast to the difference in levels, the relative measure is trending upwards throughout the sample. While CDS premiums have declined in the post-GFC period, the relative contribution of the risk premium has increased.

In Figure 9, we conduct an exercise that helps us better gauge the impact of modeling the default risk of the U.S. Treasury. We compare the sensitivity to all state variables of the “U.S. credit spread” that is displayed in Figure 7. We measure the sensitivities as factor loadings appearing in the theoretical linear relation between the credit spread and the state variables. To facilitate the quantitative interpretation of the results, we multiply these loadings by unconditional standard deviations of the respective state variables. Thus the reported numbers represent a monthly change in the credit spread (expressed in decimals) in response to a one standard deviation change in a given state variable.

Our discussion focuses on the four quantitatively most important variables. Higher government expenditures elevate the risky yield relative to the nominal one, and this effect is

especially pronounced at the short end of the term structure. That is intuitive, as, in expectation, the government can balance its budget in the long run either by raising taxes or by issuing more debt. Either measure is likely accompanied with dimmer default prospects, either directly or through the negative effects of elevated taxes on growth projections, as in [Chernov, Schmid, and Schneider \(2019\)](#). Quantitatively, a one standard deviation increase in the government expenditures to output ratio increases the credit spread by approximately 20 bps at the 5-year maturity.

Higher macroeconomic uncertainty also leads to greater risky yields, as the representative agent in our model dislikes economic uncertainty that come with a higher likelihood of extreme events. Inflation variance has a greater impact at the short end of the yield curve, as inflation surprises are more relevant for that maturity segment. Consumption variance has a greater impact at the long end of the curve. This is reminiscent of long-run risk in volatility, which has an impact due to the combination of recursive preferences with a preference for early resolution of uncertainty.

The convenience yield affects the risky Treasury directly. A higher convenience yield implies a lower yield. This effect is especially pronounced for short-term bills, perhaps because of the importance of Treasuries in short-horizon repo transactions, and impacts the credit spread by as much as 45 bps in response to a one standard deviation move. At longer maturities, this effect stabilizes around 10 bps.

Bank risk and the cost of collateral matter indirectly via the interactions with the macroeconomic fundamentals and all spread factors. The LIBOR-OIS spread captures bank risk. Bank risk interacts positively with U.S. credit risk, and so the effect on the credit spread is positive. The cost of collateral is indirectly reflected through a negative impact on the credit spread.

4.5 Swap spreads

Figure 10 displays our headline result – the model-implied OIS-Treasury spread. Importantly, we note that OIS information was not used in the model estimation. The model captures both the positive spread before the crisis when U.S. credit risk was next to nil, and the negative spread in the post-crisis period. The results are quantitatively realistic for all maturities.

In Figure 11, we also plot the model-implied IRS-Treasury spread. Recall that we only use the 1-year maturity in our estimation. As for OIS-Treasury spreads, we qualitatively fit the evolution of the swap spreads well. We match positive swaps spreads before the crisis, and negative ones thereafter.

In our analysis in section 2.4 we offer qualitative arguments and suggestive evidence linking U.S. credit risk to swap spreads. Our quantitative model allows for a rich set of different

effects beyond the sovereign risk channel, including the convenience yield, bank risk, cost of collateral, and time-varying risk premiums. Thus, a natural question is whether the quantitative effect due to a U.S. credit risk premium is large enough to support our qualitative analysis.

In a counterfactual analysis, we can use our model to evaluate the contribution of U.S. credit risk to the spreads. Figure 12 reports the results of a decomposition of the OIS-Treasury spread into the respective contributions coming from default and non-default risk. That helps to gauge the contribution of the default risk premium to the negative swap spreads in our model. We plot the decomposition for maturities of 1, 3, 5, 10, 20, and 30 years. We provide a similar decomposition for IRS-Treasury spreads in Figure 13.

The quantitative implication is clear. The model implied OIS-Treasury spreads are uniformly positive when we only account for liquidity and bank frictions. The few negative swap spread realizations are quantitatively tiny. Accounting for the U.S. credit risk premium, however, shifts the OIS-Treasury spread significantly downwards. That downward shift is increasing in maturity. This clearly illustrates the critical role of U.S. credit risk in matching negative OIS-Treasury spreads in an equilibrium model that explains multiple benchmark rates jointly, even if we account for realistic liquidity and bank frictions.

In Table 8, we report model-implied regressions of changes in swap spreads on changes in CDS premiums, similar to the ones reported in Table 3. In these regressions, we do not control for common time fixed effects because, by construction, our model is driven by a limited number of state variables that drive the common variation across swap spreads. The relation between swap spreads and U.S. credit risk in the model reflects the salient features of the data well. The relation is weakly significant for short-term maturities (column 1), highly significant for maturities above 7 years (column 2), and becomes stronger over time (columns 3 and 4). The economic magnitudes are also similar than those in the data, slightly weaker at short-term maturities, and stronger at longer maturities. For example, according to the results in column (5), a 10 bps increase in CDS premiums lowers swap spreads by 0.4 bps, with an R^2 of 16%. The most comparable regression in Table 3 is that in column (5), which indicates a 0.7 bps change for a 10 bps change in CDS premiums, with an R^2 of 2%. A regression at the weekly frequency (unreported results) yields an R^2 of 5% with a regression coefficient of 2.1 bps. Post 2014, the coefficient in the data is negative 0.13, while it is negative 0.11 in the model.

Thus, our model suggests that, quantitatively, sovereign credit risk is a relevant ingredient needed to account for negative swap-Treasury spread. The sovereign risk channel operates through the U.S. credit risk premium, which can be large, even if the physical default probability is small. Such a risk premium channel complements existing explanations based on frictions. We reach this conclusion based on a realistic model of benchmark interest rates, in which frictions are identified via observable quantities (convenience yield and LIBOR-OIS spread) and a latent factor (cost of collateral); time-varying risk premia are pinned down by the preferences of a representative risk averse agent and observed macroeconomic fundamentals.

5 Conclusion

Researchers have been struggling to explain the puzzling behavior of benchmark interest rates since the financial crisis. Most prominently, short-term and long-term overnight bank borrowing costs, reflected in overnight index and interest rate swap contracts, have been lower than maturity-matched Treasury rates. Leading explanations of these negative swap spread puzzles are based on frictions, such as demand for duration, caps on leverage, or fading convenience yields for U.S. Treasuries.

We show that it is important to account for high-quality sovereign credit risk to enhance our understanding of post-crisis pricing phenomena. A small probability of U.S. Treasury default lowers no-arbitrage bounds of swap spreads to negative levels. Specifically, accounting for a U.S. credit risk premium in Treasuries is crucial if one wants to explain the dynamics of the term structures of multiple benchmark interest rates jointly. Even if the probability of a U.S. credit event is small, the risk premium associated with it may be large.

References

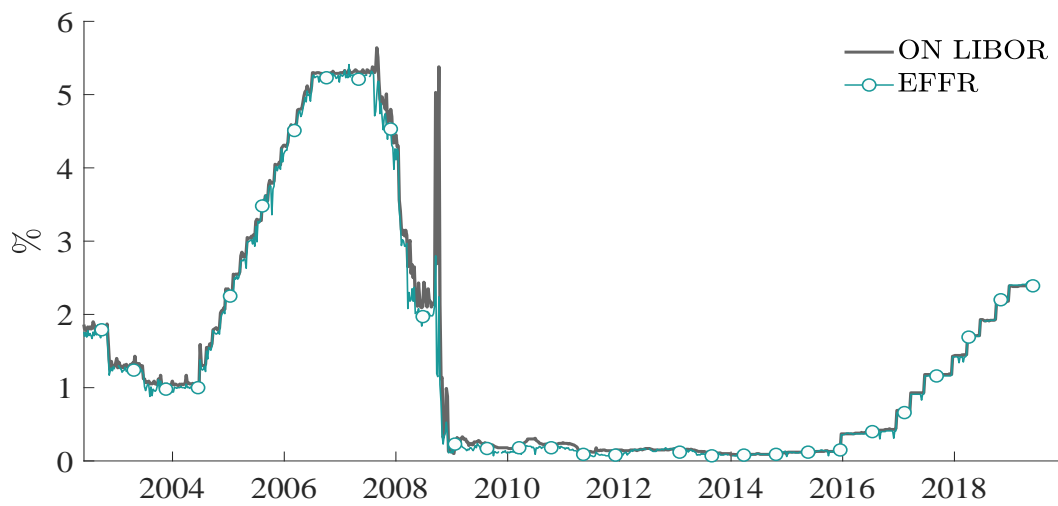
- Acharya, Viral V., Itamar Drechsler, and Philipp Schnabl, 2014, A pyrrhic victory? - Bank bailouts and sovereign credit risk, *The Journal of Finance* 69, 2689–2739.
- Arias, Jonas, Christopher Erceg, and Matthias Trabandt, 2016, The Macroeconomic Risks of Undesirably Low Inflation, *European Economic Review* 88, 88–107.
- Augustin, Patrick, 2018, The term structure of CDS spreads and sovereign credit risk, *Journal of Monetary Economics* 96, 53–76.
- Backus, David, Mikhail Chernov, and Stanley Zin, 2014, Sources of Entropy in Representative Agent Models, *Journal of Finance* 69, 51–99.
- Bansal, Ravi, and Ivan Shaliastovich, 2012, A Long-Run Risks Explanation of Predictability Puzzles in Bond and Currency Markets, *Review of Financial Studies*.
- Bansal, Ravi, and Amir Yaron, 2004, Risks for the Long Run: A Potential Resolution of Asset Pricing Puzzles, *The Journal of Finance* 59, 1481–1509.
- Bongaerts, Dion, Frank De Jong, and Joost Driessen, J., 2011, Derivative pricing with liquidity risk: Theory and evidence from the credit default swap market, *Journal of Finance* 66, 203–240.
- Boyarchenko, Nina, Pooja Gupta, Nick Steele, and Jacqueline Yen, 2018, Negative Swap Spreads, *Federal Reserve Bank of New York Economic Policy Review* 24.
- Brenner, Menachem, Rafi Eldor, and Shmuel Hauser, 2001, The Price of Options Illiquidity, *Journal of Finance* 56, 789–805.
- Cameron, Matt, 2013, Goldman and the OIS Gold Rush, *Risk Magazine* June, 15–19.
- Chen, Hui, Winston Dou, and Leonid Kogan, 2017, Measuring the “Dark Matter” in Asset Pricing Models, *Working Paper MIT*.
- Chernov, Mikhail, and Drew D. Creal, 2016, The PPP view of multihorizon currency returns, *Working paper*.
- Chernov, Mikhail, Lukas Schmid, and Andres Schneider, 2019, A macrofinance view of US Sovereign CDS premiums, *Journal of Finance* Forthcoming.
- Collin-Dufresne, Pierre, and Bruno Solnik, 2001, On the Term Structure of Default Premia in the Swap and LIBOR Markets, *The Journal of Finance* 56, 1095–1115.
- Deuskar, Prachi, Anurag Gupta, and Marti G. Subrahmanyam, 2011, Liquidity effect in OTC options markets: Premium or discount?, *Journal of Financial Markets* 14, 127–160.
- Dittmar, Robert, Alex C. Hsu, Guillaume Roussellet, and Peter Simasek, 2019, Default Risk and the Pricing of U.S. Sovereign Bonds, *Working Paper*.

- Du, Wenxin, Joanne Im, and Jesse Schreger, 2018, The U.S. Treasury Premium, *Journal of International Economics* 112, 167–181.
- Duffie, Darrell, and Ming Huang, 1996, Swap Rates and Credit Quality, *Journal of Finance* 51, 921–949.
- Duffie, Darrell, and David Lando, 2001, Term structures of credit spreads with incomplete accounting information, *Econometrica* 69, 633–664.
- Duffie, Darrell, and Kenneth J. Singleton, 1997, An Econometric Model of the Term Structure of Interest-Rate Swap Yields, *The Journal of Finance* 52, 1287–1321.
- Duffie, Darrell, and Kenneth J. Singleton, 1999, Modeling Term Structures of Defaultable Bonds, *Review of Financial Studies* 12, 687–720.
- Duffie, Darrell, and Kenneth J. Singleton, 2003, *Credit Risk: Pricing, Measurement and Management*. (Princeton University Press).
- Duffie, Darrell, and Jeremy Stein, 2015, *Journal of Economic Perspectives*, 29, 191–212.
- English, William B., 1996, Understanding the Costs of Sovereign Default: American State Debts in the 1840's, *American Economic Review* 86, 259–275.
- Feldhutter, Peter, and David Lando, 2008, Decomposing swap spreads, *Journal of Financial Economics* 88, 375–405.
- Filipovic, Damir, and Anders B. Trolle, 2013, The term structure of interbank risk, *Journal of Financial Economics* 109, 707–733.
- Fleckenstein, Matthias, Francis A. Longstaff, and Hanno Lustig, 2013, Deflation Risk, *NBER Working Paper No. 19238*.
- Gourieroux, Christian, and Joann Jasiak, 2006, Autoregressive gamma processes, *Journal of Forecasting* 25, 129–152.
- Goyenko, Ruslan, Avanidhar Subrahmanyam, and Andrey Ukhov, 2011, The Term Structure of Bond Market Liquidity and Its Implications for Expected Bond Returns, *Journal of Financial and Quantitative Analysis* 46, 111–139.
- Grinblatt, Mark, 2001, An analytic solution for interest rate swap spreads, *International Review of Finance* 2, 113–149.
- Gupta, Anurag, and Marti G. Subrahmanyam, 2000, An empirical examination of the convexity bias in the pricing of interest rate swaps, *Journal of Financial Economics* 55, 239–279.
- Gurkaynak, Refet S., Brian Sack, and Jonathan H. Wright, 2007, The U.S. Treasury yield curve: 1961 to the present, *Journal of Monetary Economics* 54, 2291–2304.

- Hansen, Lars Peter, John C. Heaton, and Nan Li, 2008, Consumption Strikes Back? Measuring Long-Run Risk, *The Journal of Political Economy* 116, pp. 260–302.
- He, Hua, 2001, Modeling term structures of swap spreads, *Working Paper*.
- Hilscher, Jens, Alon Raviv, and Ricardo Reis, 2014, Inflating Away the Public Debt? An Empirical Assessment, *NBER Working Paper No. 20339*.
- Hull, John, and Alan White, 2013, LIBOR vs. OIS: The Derivatives Discounting Dilemma, *Journal Of Investment Management* 11, 14–27.
- Jermann, Urban J., 2019, Negative Swap Spreads and Limited Arbitrage, *Review of Financial Studies* Forthcoming.
- Johannes, Michael, and Suresh M. Sundaresan, 2007, The Impact of Collateralization on Swap Rates, *The Journal of Finance* 62, 383–410.
- Klingler, Sven, and Suresh Sundaresan, 2019, How Safe Are Safe Havens?, *Working Paper Columbia University*.
- Klingler, Sven, and Suresh M. Sundaresan, 2018, An Explanation of Negative Swap Spreads: Demand for Duration from Underfunded Pension Plans, *The Journal of Finance* Forthcoming.
- Krishnamurthy, Arvind, 2002, The bond/old-bond spread, *Journal of Financial Economics* 66, 463–506.
- Krishnamurthy, Arvind, and Annette Vissing-Jorgensen, 2012, The Aggregate Demand for Treasury Debt, *Journal of Political Economy* 120, 233–267.
- Lando, David, and Sven Klingler, 2018, Safe-Haven CDS Premia, *Review of Financial Studies* 31, 1856–1895.
- Le, Anh, Kenneth J. Singleton, and Qiang Dai, 2010, Discrete-Time AffineQ Term Structure Models with Generalized Market Prices of Risk, *Review of Financial Studies* 23, 2184–2227.
- Litzenberger, Robert, 1992, Swaps: Plain and fanciful, *Journal of Finance* 47, 831–850.
- Liu, Jun, Francis Longstaff, and Ravit E. Mandell, 2006, The Market Price of Risk in Interest Rate Swaps: The Roles of Default and Liquidity Risks, *The Journal of Business* 79, 2337–2360.
- Longstaff, Francis A., 2004, The Flight-to-Liquidity Premium in U.S. Treasury Bond Prices, *Journal of Business* 77, 511–526.
- Longstaff, Francis A., Sanjay Mithal, and Eric Neis, 2005, Corporate Yield Spreads: Default Risk or Liquidity? New Evidence from the Credit Default Swap Market, *Journal of Finance* 60, 2213–2253.

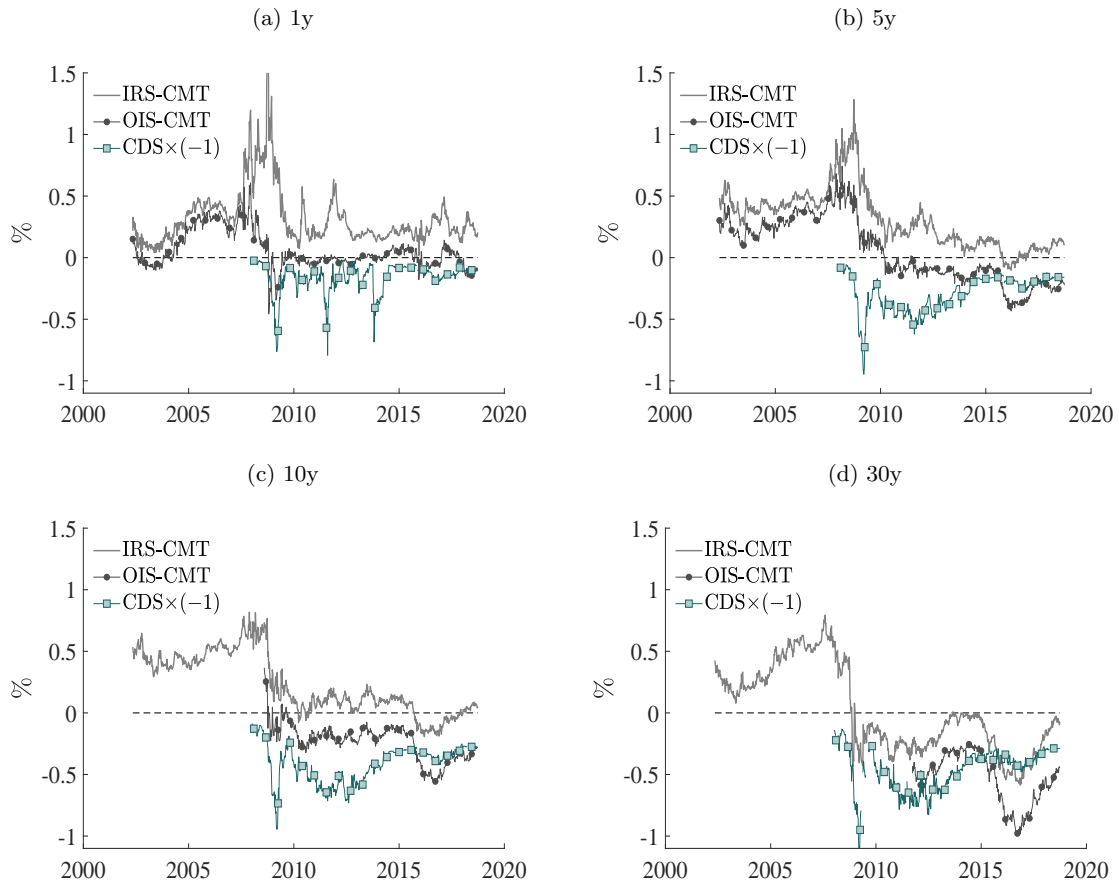
- Lou, Wujiang, 2009, On asymmetric funding of swaps and derivatives—a funding cost explanation of negative swap spreads, *SSRN Working Paper 1610338*.
- Monfort, A., J.-P. Renne, and G. Roussellet, 2016, A Quadratic Kalman Filter, *Journal of Banking and Finance* Forthcoming.
- Nagel, Stefan, 2016, The Liquidity Premium of Near-Money Assets, *Quarterly Journal of Economics* 131, 1927–1971.
- Pan, Jun, and Kenneth J. Singleton, 2008, Default and Recovery Implicit in the Term Structure of Sovereign CDS Spreads, *Journal of Finance* 63, 2345–2384.
- Reinhart, Carmen M., and Kenneth S. Rogoff, 2008, This Time is Different: A Panoramic View of Eight Centuries of Financial Crises, NBER Working Papers 13882 National Bureau of Economic Research, Inc.
- Reis, Ricardo, 2015, Different Types of Central Bank Insolvency and the Central Role of Seignorage, *Journal of Monetary Economics* 73, 20–25.
- Schorfheide, F., D. Song, and A. Yaron, 2018, Identifying Long-Run Risks: A Bayesian Mixed-Frequency Approach, *Econometrica* 86, 617–654.
- Spears, Taylor, 2019, Discounting collateral: quants, derivatives and the reconstruction of the ‘risk-free rate’ after the financial crisis, *Economy and Society, forthcoming*.
- Sun, Tong-Sheng, Suresh Sundaresan, and Ching Wang, 1993, Interest rate swaps: An empirical investigation, *Journal of Financial Economics* 34, 77–99.
- Wang, Zhenyu, and Wei Yang, 2018, OIS Risk Premiums, *Working Paper*.
- Zivney, Terry L., and Richard D. Marcus, 1989, The Day the United States Defaulted on Treasury Bills, *The Financial Review* 24, 475–489.
- Zviadadze, Irina, 2016, Term-Structure of Consumption Risk Premia in the Cross-Section of Currency Returns, *The Journal of Finance* Forthcoming.

Figure 1: USD overnight LIBOR and EFFR



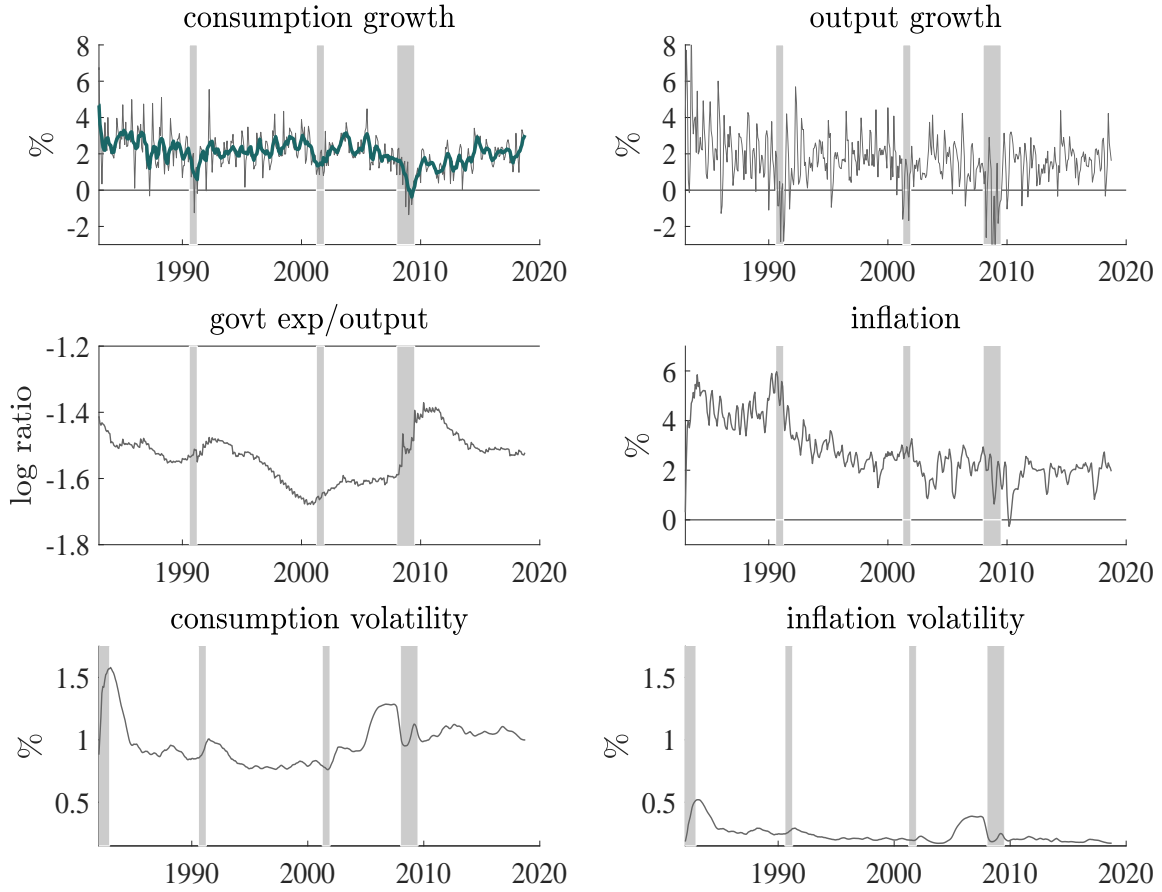
Notes: In this figure, we report the time series of the difference between the overnight London Interbank Offered Rate (LIBOR) and the Effective Federal Funds Rate (EFFR). LIBOR is the average interest rate at which leading banks borrow funds of a sizeable amount from other banks in the Eurodollar area. The EFFR is calculated as a volume-weighted median of overnight federal funds transactions provided by domestic banks, U.S. branches, and agencies of foreign banks, as reported in the reporting form FR 2420. The data frequency is weekly based on Wednesday rates. All spreads are expressed in percent. The sample period is 8 May 2002 to 26 September 2018. Source: Federal Reserve Bank of St. Louis. The y -axis is in annualized percentage terms.

Figure 2: IRS-Treasury and OIS-Treasury spreads



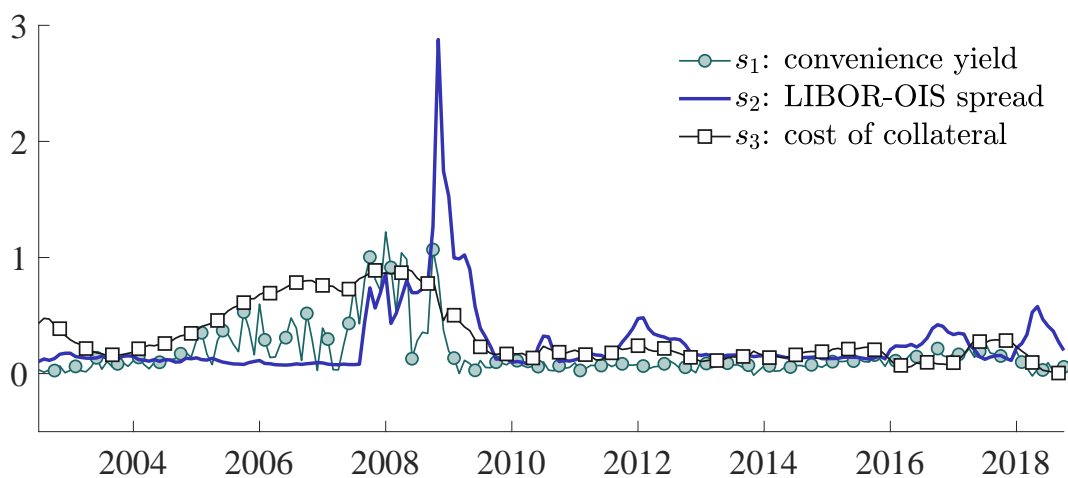
Notes: In these figures, we report the time series of the USD denominated IRS-Treasury and OIS-Treasury swap spreads, defined as the difference between the interest rate swap (IRS) rate or the overnight indexed swap (OIS) rate and the maturity-matched constant maturity Treasury (CMT) rate. Spreads for the 6-month maturity are based on LIBOR. Spreads for maturities of 5 years and higher are based on IRS rates. We overlay the (negative of the) USD maturity-matched U.S. CDS premium, i.e., the CDS premium multiplied by (-1). The data frequency is weekly based on Wednesday rates. All spreads are expressed in percent. The sample period is 8 May 2002 to 26 September 2018. Source: Bloomberg (OIS, IRS, LIBOR), FRED (CMT), Markit (CDS).

Figure 3: Macro factors



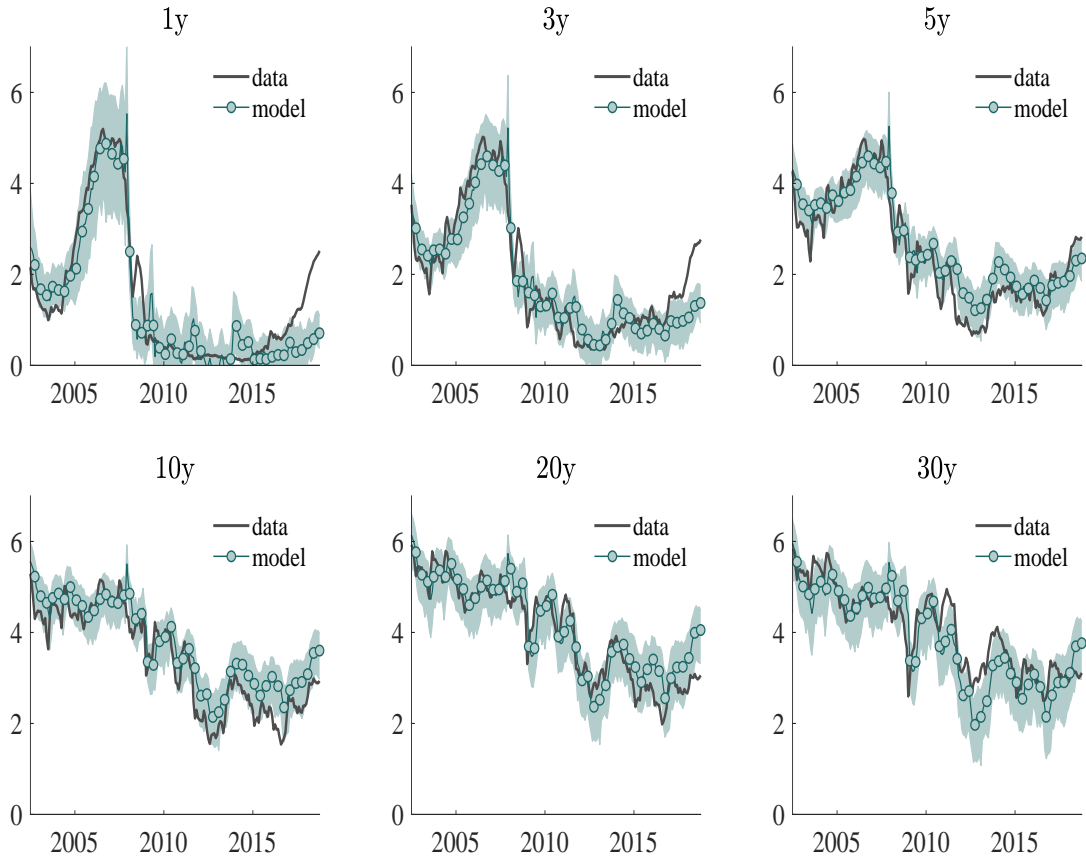
Notes: In these figures, we plot the dynamics of the macroeconomic state variables in our model: log consumption growth (z_1), output growth (z_2), government expenditures to output ratio (z_3), and inflation (z_4), as well as consumption volatility (v_1) and inflation volatility (v_2). All variables are annualized and represented in percentage terms, except for the government expenditures to output ratio, which is represented in logs. The sample period is 1982 to 2018. The data frequency is quarterly for z_1 , z_2 , and z_3 , and monthly for z_4 . Source: Federal Reserve Bank of St. Louis H.15 Report.

Figure 4: **Finance factors**



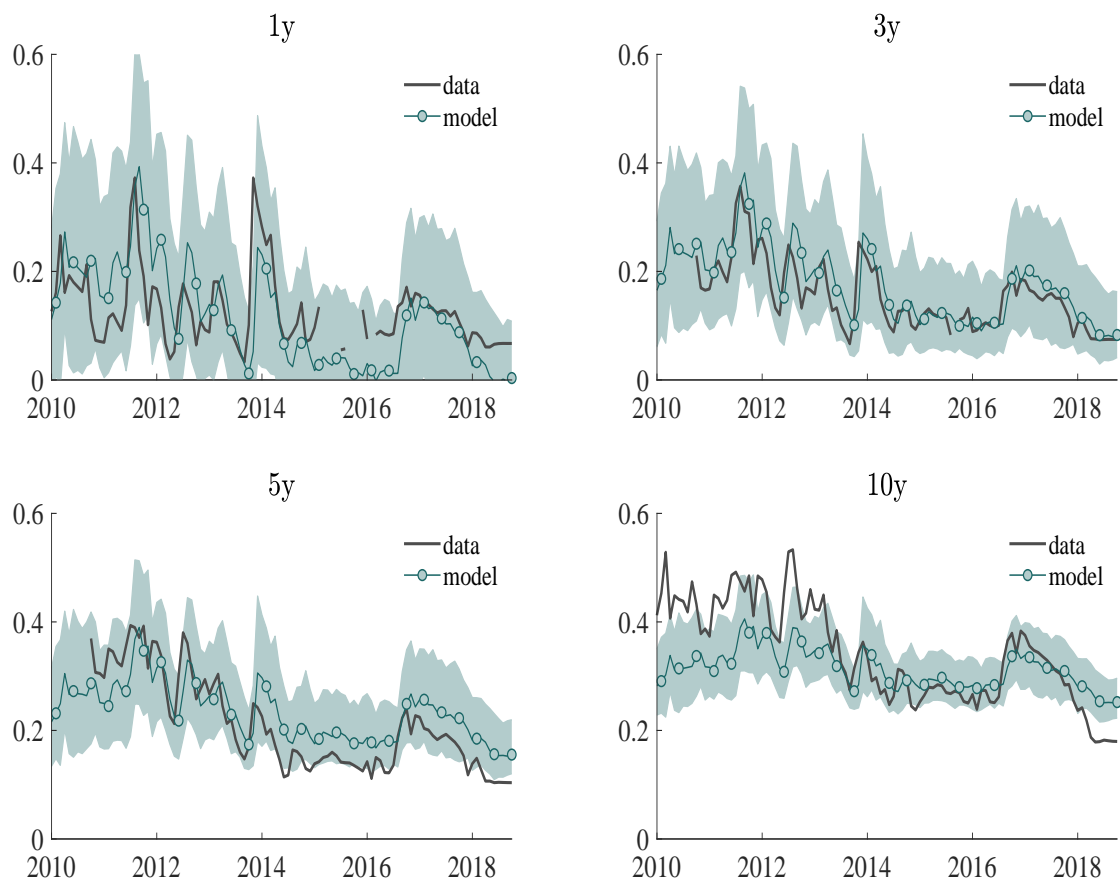
Notes: We plot the spread factors: s_1 is the convenience yield, defined as the one-month OIS-Treasury spread; s_2 captures the interbank credit and funding liquidity risk, defined as the one-month LIBOR-OIS spread; s_3 is latent and captures the opportunity cost of collateral. The sample period is May 2002 to September 2018. All variables are plotted at a monthly frequency, and are expressed in percent. Source: Bloomberg (OIS, LIBOR), FRED (CMT).

Figure 5: Model-implied risky zero-coupon yields and nominal Treasury yields



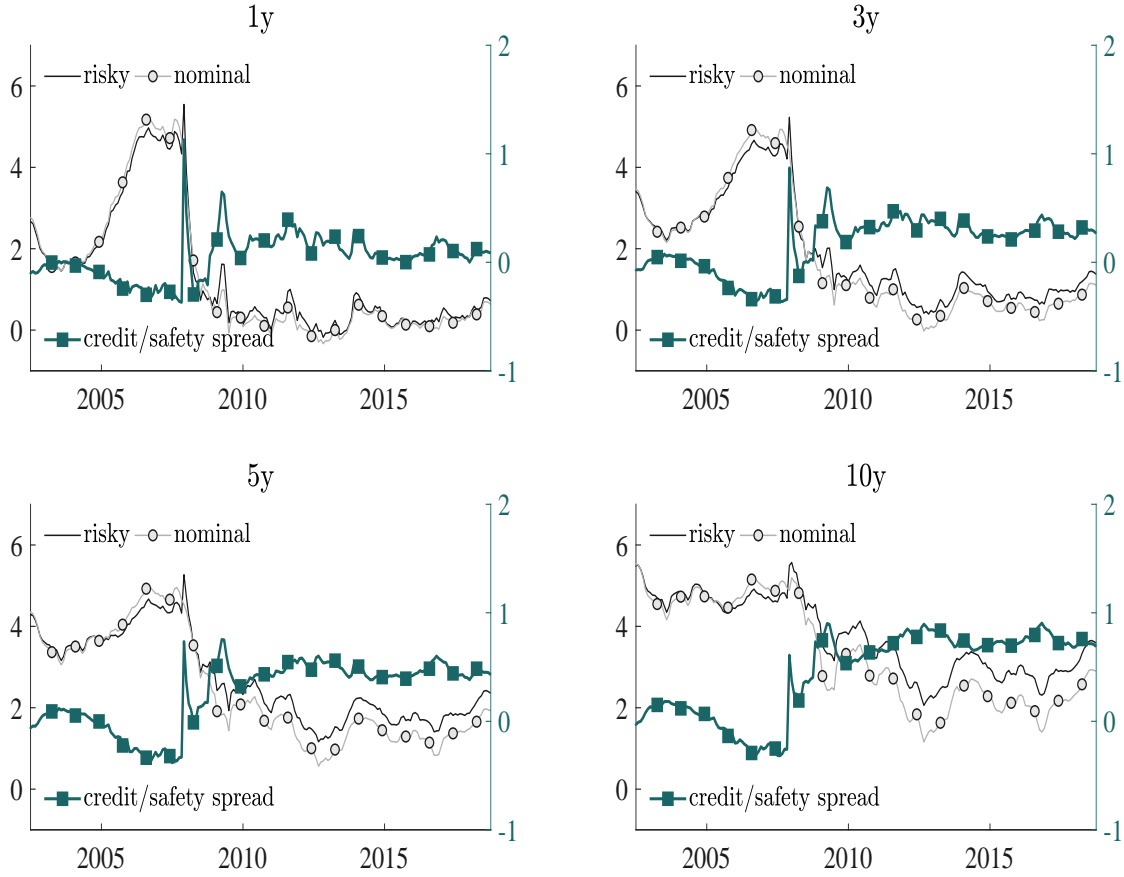
Notes: In these figures, we plot the model-implied risky zero-coupon bond yields (green line with bullets) together with their 90% confidence bands, and compare them with the observed nominal zero-coupon Treasury yields (solid black line) from [Gurkaynak, Sack, and Wright \(2007\)](#). We plot observed and model-implied yields for maturities of 1y, 3y, 5y, 10y, 20y, and 30y. All variables are plotted at a monthly frequency and are expressed in annualized percentage terms. The sample period is May 2002 to September 2018.

Figure 6: Model-implied and actual CDS premiums



Notes: In these figures, we plot the model-implied (green line with bullets), their 90% confidence bands, and observed (solid black line) CDS premiums. We plot observed and model-implied CDS premiums for maturities of 1y, 3y, 5y, and 10y. All variables are plotted at a monthly frequency, and are expressed in annualized percentage terms. The sample period is May 2002 to September 2018. Source: Markit.

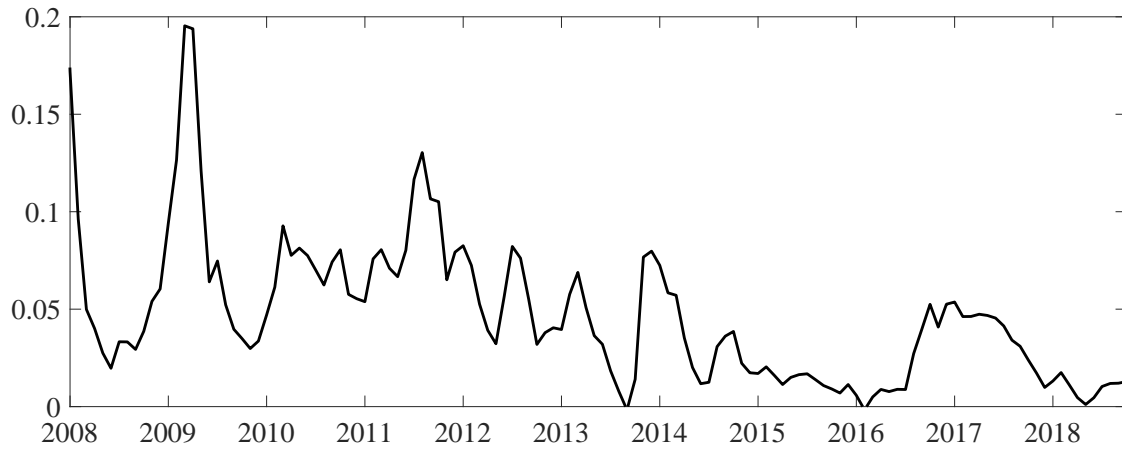
Figure 7: Model-implied zero-coupon yields



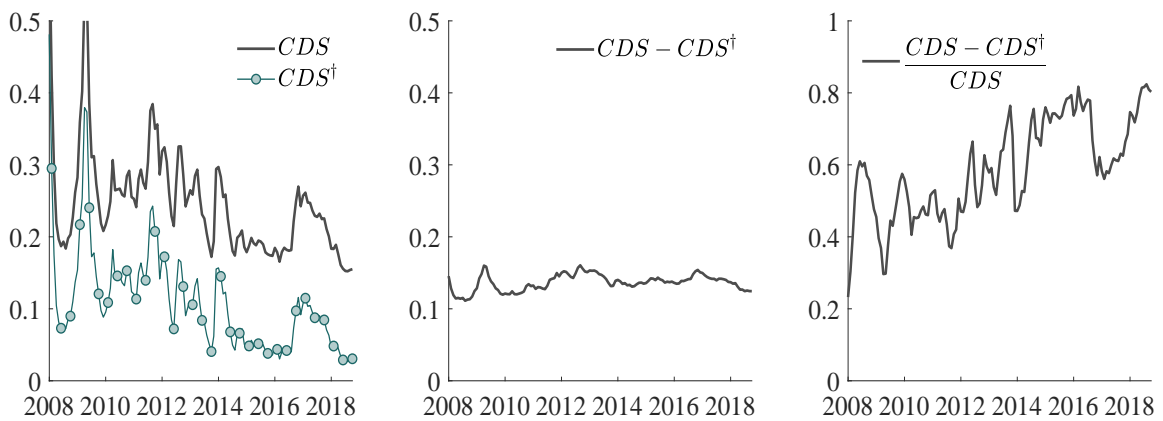
Notes: In these figures, we plot the model-implied zero-coupon yields for nominal bonds (gray line with bullets), risky Treasury bonds (solid black line), and the “credit/safety” spread (green line with squares). We plot model-implied zero-coupon yields for maturities of 1y, 3y, 5y, and 10y. All variables are plotted at a monthly frequency, and are expressed in annualized percentage terms. The sample period is May 2002 to September 2018. Source: Authors’ computations.

Figure 8: **Default intensity and credit risk premium**

(A) Default intensity

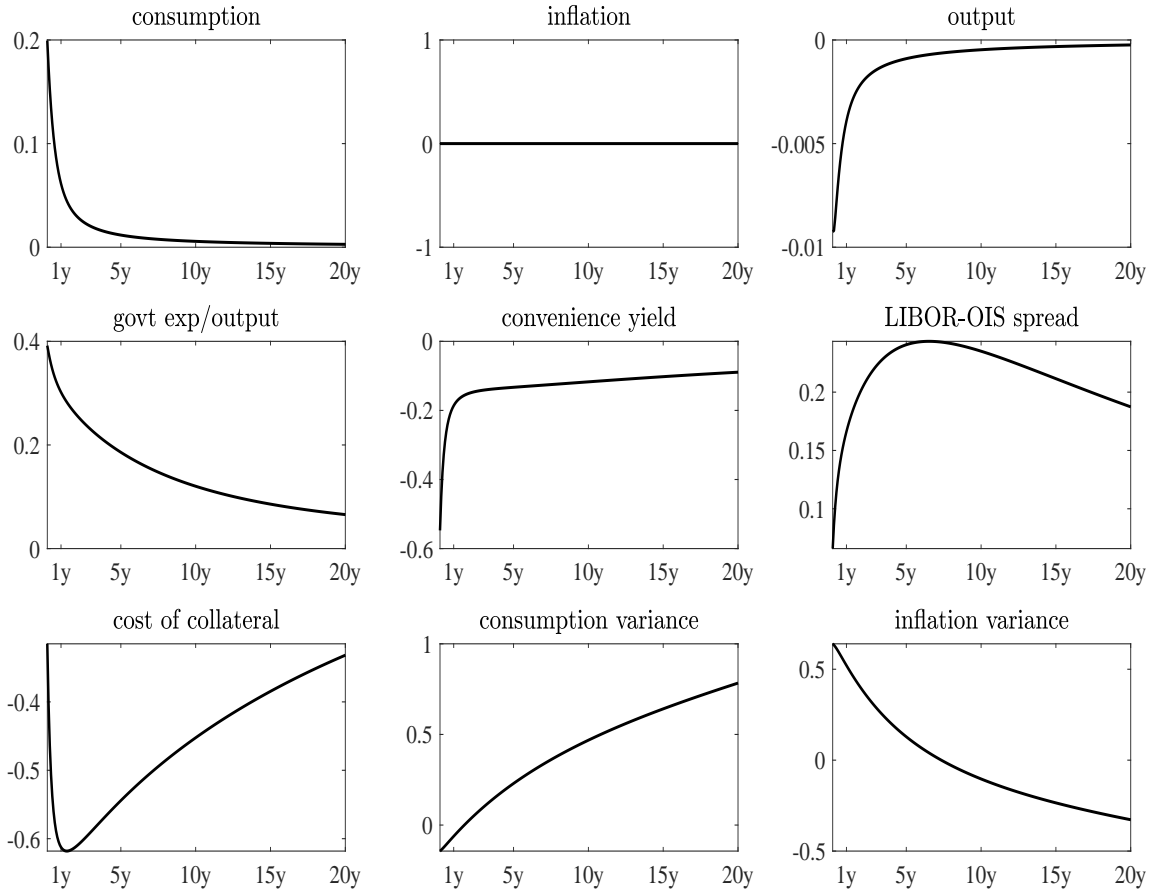


(B) Model-implied CDS premiums under the risk-neutral and physical measures



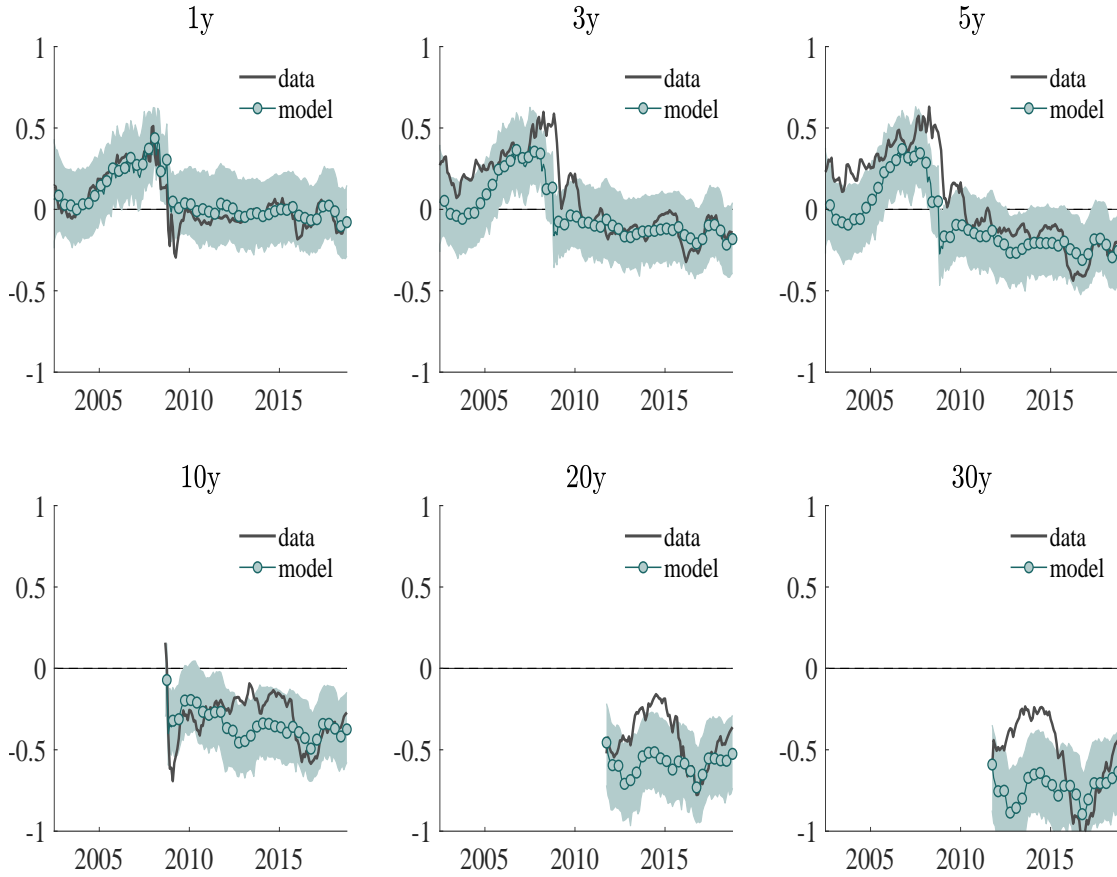
Notes: In Panel (A), we plot the model-implied physical default intensity for U.S. credit risk from January 2008 to September 2018. In Panel (B), we plot the model implied CDS premiums for maturity 5 years under the risk-neutral CDS and physical CDS^\dagger measures from January 2008 to September 2018. The y -axis is expressed in annualized percentage terms. Source: authors' computations.

Figure 9: Credit/safety spread loadings: Risky - nominal rate



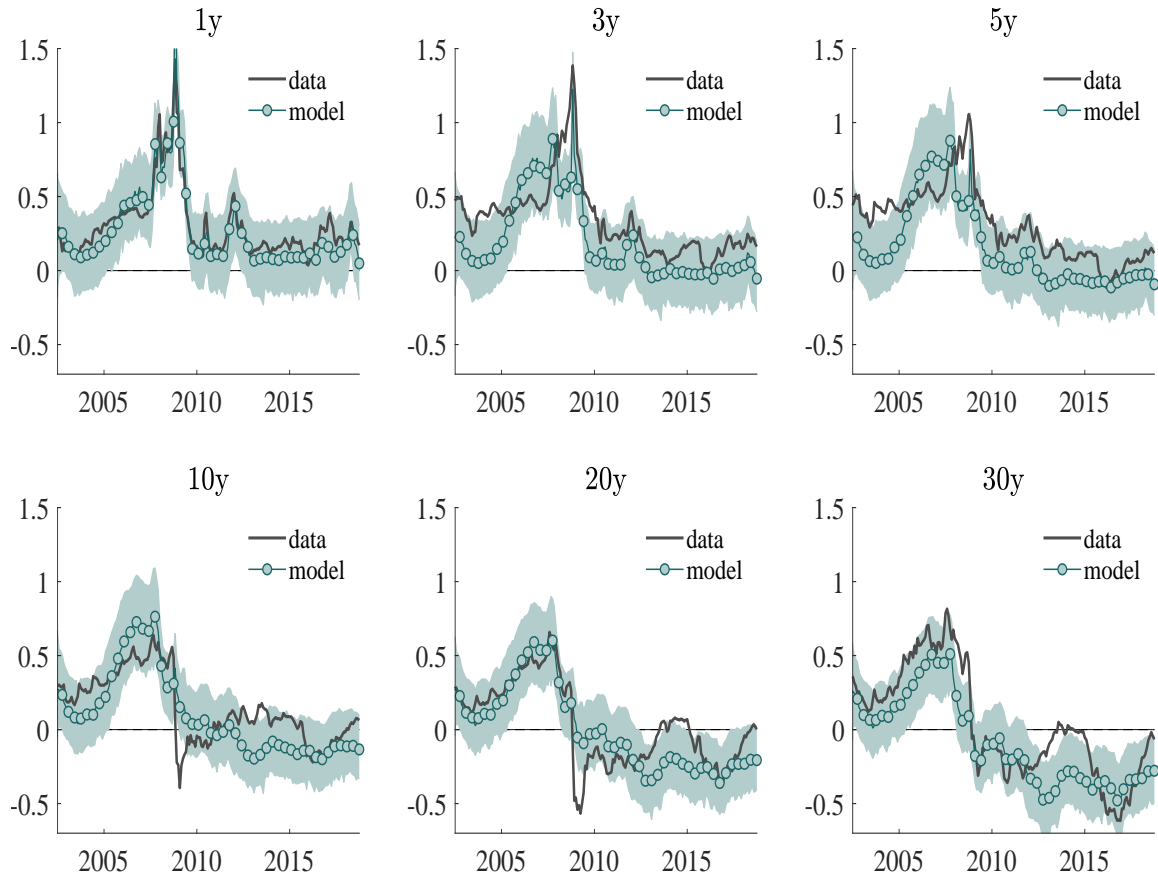
Notes: In these figures, we examine the sensitivity of model-implied risky zero-coupon Treasury yields (which incorporate the convenience yield) to all state variables over and above the sensitivity of model-implied nominal Treasury yields (which exclude the convenience yield). Specifically, we plot the difference of the sensitivity loadings with respect to the state variables as a function of the maturity horizon, up to 20 years. The state variables are log consumption growth (z_1), inflation (z_2), output growth (z_3), government expenditures to output ratio (z_4), the convenience yield (s_1), the LIBOR-OIS spread (s_2), the opportunity cost of collateral (s_3), consumption volatility (v_1), and inflation volatility (v_2). Source: Authors' computations.

Figure 10: Model-implied spread between OIS and CMT



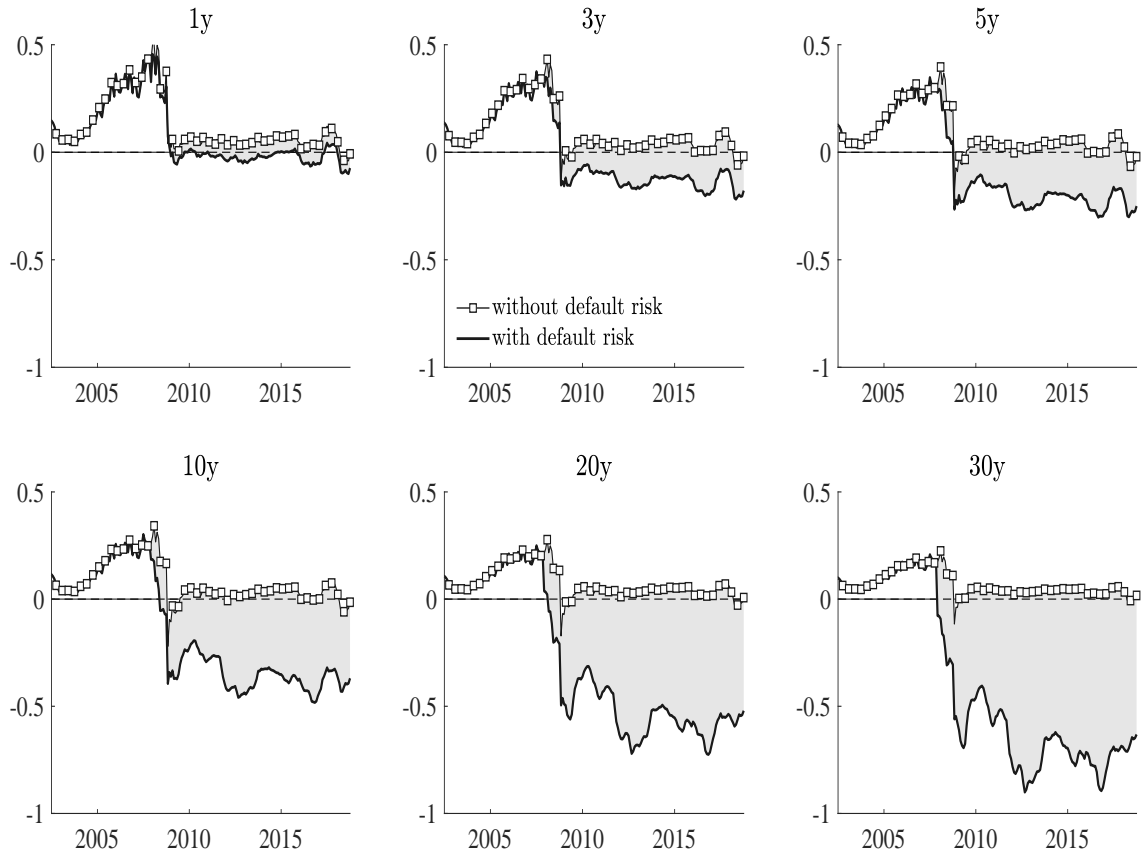
Notes: In these figures, we plot the model-implied (green line with bullets), their 90% confidence bands, and observed (solid black line) OIS-Treasury spreads, where we use the constant maturity Treasury par rates. We plot observed and model-implied OIS-CMT spreads for maturities of 1y, 3y, 5y, 10y, 20y, 30y. All variables are plotted at a monthly frequency and are expressed in annualized percentage terms. The sample period is May 2002 to September 2018. Source: Bloomberg (OIS) and FRED (CMT).

Figure 11: Model-implied spread between IRS and CMT



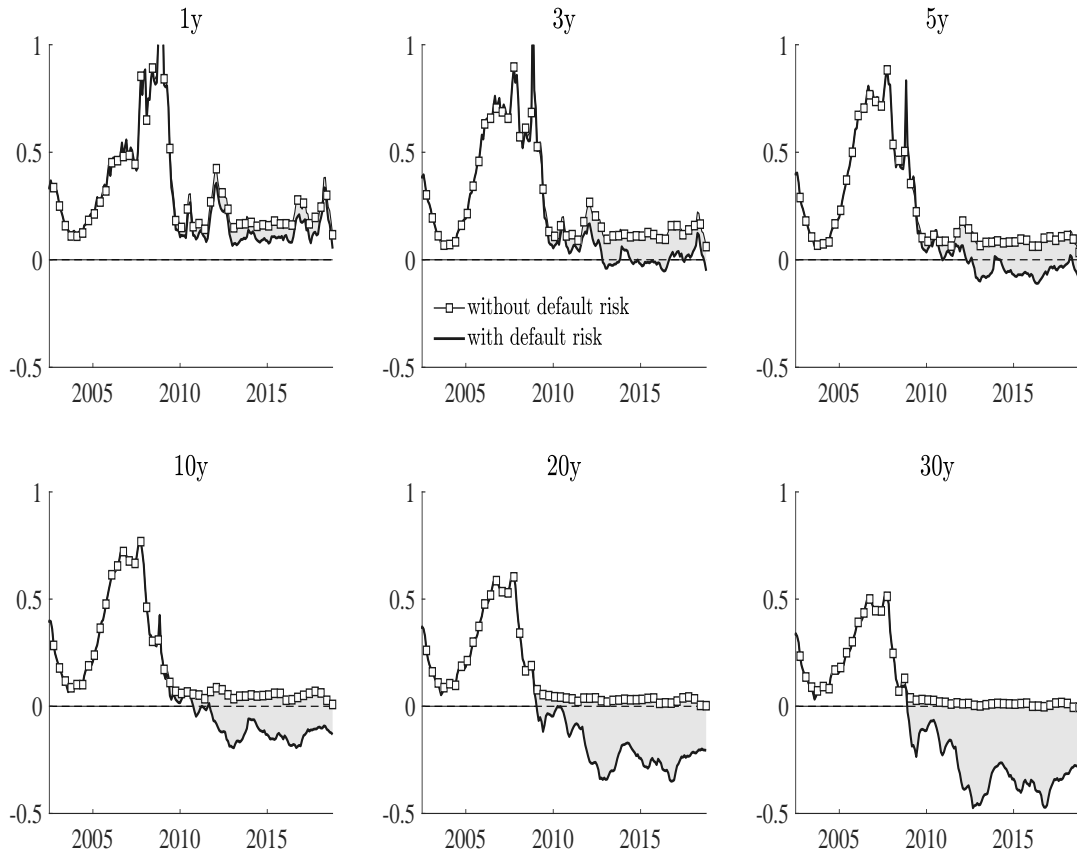
Notes: In these figures, we plot the model-implied (green line with bullets), their 90% confidence bands, and observed (solid black line) IRS-Treasury spreads, where we use the constant maturity Treasury par rates. We plot observed and model-implied IRS-CMT spreads for maturities of 1y, 3y, 5y, 10y, 20y, and 30y. All variables are plotted at a monthly frequency, and are expressed in annualized percentage terms. The sample period is May 2002 to September 2018. Source: Bloomberg (IRS) and FRED (CMT).

Figure 12: Model-implied spread between OIS and CMT: Counterfactual



Notes: In these figures, we compare the fitted OIS-CMT spreads (black line) with their counterfactual values when U.S. credit risk is shut down (gray boxes). All rates are expressed on a par basis. We plot the OIS-CMT spreads for maturities of 1y, 3y, 5y, 10y, 20y, 30y. All variables are plotted at a monthly frequency, and are expressed in annualized percentage terms. The sample period is May 2002 to September 2018. Source: Authors' computations.

Figure 13: Model-implied spread between IRS and CMT: Counterfactual



Notes: In these figures, we compare the fitted IRS-CMT spreads (black line) with their counterfactual values when U.S. credit risk is shut down (gray boxes). All rates are expressed on a par basis. We plot the IRS-CMT spreads for maturities of 1y, 3y, 5y, 10y, 20y, 30y. All variables are plotted at a monthly frequency, and are expressed in annualized percentage terms. The sample period is May 2002 to September 2018. Source: Authors' computations.

Table 1: Literature on negative IRS-Treasury and OIS-Treasury spreads

Study	Focus		Type		Explanations			
	IRS-Treasury	OIS-Treasury	Empirics	Theory	Funding costs	Hedging demand	Leverage ratios	Convenience yield
Lou (2009)	✓		✓		✓			
Klingler and Sundaresan (2018)	✓		✓	✓		✓		
Boyarchenko, Gupta, Steele, and Yen (2018)	✓		✓				✓	
Klingler and Sundaresan (2019)		✓	✓					✓
Jermann (2019)	✓			✓		✓		
The present study	✓	✓	✓	✓				✓

Notes. This table summarizes the main studies explaining negative OIS-Treasury or IRS-Treasury swap spreads. We describe the focus of the paper (IRS-Treasury or OIS-Treasury), the type of study (empirical or theoretical), and the main explanation proposed by each study.

Table 2: **Descriptive statistics of USD interest and CDS rates.** In this table, we report summary statistics (mean, sd, p1, p50, p99) and the number of observations (Obs.) for the term structure of various U.S. interest and credit default swap (CDS) rates with maturities ranging between 3 months and 30 years. We use weekly observations based on Wednesday rates. Statistics are reported for USD denominated overnight index swap (OIS) rates (Panel A), USD denominated interest rate swap (IRS) rates, where maturities below one year correspond to London interbank offered (LIBOR) rates (Panel B), USD denominated constant maturity Treasury yields (Panel C), USD denominated zero coupon Treasury (ZCT) yields from [Gurkaynak, Sack, and Wright \(2007\)](#) (Panel D), USD denominated CDS spreads (Panel E), and EUR denominated CDS spreads (Panel F). All rates are expressed in percentage terms. The sample period is May 8, 2002 through September 26, 2018. Source: Bloomberg (OIS, IRS), [Gurkaynak, Sack, and Wright \(2007\)](#) (ZCT), Federal Reserve Bank of St. Louis (CMT, LIBOR), Markit (CDS).

Maturity	3m	6m	1y	3y	5y	7y	10y	20y	30y	3m	6m	1y	3y	5y	7y	10y	20y	30y	
Panel A: USD OIS Rates																			
Mean	1.40	1.44	1.54	2.07	2.54	1.67	2.31	2.39	2.48	1.66	1.83	1.81	2.33	2.79	3.13	3.46	3.89	3.97	
SD	1.66	1.67	1.67	1.53	1.43	0.49	0.71	0.49	0.51	1.67	1.62	1.64	1.48	1.37	1.30	1.25	1.22	1.21	
P1	0.08	0.09	0.09	0.22	0.53	0.82	1.00	1.24	1.30	0.23	0.32	0.26	0.46	0.79	1.19	1.42	1.70	1.78	
P50	0.68	0.73	0.88	1.57	2.24	1.76	2.22	2.33	2.44	1.12	1.24	1.26	1.87	2.54	2.91	3.23	3.80	3.93	
P99	5.32	5.37	5.41	5.39	5.45	2.68	4.04	3.45	3.59	5.50	5.52	5.51	5.48	5.55	5.61	5.70	5.91	5.94	
Obs.	856	856	856	856	856	333	530	366	366	853	853	856	856	856	856	856	856	856	
Panel B: USD LIBOR/IRS Rates																			
Panel C: Constant Maturity Treasury Rates																			
Mean	1.25	1.37	1.49	1.99	2.48	2.87	3.23	3.81	3.95	-	-	1.50	1.73	1.99	2.50	2.93	4.04	4.07	
SD	1.56	1.60	1.55	1.37	1.22	1.11	1.04	1.06	0.93	-	-	1.53	1.44	1.34	1.19	1.12	1.06	0.91	
P1	0.01	0.04	0.10	0.32	0.64	1.04	1.54	1.90	2.29	-	-	0.11	0.22	0.34	0.67	1.07	2.05	2.49	
P50	0.52	0.66	0.89	1.52	2.23	2.79	3.12	3.96	4.13	-	-	0.90	1.22	1.53	2.23	2.83	4.36	4.18	
P99	5.12	5.17	5.09	5.02	5.03	5.06	5.14	5.55	5.58	-	-	5.04	5.00	4.95	4.95	5.03	5.86	5.82	
Obs.	856	856	856	856	856	856	856	856	856	-	-	856	856	856	856	856	856	856	
Panel D: Zero-coupon Rates																			
Panel E: USD CDS Premiums																			
Mean	-	0.11	0.13	0.14	0.18	0.24	0.27	0.36	0.37	-	0.13	0.14	0.16	0.22	0.29	0.32	0.43	0.44	
SD	-	0.08	0.11	0.12	0.16	0.16	0.18	0.15	0.16	-	0.10	0.12	0.14	0.18	0.18	0.21	0.18	0.19	
P1	-	0.01	0.01	0.01	0.01	0.02	0.02	0.03	0.03	-	0.01	0.01	0.01	0.01	0.02	0.02	0.03	0.03	
P50	-	0.09	0.10	0.13	0.15	0.24	0.28	0.37	0.38	-	0.11	0.12	0.14	0.19	0.27	0.33	0.41	0.42	
P99	-	0.38	0.61	0.67	0.66	0.72	0.74	0.80	0.85	-	0.50	0.63	0.64	0.66	0.72	0.74	0.80	0.85	
Obs.	-	502	538	681	747	677	721	527	513	-	575	608	720	755	685	729	557	572	

Table 3: Link between OIS-Treasury spreads and CDS premiums.

In this table, we report the results from a regression of monthly changes in OIS-Treasury spreads (ΔSS) on monthly changes of the maturity-matched U.S. CDS premium (USD, CR restructuring clause). The 3-month OIS-Treasury spread is matched with the 6-month CDS premium. Maturities for OIS-Treasury spreads are 3/6 months, and 1/2/3/5/7/10/20/30 years to maturity. The sample period is January 2010 to September 2018. All specifications include maturity and/or week fixed effects. In row *Mat.*, we indicate maturity restrictions; in row *YEAR*, we indicate sample period restrictions. Standard errors are heteroscedasticity-robust (*RO*), clustered by time (*CL*) or adjusted for cross-sectional dependence and serial dependence up to 3 weeks using Driscoll-Kraay standard errors. We report the within R^2 of the regression. Control variables include the CBOE VIX index, the exchange rate of the USD against a basket of a broad group of major U.S. trading partners, the West Texas Intermediate oil price index, the economic policy uncertainty index, the high-yield and investment-grade bond indices, inflation, the TED spread, the 3-month LIBOR-OIS spread, the 3-month T-bill rate, the U.S. Treasury total cash balances, and CDS depth defined as the number of dealer quotes used to compute the mid-market spread. ***, **, and * denote significance at the 1%, 5%, and 10%, respectively. CDS data is from Markit; OIS data is from Bloomberg; constant-maturity Treasury rates are from the Federal Reserve Bank of St. Louis H.15 report.

VARIABLES	(1) ΔSS	(2) ΔSS	(3) ΔSS	(4) ΔSS	(5) ΔSS	(6) ΔSS	(7) ΔSS	(8) ΔSS	(9) ΔSS	(10) ΔSS	(11) ΔSS	(12) ΔSS
ΔCDS	-0.07*** (0.02)	-0.08** (0.04)	-0.07*** (0.02)	-0.13* (0.08)	-0.07*** (0.02)	-0.08*** (0.02)	-0.06*** (0.02)	-0.13* (0.08)	-0.07*** (0.02)	-0.07*** (0.02)	-0.07*** (0.02)	-0.23*** (0.08)
ΔSS_{t-1}					-0.09** (0.04)	-0.27*** (0.04)	-0.44*** (0.05)	-0.09* (0.05)	-0.16*** (0.04)	-0.16*** (0.05)	-0.16*** (0.05)	-0.13** (0.06)
ΔVIX									0.00 (0.00)	0.00 (0.00)	0.00 (0.00)	-0.00 (0.00)
ΔFX									0.00** (0.00)	0.00 (0.00)	0.00 (0.00)	0.00 (0.00)
ΔWTI									-0.00 (0.00)	-0.00 (0.00)	-0.00 (0.00)	-0.00 (0.00)
ΔEPU									-0.00 (0.00)	-0.00 (0.00)	-0.00 (0.00)	0.00 (0.00)
ΔIG									-0.06*** (0.02)	-0.06** (0.03)	-0.06** (0.03)	-0.06 (0.04)
ΔHY									-0.01 (0.01)	-0.01 (0.02)	-0.01 (0.02)	-0.02 (0.02)
$\Delta \Pi$									-0.06*** (0.01)	-0.06*** (0.02)	-0.06** (0.02)	-0.02 (0.05)
ΔTED									0.41*** (0.06)	0.41*** (0.10)	0.41*** (0.09)	0.54*** (0.08)
$\Delta LIBOR - OIS_{3m}$									-0.36*** (0.06)	-0.36*** (0.10)	-0.36*** (0.09)	-0.59*** (0.09)
$\Delta TB3$									0.09 (0.06)	0.09 (0.10)	0.09 (0.08)	0.17** (0.07)
ΔCB									0.00 (0.00)	0.00 (0.00)	0.00 (0.00)	0.00 (0.00)
ΔLIQ									0.00** (0.00)	0.00 (0.00)	0.00 (0.00)	0.01*** (0.01)
OBS.	591	347	938	411	935	935	923	411	935	935	935	411
MATURITY FE	YES	YES	YES	YES	YES	YES	NO	YES	YES	YES	YES	YES
QUARTER FE	NO	NO	NO	NO	NO	YES	NO	NO	YES	YES	YES	YES
MATURITY-QUARTER FE	NO	NO	NO	NO	NO	NO	YES	NO	NO	NO	NO	NO
CLUSTER TIME	NO	YES	NO	NO								
SE	RO	CL	DK-3	RO								
MAT	<=5	>=7	ALL	ALL	ALL							
YEAR	>2009	>2009	>2009	>2014	>2009	>2009	>2009	>2014	>2009	>2009	>2009	>2014
CONTROLS	NO	YES	YES	YES	YES							
WITHIN R ²	0.02	0.01	0.01	0.01	0.02	0.09	0.20	0.02	0.24	0.24	0.34	0.32

Table 4: Cash flows from swap-spread trading strategy: Assuming Treasury cannot default

Strategy	Cash flows at time		
	0	t	T
Long Treasury bond	-1	CMT	$CMT + 1$
Repo financing cash flows	1	$-r_{t-1}$	$-r_{T-1} - 1$
Pay fixed on swap	-	$-CMS$	$-CMS$
Receive floating on swap	-	f_{t-1}	f_{T-1}
Total	0	$S_{t-1} - SS$	$S_{T-1} - SS$

Notes: This table illustrates the cash flows generated by a stylized form of a swap-spread trading strategy. CMS and CMT denote the fixed swap and Treasury coupon rates. f_t denotes the EFFR rate compounded from the beginning of month t to the end of month $t + 2$, or LIBOR at time t , and r_t denotes the three-month repo rate determined at time t . For expositional simplicity, this table assumes that floating and fixed payments are paid each period. SS denotes the swap spread and equals $CMS - CMT$. The term S_t denotes the difference $f_t - r_t$.

Table 5: Cash flows from swap-spread trading strategy: Assuming Treasury can default

Strategy	Cash flows at time			
	0	t	τ	T
Long Treasury bond	-1	CMT	-	$CMT + 1$
Repo financing cash flows	1	$-r_{t-1}$	-	$-r_{T-1} - 1$
Pay fixed on swap	-	$-CMS$	-	$-CMS$
Receive floating on swap	-	f_{t-1}	-	f_{T-1}
Pay CDS premia	-	$-CDS$	-	$-CDS$
Sell Treasury bond at default	-	-	$1 - L$	-
Receive CDS payoff at default	-	-	L	-
Payoff repo loan at default	-	-	-1	-
Unwind swap at default	-	-	U_τ	-
Total	0	$S_{t-1} - SS - CDS$	U_τ	$S_{T-1} - SS - CDS$

Notes: This table illustrates the cash flows generated by a stylized form of a swap-spread trading strategy. CMS and CMT denote the fixed swap and Treasury coupon rates. f_t denotes the EFFR rate compounded from the beginning of month t to the end of month $t + 2$, or LIBOR at time t , and r_t denotes the three-month repo rate determined at time t . For expositional simplicity, this table assumes that floating and fixed payments are paid each period. SS denotes the swap spread and equals $CMS - CMT$. The term S_t denotes the difference $f_t - r_t$. Upon random default τ before maturity T , the bond is worth $1 - L$, but the CDS hedge pays L and terminates. The swap contract is unwound at the current market value of U_τ .

Table 6: **Parameter estimates: Macroeconomic factors**

$$\begin{aligned}
 z_{t+1} &= (\Delta c_{t+1}, d_{t+1}, g_{t+1}, \pi_{t+1})^\top \\
 z_{t+1} &= \mu_z + \Phi_z z_t + \Phi_{zv} v_t + \Sigma_z V_{z,t}^{1/2} \varepsilon_{z,t+1} + \Theta_z \Sigma_z V_{z,t-1}^{1/2} \varepsilon_{z,t} \\
 &= \begin{bmatrix} 0.0000 \\ [-0.0003, 0.0004] \\ -0.0019 \\ [-0.0032, -0.0011] \\ 0.0181 \\ [0.0134, 0.0197] \\ -0.0007 \\ [-0.0009, -0.0003] \end{bmatrix} + \begin{bmatrix} 0.78 & -0.05 & -0.03 & 0 \\ [0.69, 0.84] & [-0.07, -0.04] & [-0.04, 0.01] & \\ 0.39 & 0.21 & 0.17 & 0 \\ [0.29, 0.43] & [0.16, 0.28] & [0.14, 0.24] & \\ 0.00 & -0.00 & 0.98 & 0 \\ [-0.02, 0.01] & [-0.01, 0.00] & [0.97, 0.99] & \\ 0.00 & 0.01 & -0.12 & 0.71 \\ [-0.07, 0.04] & [-0.00, 0.04] & [-0.15, -0.08] & [0.62, 0.76] \end{bmatrix} z_t \\
 &+ 10^{-4} \begin{bmatrix} 0 & 0 \\ 0 & 0 \\ 0 & 0 \\ 5.45 & -4.95 \\ [2.92, 6.92] & [-6.21, -1.14] \end{bmatrix} v_t + 10^{-3} \text{Diag} \begin{bmatrix} 2.84 + 2.80 v_{1,t} + 5.30 v_{2,t} \\ [2.58, 3.66] & [1.24, 3.40] & [3.01, 7.08] \\ 2.38 + 0.11 v_{1,t} + 1.39 v_{2,t} \\ [1.53, 2.64] & [0.07, 0.14] & [1.00, 1.97] \\ 0.13 + 1.79 v_{1,t} + 4.92 v_{2,t} \\ [0.10, 0.25] & [1.38, 2.34] & [3.12, 6.19] \\ 0.12 + 0.40 v_{1,t} + 0.10 v_{2,t} \\ [0.09, 0.22] & [0.32, 0.44] & [0.05, 0.90] \end{bmatrix}^{1/2} \varepsilon_{z,t+1} \\
 &+ \begin{bmatrix} -1.23 & 0.68 & -0.80 & 0 \\ [-1.44, -0.94] & [0.62, 0.75] & [-0.92, -0.75] & \\ 0.44 & 0.75 & -0.06 & 0 \\ [0.36, 0.62] & [0.43, 1.07] & [-0.17, 0.00] & \\ -0.01 & -0.01 & -0.68 & 0 \\ [-0.09, 0.00] & [-0.03, 0.04] & [-0.73, -0.54] & \\ 0.05 & 0.01 & 0.17 & -0.06 \\ [-0.02, 0.10] & [-0.01, 0.03] & [0.11, 0.21] & [-0.09, -0.02] \end{bmatrix} V_{z,t-1}^{1/2} \varepsilon_{z,t}
 \end{aligned}$$

$$\begin{aligned}
 v_{1,t+1} &\sim \text{ARG}(\nu_1, \phi_1, \frac{1-\phi_1}{\nu_1}) = \text{ARG}(\underset{[1.04, 5.99]}{2.43}, \underset{[0.951, 0.992]}{0.908}, 0.0377) \\
 v_{2,t+1} &\sim \text{ARG}(\nu_2, \phi_2, \frac{1-\phi_2}{\nu_2}) = \text{ARG}(\underset{[0.75, 5.43]}{2.43}, \underset{[0.985, 0.999]}{0.998}, 0.0008)
 \end{aligned}$$

Notes: We provide the estimates for the dynamics of the macroeconomic fundamentals z_t . We set Σ_z to be an identity matrix for identification reasons.

Table 7: **Parameter estimates: Finance factors, default intensity, preferences**

$$\begin{aligned}
 s_{t+1} &= \mu_s + \Phi_{sv}v_t + \Phi_s s_t + \Sigma_s \varepsilon_{s,t+1} \\
 &= 10^{-4} \begin{bmatrix} -0.20 & -0.04 \\ [-0.33,0.09] & [-0.08,0.06] \\ -0.00 & 0.00 \\ [-0.00,0.00] & [0.00,0.00] \\ 0.20 & -0.17 \\ [0.13,0.28] & [-0.23,-0.08] \end{bmatrix} v_t + \begin{bmatrix} 0.61 & -0.05 & 0.19 \\ [0.43,0.68] & [-0.08,0.04] & [0.04,0.22] \\ -0.20 & 0.94 & 0.09 \\ [-0.31,0.03] & [0.74,0.98] & [-0.10,0.23] \\ 0.04 & -0.02 & 0.97 \\ [0.03,0.19] & [-0.04,0.10] & [0.89,0.99] \end{bmatrix} s_t \\
 &\quad + 10^{-4} \begin{bmatrix} 0.17 & 0 & 0 \\ [0.12,0.24] & & \\ 0 & 3.17 & 0 \\ & [2.32,4.11] & \\ 0 & 0 & 0.36 \\ & & [0.13,0.73] \end{bmatrix} \varepsilon_{s,t+1} \\
 h_t &= h + h_c \Delta c_t + h_d d_t + h_g g_t + h_{v_1} v_{1,t} + h_{v_2} v_{2,t} \\
 &= \frac{0.0009}{[0.0003,0.0011]} + \frac{0.13}{[0.01,0.15]} \Delta c_t + \frac{0.00}{[-0.01,0.02]} d_t + \frac{0.88}{[0.47,1.11]} g_t + \frac{0.0024}{[0.0015,0.0033]} v_{1,t} + \frac{0.0001}{[0.0000,0.0003]} v_{2,t} \\
 U_t &= [(1 - \beta)C_t^\rho + \beta\mu_t(U_{t+1})^\rho]^{1/\rho}, \quad \mu(U_{t+1}) = E_t(U_{t+1}^\alpha)^{1/\alpha} \\
 \beta &= \frac{0.9984}{[0.9981,0.9990]}, \quad \alpha = \frac{-3.91}{[-4.90,-2.12]}, \quad \rho = \frac{0.25}{[0.22,0.45]} \\
 L &= 0.3
 \end{aligned}$$

Notes: We provide the estimates for the dynamics of the financial variables s_t and the default intensity h_t . We set μ_s, Φ_{sv} to zero for parsimony. Risk aversion is $1 - \alpha$ and intertemporal elasticity of substitution is $(1 - \rho)^{-1}$. We calibrate the value of L .

Table 8: Model-implied link between OIS-Treasury spreads and CDS premiums.

In this table, we report the model-implied results from a regression of monthly changes in OIS-Treasury spreads (ΔSS) on monthly changes of the maturity-matched U.S. CDS premiums denominated in USD. Maturities for OIS-Treasury spreads are 1, 3, 5, 7, 10, 20, and 30 years to maturity. The sample period is January 2010 to September 2018. As in the data, results are based on an unbalanced sample. All specifications include maturity fixed effects. In row *Mat.*, we indicate maturity restrictions; in row *YEAR*, we indicate sample period restrictions. Standard errors are heteroscedasticity-robust. We report the within R^2 of the regression. ***, **, and * denote significance at the 1%, 5%, and 10%, respectively. Source: Authors' computations.

VARIABLES	(1) ΔSS	(2) ΔSS	(3) ΔSS	(4) ΔSS	(5) ΔSS	(8) ΔSS
ΔCDS	-0.02* (0.01)	-0.37*** (0.07)	-0.06*** (0.01)	-0.16*** (0.06)	-0.04*** (0.01)	-0.11* (0.06)
ΔSS_{t-1}					0.36*** (0.04)	0.40*** (0.06)
OBS.	591	347	938	411	935	411
MATURITY FE	YES	YES	YES	YES	YES	YES
MAT	≤ 5	≥ 7	ALL	ALL	ALL	ALL
YEAR	>2009	>2009	>2009	>2014	>2009	>2014
WITHIN R^2	0.00	0.09	0.01	0.01	0.16	0.16

A Derivation of the real pricing kernel

Since utility is defined by a constant elasticity of substitution recursion and the certainty equivalent is homogeneous of degree one, we can scale utility and take logs:

$$\log(U_t/C_t) \equiv u_t = \rho^{-1} \log \left[(1 - \beta) + \beta \mu_t \left(e^{\Delta c_{t+1} + u_{t+1}} \right)^\rho \right].$$

Taking a first-order Taylor approximation of u_t around the point $E[\log \mu_t] = \log \mu$, we obtain the log-linearized form

$$\begin{aligned} u_t &\approx \rho^{-1} \log \left[(1 - \beta) + \beta e^{\rho \log \mu} \right] + \rho^{-1} \frac{\beta e^{\rho \log \mu} \rho}{[(1 - \beta) + \beta e^{\rho \log \mu}]} \left[\log \mu_t \left(e^{\Delta c_{t+1} + u_{t+1}} \right) - \log \mu \right] \\ &\approx b_0 + b_1 \log \mu_t \left(e^{\Delta c_{t+1} + u_{t+1}} \right), \end{aligned}$$

where

$$\begin{aligned} b_1 &= \beta e^{\rho \log \mu} \left((1 - \beta) + \beta e^{\rho \log \mu} \right)^{-1} \\ b_0 &= \rho^{-1} \log \left[(1 - \beta) + \beta e^{\rho \log \mu} \right] - b_1 \log \mu. \end{aligned}$$

The state vector $x_t = (\Delta c_t, \pi_t, d_t, g_t, w_{c,t}, w_{\pi,t}, w_{y,t}, w_{g,t}, v_{1,t}, v_{2,t})$ describes the economy, where $\Delta c_t = \log(C_{t+1}/C_t)$ is log consumption growth, π_t is inflation, d_t is log output growth, g_t is the government expenditure to output ratio, $w_t = [w_{c,t}, w_{\pi,t}, w_{d,t}, w_{g,t}]^\top$ is the vector of moving average components, and $v_t = [v_{1,t}, v_{2,t}]^\top$ is a vector of common stochastic variance processes.

Guess that the log scaled utility is affine in the state vector x_t

$$\begin{aligned} u_t &= \log u + P_x^\top x_t = \log u + P_y^\top y_t + p_v^\top v_t \\ &= \log u + p_c \Delta c_t + p_\pi \pi_t + p_d d_t + p_g g_t + p_{v1} v_{1,t} + p_{v2} v_{2,t}, \end{aligned}$$

which implies that $P_x = [P_y^\top, p_v^\top]^\top = [p_c, p_\pi, p_d, p_g, 0, 0, 0, 0, p_{v1}, p_{v2}]^\top$.

Next compute $\log(e^{\Delta c_{t+1} + u_{t+1}})$ and $\log \mu_t(e^{\Delta c_{t+1} + u_{t+1}})$, plug terms into the log-linearized scaled utility u_t and verify. Given the initial guess, this results in a system of seven equations, which can be solved using the method of undetermined coefficients for the constant and the loadings of the log scaled utility on x_t . For the derivations, define the coordinate vectors e_i ($i = 1, 2, \dots, 8$) and e_{v_i} ($i = 1, 2$) with all elements equal to zero except element i , which is equal to one.

Step 1: Compute $\log(e^{\Delta c_{t+1} + u_{t+1}})$:

$$\begin{aligned} \log(e^{\Delta c_{t+1} + u_{t+1}}) &= \Delta c_{t+1} + u_{t+1} = e_1^\top y_{t+1} + \log u + P_y^\top y_{t+1} + p_v^\top v_{t+1} \\ &= \log u + (P_y + e_1)^\top \mu_y + (P_y + e_1)^\top \Phi_y y_t + (P_y + e_1)^\top \Phi_{y_v} v_t \\ &\quad + (P_y + e_1)^\top \Sigma_y V_{y,t}^{1/2} \varepsilon_{y,t+1} + p_v^\top v_{t+1}. \end{aligned}$$

Step 2: Compute $\log \mu_t(e^{\Delta c_{t+1} + u_{t+1}})$:

$$\begin{aligned} \log \mu_t(e^{\Delta c_{t+1} + u_{t+1}}) &= \log \left[E_t \left(e^{\Delta c_{t+1} + u_{t+1}} \right)^\alpha \right]^{1/\alpha} = \alpha^{-1} \log \left[E_t \left(e^{\alpha(\Delta c_{t+1} + u_{t+1})} \right) \right] \\ &= \log u + (P_y + e_1)^\top \mu_y + (P_y + e_1)^\top \Phi_y y_t + (P_y + e_1)^\top \Phi_{y_v} v_t \\ &\quad + \frac{\alpha}{2} (P_y + e_1)^\top \Omega_{y,t} (P_y + e_1) + \sum_{j=1}^2 \frac{-v_{v_j}}{\alpha} \log(1 - \alpha p_{v_j} c_{v_j}) + \frac{p_{v_j} \phi_{v_j}}{1 - \alpha p_{v_j} c_{v_j}} v_{j,t}, \end{aligned}$$

where $\Omega_{y,t} = \Sigma_y V_{y,t} \Sigma_y^\top$.

Step 3: Plug into u_t and verify:

$$\begin{aligned}
u_t &\approx b_0 + b_1 \log \mu_t \left(e^{\Delta c_{t+1} + u_{t+1}} \right) \\
&= b_0 + b_1 \left[\log u + (P_y + e_1)^\top \mu_y - \sum_{j=1}^2 \frac{v_{v_j}}{\alpha} \log(1 - \alpha p_{v_j} c_{v_j}) \right] + b_1 \left[(P_y + e_1)^\top \Phi_y y_t \right] \\
&+ b_1 \left[(P_y + e_1)^\top \Phi_{y_v} v_t + \frac{\alpha}{2} (P_y + e_1)^\top \Omega_{y,t} (P_y + e_1) + \sum_{j=1}^2 \frac{p_{v_j} \phi_{v_j}}{1 - \alpha p_{v_j} c_{v_j}} v_{j,t} \right].
\end{aligned}$$

Given the initial guess, this results in a system of seven equations:

$$\begin{aligned}
\log u &= b_0 + b_1 \left[\log u + (P_y + e_1)^\top \mu_y + \frac{\alpha}{2} (P_y + e_1)^\top \Sigma_y \left[\mathbf{I} \odot \left(\mathbf{1}^\top \otimes \mathbf{A} \right) \right] \Sigma_y^\top (P_y + e_1) \right. \\
&\quad \left. - \sum_{j=1}^2 \frac{v_{v_j}}{\alpha} \log(1 - \alpha p_{v_j} c_{v_j}) \right] \\
p_c &= b_1 (P_y + e_1)^\top \Phi_y e_1 \\
p_\pi &= u_1 (P_y + e_1)^\top \Phi_y e_2 \\
p_d &= b_1 (P_y + e_1)^\top \Phi_y e_3 \\
p_g &= b_1 (P_y + e_1)^\top \Phi_y e_4 \\
p_{v_1} &= b_1 \left[(P_y + e_1)^\top \Phi_{y_v} e_{v_1} + \frac{\alpha}{2} (P_y + e_1)^\top \Sigma_y \left[\mathbf{I} \odot \left(\mathbf{1}^\top \otimes \mathbf{B}_1 \right) \right] \Sigma_y^\top (P_y + e_1) + \frac{p_{v_1} \phi_{v_1}}{1 - \alpha p_{v_1} c_{v_1}} \right] \\
p_{v_2} &= b_1 \left[(P_y + e_1)^\top \Phi_{y_v} e_{v_2} + \frac{\alpha}{2} (P_y + e_1)^\top \Sigma_y \left[\mathbf{I} \odot \left(\mathbf{1}^\top \otimes \mathbf{B}_2 \right) \right] \Sigma_y^\top (P_y + e_1) + \frac{p_{v_2} \phi_{v_2}}{1 - \alpha p_{v_2} c_{v_2}} \right],
\end{aligned}$$

where \otimes defines the Kronecker product, \odot the Hadamar product, \mathbf{I} is the identity matrix, and $\mathbf{1}$ is a column vector of ones, and where we have defined the column vectors \mathbf{A} , \mathbf{B}_1 , \mathbf{B}_2 as follows:

$$\begin{aligned}
\mathbf{A} &= [a_c, a_\pi, a_d, a_g, 0, 0, 0, 0]^\top \\
\mathbf{B}_1 &= [b_{cv_1}, b_{\pi v_1}, b_{dv_1}, b_{gv_1}, 0, 0, 0, 0]^\top \\
\mathbf{B}_2 &= [b_{cv_2}, b_{\pi v_2}, b_{dv_2}, b_{gv_2}, 0, 0, 0, 0]^\top.
\end{aligned} \tag{A.1}$$

Since, the equations for p_c , p_π , p_d , and p_g are linear, their solutions are given by

$$\begin{aligned}
p_c &= -e_1^\top (b_1^2 [\Phi_z - \mathbf{I}]^{-1} \phi_c) \\
p_\pi &= -e_2^\top (b_1^2 [\Phi_z - \mathbf{I}]^{-1} \phi_c) \\
p_y &= -e_3^\top (b_1^2 [\Phi_z - \mathbf{I}]^{-1} \phi_c) \\
p_g &= -e_4^\top (b_1^2 [\Phi_z - \mathbf{I}]^{-1} \phi_c).
\end{aligned}$$

The equations for p_v are quadratic and have two roots. We choose the root such that $\lim c_j p_{v_j} = 0$ as $c_j \rightarrow 0$. We have that for $j = 1, 2$:

$$\begin{aligned}
&\underbrace{\left[b_1 \left(\phi_{v_j} - \alpha c_{v_j} \left[(P_y + e_1)^\top \Phi_{y_v} e_{v_j} + \frac{\alpha}{2} (P_y + e_1)^\top \Sigma_y \left[\mathbf{I} \odot \left(\mathbf{1}^\top \otimes \mathbf{B}_j \right) \right] \Sigma_y^\top (P_y + e_1) \right] \right) - 1 \right]}_{B_j^*} p_{v_j} \\
&+ \underbrace{\alpha c_{v_j} p_{v_j}^2}_{A_j^*} + b_1 \underbrace{\left[(P_y + e_1)^\top \Phi_{y_v} e_{v_j} + \frac{\alpha}{2} (P_y + e_1)^\top \Sigma_y \left[\mathbf{I} \odot \left(\mathbf{1}^\top \otimes \mathbf{B}_j \right) \right] \Sigma_y^\top (P_y + e_1) \right]}_{C_j^*} = 0,
\end{aligned}$$

where the roots to the quadratic equation are determined by:

$$p_{v_j} = \frac{-B_j^* + / - \sqrt{(B_j^*)^2 - 4A_j^*C_j^*}}{2A_j^*}.$$

Finally, we have that

$$\begin{aligned} \log u &= (1 - b_1)^{-1} \left[b_0 + b_1 \left((P_y + e_1)^\top \mu_y + \frac{\alpha}{2} (P_y + e_1)^\top \Sigma_y \left[\mathbf{I} \odot \left(\mathbf{1}^\top \otimes \mathbf{A} \right) \right] \Sigma_y^\top (P_y + e_1) \right. \right. \\ &\quad \left. \left. - \sum_{j=1}^2 \frac{v_{v_j}}{\alpha} \log(1 - \alpha p_{v_j} c_{v_j}) \right) \right]. \end{aligned}$$

Plugging terms into the expression for the marginal rate of substitution, we obtain the final solution to the real pricing kernel

$$\begin{aligned} \widehat{m}_{t,t+1} &= \bar{m} + (\rho - 1) e_1^\top \Phi_y y_t + (\rho - 1) e_1^\top \Phi_{yv} v_t \\ &\quad - \sum_{j=1}^2 \left[\frac{(\alpha - \rho) p_{v_j} \phi_{v_j}}{1 - \alpha p_{v_j} c_{v_j}} + \frac{\alpha}{2} (\alpha - \rho) (P_y + e_1)^\top \Sigma_y \left[\mathbf{I} \odot \left(\mathbf{1}^\top \otimes \mathbf{B}_j \right) \right] \Sigma_y^\top (P_y + e_1) \right] v_{j,t} \\ &\quad + [(\rho - 1) e_1 + (\alpha - \rho) (P_y + e_1)]^\top \Sigma_y V_{y,t}^{1/2} \varepsilon_{y,t+1} + (\alpha - \rho) p_v^\top v_{t+1}, \end{aligned} \quad (\text{A.2})$$

where

$$\begin{aligned} \bar{m} &= \log \beta + (\rho - 1) e_1^\top \mu_y + (\alpha - \rho) \sum_{j=1}^2 \frac{v_{v_j}}{\alpha} \log(1 - \alpha p_{v_j} c_{v_j}) \\ &\quad - \frac{\alpha}{2} (\alpha - \rho) (P_y + e_1)^\top \Sigma_y \left[\mathbf{I} \odot \left(\mathbf{1}^\top \otimes \mathbf{A} \right) \right] \Sigma_y^\top (P_y + e_1). \end{aligned} \quad (\text{A.3})$$

The numerical solution to the mean log certainty equivalent $E[\log \mu_t] = \log \mu$ depends on the approximated constants from the log-linearization of the scaled log utility b_0 and b_1 , which themselves depend on the mean log certainty equivalent $\log \mu$. Model consistency thus requires to solve a fixed-point equation for the mean log certainty equivalent. More specifically, using a convergence criterion of $10e^{-12}$, we solve for the fixed-point equation $\log \mu = f(\log \mu)$.

B Valuation

B.1 Term structure of real interest rates

The price of an n -period real zero-coupon bond must satisfy the Euler equation $\widehat{P}_t^n = E_t \left[\widehat{M}_{t,t+n} \right]$. To derive closed-form solutions for the term structure of real interest rates, we conjecture that log zero-coupon bond prices \widehat{p}_t^n are affine in the state vector x_t

$$\widehat{p}_t^n = \log \widehat{P}_t^n = -\widehat{A}_n - \widehat{B}_{y,n}^\top y_t - \widehat{B}_{v,n}^\top v_t,$$

where the coefficients of the vectors $\widehat{B}_{Y,n}$ and $\widehat{B}_{v,n}$ measure the sensitivity of real bond prices to the risk factors and where n refers to the maturity of the bond. Since the real pricing kernel is an affine function of the state vector, log bond prices are fully characterized by the cumulant-generating function of X_t . The law of iterated expectations implies that \widehat{P}_t^n satisfies the recursion

$$\widehat{P}_t^n = E_t \left[\widehat{M}_{t,t+1} \widehat{P}_{t+1}^{n-1} \right].$$

It can be shown that for all n , the scalar \widehat{A}_n and the components of the column vectors $\widehat{B}_{y_j,n}$ for $j = 1, 2, \dots, 8$ and $\widehat{B}_{v_j,n}$ for $j = 1, 2$, are given by

$$\begin{aligned}
\widehat{A}_n &= \widehat{A}_{n-1} - \bar{m} + \widehat{B}_{y,n-1}^\top \mu_y + \sum_{j=1}^2 v_{v_j} \log \left(1 - [(\alpha - \rho) p_{v_j} - \widehat{B}_{v_j,n-1}] c_{v_j} \right) \\
&\quad - \frac{1}{2} \left[(\rho - 1) e_1 + (\alpha - \rho) (P_y + e_1) - \widehat{B}_{y,n-1} \right]^\top \Sigma_y \left[\mathbf{I} \odot (\mathbf{1}^\top \otimes \mathbf{A}) \right] \Sigma_y^\top \\
&\quad \times \left[(\rho - 1) e_1 + (\alpha - \rho) (P_y + e_1) - \widehat{B}_{y,n-1} \right] \\
\widehat{B}_{y_j,n} &= \left[\widehat{B}_{y,n-1} - (\rho - 1) e_1 \right]^\top \Phi_y e_j \\
\widehat{B}_{v_j,n} &= \left[\widehat{B}_{y,n-1} - (\rho - 1) e_1 \right]^\top \Phi_{yv} e_{v_j} \\
&\quad + \frac{(\alpha - \rho) p_{v_j} \phi_{v_j}}{1 - \alpha p_{v_j} c_{v_j}} + \frac{\alpha}{2} (\alpha - \rho) (P_y + e_1)^\top \Sigma_y \left[\mathbf{I} \odot (\mathbf{1}^\top \otimes \mathbf{B}_j) \right] \Sigma_y^\top (P_y + e_1) \\
&\quad - \frac{1}{2} \left[(\rho - 1) e_1 + (\alpha - \rho) (P_y + e_1) - \widehat{B}_{y,n-1} \right]^\top \Sigma_y \left[\mathbf{I} \odot (\mathbf{1}^\top \otimes \mathbf{B}_j) \right] \\
&\quad \times \Sigma_y^\top \left[(\rho - 1) e_1 + (\alpha - \rho) (P_y + e_1) - \widehat{B}_{y,n-1} \right] - \frac{\left[(\alpha - \rho) p_{v_j} - \widehat{B}_{v_j,n-1} \right] \phi_{v_j}}{1 - [(\alpha - \rho) p_{v_j} - \widehat{B}_{v_j,n-1}] c_{v_j}},
\end{aligned}$$

with initial conditions $\widehat{A}_0 = 0$, $\widehat{B}_{y,0} = \mathbf{0}$, and $\widehat{B}_{v,0} = \mathbf{0}$, and where \otimes defines the Kronecker product, \odot the Hadamard product, \mathbf{I} is the identity matrix, $\mathbf{1}$ is a column vector of ones, e_i ($i = 1, 2, \dots, 8$) and e_{v_i} ($i = 1, 2$) are coordinate vectors with all elements equal to zero except element $i = 1$, the column vectors \mathbf{A} , and \mathbf{B}_j for $j = 1, 2$ are defined in Equation (A.1), and \bar{m} is defined in Equation (A.3).

It follows naturally that the term structure of real interest rates is given by:

$$\widehat{y}_t^n = n^{-1} \left(\widehat{A}_n + \widehat{B}_{y,n}^\top y_t + \widehat{B}_{v,n}^\top v_t \right).$$

B.2 Term structure of nominal interest rates

The price of an n -period nominal zero-coupon bond must satisfy the Euler equation $P_t^n = E_t [M_{t,t+n}]$, where $M_{t,t+1}$ defines the nominal stochastic discount factor defined in logs as

$$m_{t,t+1} = \widehat{m}_{t,t+1} - \pi_{t+1} = \widehat{m}_{t,t+1} - e_2^\top y_{t+1},$$

with the real pricing kernel $\widehat{m}_{t,t+1}$ defined in Equation (A.2). To derive closed-form solutions for the term structure of nominal interest rates, we conjecture that log zero-coupon bond prices p_t are affine in the state vector x_t

$$p_t^n = \log P_t^n = -A_n - B_{y,n}^\top y_t - B_{v,n}^\top v_t,$$

where the coefficients of the vectors $B_{y,n}$ and $B_{v,n}$ measure the sensitivity of nominal bond prices to the risk factors and where n refers to the maturity of the bond. Since the nominal pricing kernel is an affine function of the state vector, log bond prices are fully characterized by the cumulant-generating function of x_t . The law of iterated expectations implies that P_t^n satisfies the recursion

$$P_t^n = E_t [M_{t,t+1} P_{t+1}^{n-1}].$$

It can be shown that for all n , the scalar A_n and the components of the column vectors $B_{y_j,n}$ for $j = 1, 2, \dots, 8$ and $B_{v_j,n}$ for $j = 1, 2$, are given by

$$A_n = A_{n-1} - \bar{m} + [e_2 + B_{y,n-1}]^\top \mu_y + \sum_{j=1}^2 v_{v_j} \log \left(1 - [(\alpha - \rho) p_{v_j} - B_{v_j,n-1}] c_{v_j} \right)$$

$$\begin{aligned}
& - \frac{1}{2} [(\rho - 1)e_1 + (\alpha - \rho)(P_y + e_1) - e_2 - B_{y,n-1}]^\top \Sigma_y \left[\mathbf{I} \odot \left(\mathbf{1}^\top \otimes \mathbf{A} \right) \right] \\
& \times \Sigma_y^\top [(\rho - 1)e_1 + (\alpha - \rho)(P_y + e_1) - e_2 - B_{y,n-1}] \\
B_{y_j,n} & = [B_{y,n-1} + e_2 - (\rho - 1)e_1]^\top \Phi_y e_j \\
B_{v_j,n} & = [B_{y,n-1} + e_2 - (\rho - 1)e_1]^\top \Phi_{y_v} e_{v_j} \\
& + \frac{(\alpha - \rho)p_{v_j}\phi_{v_j}}{1 - \alpha p_{v_j}c_{v_j}} + \frac{\alpha}{2} (\alpha - \rho)(P_y + e_1)^\top \Sigma_y \left[\mathbf{I} \odot \left(\mathbf{1}^\top \otimes \mathbf{B}_j \right) \right] \Sigma_y^\top (P_y + e_1) \\
& - \frac{1}{2} [(\rho - 1)e_1 + (\alpha - \rho)(P_y + e_1) - e_2 - B_{y,n-1}]^\top \Sigma_y \left[\mathbf{I} \odot \left(\mathbf{1}^\top \otimes \mathbf{B}_j \right) \right] \\
& \times \Sigma_y^\top [(\rho - 1)e_1 + (\alpha - \rho)(P_y + e_1) - e_2 - B_{y,n-1}] - \frac{[(\alpha - \rho)p_{v_j} - B_{v_j,n-1}]\phi_{v_j}}{1 - [(\alpha - \rho)p_{v_j} - B_{v_j,n-1}]c_{v_j}},
\end{aligned}$$

with initial conditions $A_0 = 0$, $B_{y,0} = \mathbf{0}$, and $B_{v,0} = \mathbf{0}$, and where \otimes defines the Kronecker product, \odot the Hadamar product, \mathbf{I} is the identity matrix, $\mathbf{1}$ is a column vector of ones, e_i ($i = 1, 2, \dots, 8$) and e_{v_i} ($i = 1, 2$) are coordinate vectors with all elements equal to zero except element $i = 1$, the column vectors \mathbf{A} and \mathbf{B}_j for $j = 1, 2$ are defined in Equation (A.1), and \bar{m} is defined in Equation (A.3).

It follows naturally that the term structure of nominal interest rates is given by:

$$y_t^n = n^{-1} \left(A_n + B_{y,n}^\top y_t + B_{v,n}^\top v_t \right).$$

B.3 Term structure of risky treasury yields

U.S. default risk is driven by a default intensity h_t defined as

$$h_t = h + h_c \Delta c_t + h_d d_t + h_g g_t + h_{v_1} v_{1,t} + h_{v_2} v_{2,t} = h + h_z^\top z_t + h_v^\top v_t, \quad (\text{B.1})$$

such that $h_z = [h_c, h_\pi, h_d, h_g]^\top$ and $h_v = [h_{v_1}, h_{v_2}]^\top$. We adopt the convention that $h_y = [h_z, 0, 0, 0, 0]^\top$, and $h_{\bar{y}} = [h_y, 0, 0, 0]^\top$. We connect the default intensity to \mathcal{H}_t , the conditional default probability of a given reference entity at day t via $\mathcal{H}_t \equiv \text{Prob}(\tau = t \mid \tau \geq t; \mathcal{F}_t) = 1 - e^{-h_t}$, where \mathcal{F}_t denotes all the available information available at time t , with the exception of credit events. This implies that the probability of survival (no credit event) until time t is:

$$S_t \equiv \text{Prob}(\tau > t \mid \mathcal{F}_t) = S_0 \prod_{j=1}^t (1 - \mathcal{H}_j), \quad t \geq 1. \quad (\text{B.2})$$

To price risky zero coupon Treasury bonds, we take into account the convenience yield $s_{1,t}$ with dynamics defined in Equation (3), and loss given default L . Using the law of iterated expectations, it is possible to show that risky bond prices follow the recursion

$$\begin{aligned}
\tilde{P}_t^n & = E_t \left(M_{t,t+1} e^{s_{1,t+1}} [\mathcal{I}(\tau > t+1) + (1-L) \cdot \mathcal{I}(t < \tau \leq t+1)] \cdot \tilde{P}_{t+1}^{n-1} \right) \\
& = E_t \left(M_{t,t+1} e^{s_{1,t+1}} [1 - L\mathcal{H}_{t+1}] \cdot \tilde{P}_{t+1}^{n-1} \right) \\
& \approx E_t e^{\sum_{j=1}^n m_{t+j-1, t+j} - L \cdot h_{t+j} + s_{1,t+j}},
\end{aligned}$$

where we follow [Duffie and Singleton \(1999\)](#) by applying a first order Taylor approximation of $\log(1 - L\mathcal{H}_t)$ around 0 such that $\log(1 - L\mathcal{H}_t) \approx -L \cdot h_t$. Since all elements of the bond pricing equation are affine functions of the extended state vector, log bond prices are fully characterized by the cumulant-generating function of \tilde{x}_t . The law of iterated expectations implies that \tilde{P}_t^n satisfies the recursion

$$\tilde{P}_t^n = E_t \left[M_{t,t+1} e^{-L \cdot h_{t+1} + s_{1,t+1}} \tilde{P}_{t+1}^{n-1} \right].$$

To derive closed-form solutions for the term structure of risky Treasury rates, we conjecture that log prices of risky zero-coupon bonds \tilde{p}_t are affine in the extended state vector $\tilde{x}_t = [y_t^\top, s^\top, v_t^\top]^\top = [\tilde{y}_t^\top, v_t^\top]^\top$:

$$\tilde{p}_t^n = \log \tilde{P}_t^n = -\tilde{A}_n - \tilde{B}_{\tilde{y},n}^\top \tilde{y}_t - \tilde{B}_{v,n}^\top v_t.$$

where the coefficients of the vectors $\tilde{B}_{\tilde{y},n}$ and $\tilde{B}_{v,n}$ measure the sensitivity of risky bond prices to the risk factors and where n refers to the maturity of the bond. It can be shown that for all n , the scalar \tilde{A}_n and the components of the column vectors $\tilde{B}_{\tilde{y},n}$ for $j = 1, 2, \dots, 11$ and $\tilde{B}_{v,n}$ for $j = 1, 2$, are given by

$$\begin{aligned} \tilde{A}_n &= \tilde{A}_{n-1} + L \cdot h - \tilde{m} + \left[\tilde{e}_2 + L \cdot h_{\tilde{y}} - \tilde{e}_9 + \tilde{B}_{\tilde{y},n-1} \right]^\top \tilde{\mu}_y \\ &+ \sum_{j=1}^2 v_{v_j} \log \left(1 - \left[(\alpha - \rho) p_{v_j} - L \cdot h_{v_j} - \tilde{B}_{v_j,n-1} \right. \right. \\ &\quad \left. \left. + \left(\tilde{B}_{s_1,n-1} + 1 \right) v_{s_1 v_j} + \tilde{B}_{s_2,n-1} v_{s_2 v_j} + \tilde{B}_{s_3,n-1} v_{s_3 v_j} \right] c_{v_j} \right) \\ &- \frac{1}{2} \left[(\rho - 1) \tilde{e}_1 + (\alpha - \rho) (P_{\tilde{y}} + \tilde{e}_1) - \left(\tilde{e}_2 + L \cdot h_{\tilde{y}} - \tilde{e}_9 + \tilde{B}_{\tilde{y},n-1} \right) \right]^\top \tilde{\Sigma}_y \left[\tilde{\mathbf{I}} \odot \left(\tilde{\mathbf{I}}^\top \otimes \tilde{\mathbf{A}} \right) \right] \\ &\times \tilde{\Sigma}_y^\top \left[(\rho - 1) \tilde{e}_1 + (\alpha - \rho) (P_{\tilde{y}} + \tilde{e}_1) - \left(\tilde{e}_2 + L \cdot h_{\tilde{y}} - \tilde{e}_9 + \tilde{B}_{\tilde{y},n-1} \right) \right] \\ &- \sum_{j=1}^2 \left(\left(\tilde{B}_{s_1,n-1} + 1 \right) v_{s_1 v_j} + \tilde{B}_{s_2,n-1} v_{s_2 v_j} + \tilde{B}_{s_3,n-1} v_{s_3 v_j} \right) v_{v_j} c_{v_j} \\ \tilde{B}_{\tilde{y},n} &= \left[\left(\tilde{e}_2 + L \cdot h_{\tilde{y}} - \tilde{e}_9 + \tilde{B}_{\tilde{y},n-1} \right) - (\rho - 1) \tilde{e}_1 \right]^\top \tilde{\Phi}_y \tilde{e}_j \\ \tilde{B}_{v_j,n} &= \left(\tilde{e}_2 + L \cdot h_{\tilde{y}} - \tilde{e}_9 + \tilde{B}_{\tilde{y},n-1} \right) - [(\rho - 1) \tilde{e}_1]^\top \tilde{\Phi}_{\tilde{y}v} e_{v_j} \\ &+ \frac{(\alpha - \rho) p_{v_j} \phi_{v_j}}{1 - \alpha p_{v_j} c_{v_j}} + \frac{\alpha}{2} (\alpha - \rho) (P_{\tilde{y}} + \tilde{e}_1)^\top \tilde{\Sigma}_y \left[\tilde{\mathbf{I}} \odot \left(\tilde{\mathbf{I}}^\top \otimes \tilde{\mathbf{B}}_j \right) \right] \tilde{\Sigma}_y^\top (P_{\tilde{y}} + \tilde{e}_1) \\ &- \frac{1}{2} \left[(\rho - 1) \tilde{e}_1 + (\alpha - \rho) (P_{\tilde{y}} + \tilde{e}_1) - \left(\tilde{e}_2 + L \cdot h_{\tilde{y}} - \tilde{e}_9 + \tilde{B}_{\tilde{y},n-1} \right) \right]^\top \tilde{\Sigma}_y \left[\tilde{\mathbf{I}} \odot \left(\tilde{\mathbf{I}}^\top \otimes \tilde{\mathbf{B}}_j \right) \right] \\ &\times \tilde{\Sigma}_y^\top \left[(\rho - 1) \tilde{e}_1 + (\alpha - \rho) (P_{\tilde{y}} + \tilde{e}_1) - \left(\tilde{e}_2 + L \cdot h_{\tilde{y}} - \tilde{e}_9 + \tilde{B}_{\tilde{y},n-1} \right) \right] \\ &- \frac{\left[(\alpha - \rho) p_{v_j} - L \cdot h_{v_j} - \tilde{B}_{v_j,n-1} + \left(\tilde{B}_{s_1,n-1} + 1 \right) v_{s_1 v_j} + \tilde{B}_{s_2,n-1} v_{s_2 v_j} + \tilde{B}_{s_3,n-1} v_{s_3 v_j} \right] \phi_{v_j}}{1 - \left[(\alpha - \rho) p_{v_j} - L \cdot h_{v_j} - \tilde{B}_{v_j,n-1} + \left(\tilde{B}_{s_1,n-1} + 1 \right) v_{s_1 v_j} + \tilde{B}_{s_2,n-1} v_{s_2 v_j} + \tilde{B}_{s_3,n-1} v_{s_3 v_j} \right] c_{v_j}} \\ &+ \left(\left(\tilde{B}_{s_1,n-1} + 1 \right) v_{s_1 v_j} + \tilde{B}_{s_2,n-1} v_{s_2 v_j} + \tilde{B}_{s_3,n-1} v_{s_3 v_j} \right) \phi_{v_j}, \end{aligned}$$

with initial conditions $\tilde{A}_0 = 0$, $\tilde{B}_{\tilde{y},0} = \mathbf{0}$, and $\tilde{B}_{v,0} = \mathbf{0}$, and where \otimes defines the Kronecker product, \odot the Hadamar product, $\tilde{\mathbf{I}}$ is the identity matrix, $\tilde{\mathbf{1}}$ is a column vector of ones, \tilde{e}_i ($i = 1, 2, \dots, 11$) and e_{v_i} ($i = 1, 2$) are coordinate vectors with all elements equal to zero except element $i = 1$, \tilde{m} is defined in Equation (A.3), and the column vectors $\tilde{\mathbf{A}}$ and $\tilde{\mathbf{B}}_j$ for $j = 1, 2$ are given by

$$\begin{aligned} \tilde{\mathbf{A}} &= [a_c, a_\pi, a_d, a_g, 0, 0, 0, 0, 1, 1, 1]^\top \\ \tilde{\mathbf{B}}_j &= [b_{cv_j}, b_{\pi v_j}, b_{dv_j}, b_{gv_j}, 0, 0, 0, 0, 0, 0, 0]^\top. \end{aligned} \quad (\text{B.3})$$

It follows naturally that the term structure of risky interest rates is given by:

$$\tilde{y}_t^n = n^1 \left(\tilde{A}_n + \tilde{B}_{\tilde{y},n}^\top \tilde{y}_t + \tilde{B}_{v,n}^\top v_t \right).$$

B.4 Term structure of LIBOR rates

We work with hypothetical zero-coupon LIBOR bonds L_t^n discounted at the continuously compounded yield ℓ_t^n (defined at the monthly frequency), such that $L_t^n = \exp(-\ell_t^n \cdot n)$, where $n \leq 12$ corresponds to LIBOR

rate maturities of up to 12 months. To price LIBOR bonds, we take into account the convenience yield $s_{1,t}$ and bank risk $s_{2,t}$, with dynamics defined in Equation (3), and loss given default L . The LIBOR rate is defined as $\ell_t = \tilde{y}_t^1 + s_{1,t} + s_{2,t}$. Using the law of iterated expectations, it is possible to show that LIBOR bond prices follow the recursion

$$L_t^n \approx E_t e^{\sum_{j=1}^n m_{t+j-1,t+j} - L \cdot h_{t+j} - s_{2,t+j}}.$$

Following the logic developed for risky Treasury bonds in appendix B.3, it is straightforward to show that the log price of a risky n -period zero coupon LIBOR bond is affine in the extended state space \tilde{x}_t :

$$\log L_t^n = -\bar{A}_n - \bar{B}_{\tilde{y},n}^\top \tilde{y}_t - \bar{B}_{v,n}^\top v_t. \quad (\text{B.4})$$

where the constant \bar{A}_n and the coefficients of the column vectors $\bar{B}_{\tilde{y},n}$ and $\bar{B}_{v,n}$ measure the sensitivity of LIBOR bond prices to the risk factors and where n refers to the maturity of the bond. It can be shown that for all n , the scalar \bar{A}_n and the components of the column vectors $\bar{B}_{\tilde{y},n}$ for $j = 1, 2, \dots, 11$ and $\bar{B}_{v_j,n}$ for $j = 1, 2$, are given by

$$\begin{aligned} \bar{A}_n &= \bar{A}_{n-1} + L \cdot h - \bar{m} + (\tilde{e}_2 + L \cdot h_{\tilde{y}} + \tilde{e}_{10} + \bar{B}_{\tilde{y},n-1})^\top \tilde{\mu}_y \\ &+ \sum_{j=1}^2 v_{v_j} \log \left(1 - [(\alpha - \rho) p_{v_j} - L \cdot h_{v_j} - \bar{B}_{v_j,n-1} \right. \\ &\quad \left. + \bar{B}_{s_1,n-1} v_{s_1 v_j} + (\bar{B}_{s_2,n-1} - 1) v_{s_2 v_j} + \bar{B}_{s_3,n-1} v_{s_3 v_j}] c_{v_j} \right) \\ &- \frac{1}{2} [(\rho - 1) \tilde{e}_1 + (\alpha - \rho) (P_{\tilde{y}} + \tilde{e}_1) - (\tilde{e}_2 + L \cdot h_{\tilde{y}} + \tilde{e}_{10} + \bar{B}_{\tilde{y},n-1})]^\top \tilde{\Sigma}_y [\tilde{\mathbf{I}} \odot (\tilde{\mathbf{I}}^\top \otimes \tilde{\mathbf{A}})] \\ &\times \tilde{\Sigma}_y^\top [(\rho - 1) \tilde{e}_1 + (\alpha - \rho) (P_{\tilde{y}} + \tilde{e}_1) - (\tilde{e}_2 + L \cdot h_{\tilde{y}} + \tilde{e}_{10} + \bar{B}_{\tilde{y},n-1})] \\ &+ \sum_{j=1}^2 \bar{B}_{s_1,n-1} v_{s_1 v_j} + ((\bar{B}_{s_2,n-1} - 1) v_{s_2 v_j} + \bar{B}_{s_3,n-1} v_{s_3 v_j}) v_{v_j} c_{v_j} \\ \bar{B}_{\tilde{y}_j,n} &= [(\tilde{e}_2 + L \cdot h_{\tilde{y}} + \tilde{e}_{10} + \bar{B}_{\tilde{y},n-1}) - (\rho - 1) \tilde{e}_1]^\top \tilde{\Phi}_y \tilde{e}_j \\ \bar{B}_{v_j,n} &= [(\tilde{e}_2 + L \cdot h_{\tilde{y}} + \tilde{e}_{10} + \bar{B}_{\tilde{y},n-1}) - (\rho - 1) \tilde{e}_1]^\top \tilde{\Phi}_{\tilde{y}v} e_{v_j} \\ &+ \frac{(\alpha - \rho) p_{v_j} \phi_{v_j}}{1 - \alpha p_{v_j} c_{v_j}} + \frac{\alpha}{2} (\alpha - \rho) (P_{\tilde{y}} + \tilde{e}_1)^\top \tilde{\Sigma}_y [\tilde{\mathbf{I}} \odot (\tilde{\mathbf{I}}^\top \otimes \tilde{\mathbf{B}}_j)] \tilde{\Sigma}_y^\top (P_{\tilde{y}} + \tilde{e}_1) \\ &- \frac{1}{2} [(\rho - 1) \tilde{e}_1 + (\alpha - \rho) (P_{\tilde{y}} + \tilde{e}_1) - (\tilde{e}_2 + L \cdot h_{\tilde{y}} + \tilde{e}_{10} + \bar{B}_{\tilde{y},n-1})]^\top \tilde{\Sigma}_y [\tilde{\mathbf{I}} \odot (\tilde{\mathbf{I}}^\top \otimes \tilde{\mathbf{B}}_j)] \\ &\times \tilde{\Sigma}_y^\top [(\rho - 1) \tilde{e}_1 + (\alpha - \rho) (P_{\tilde{y}} + \tilde{e}_1) - (\tilde{e}_2 + L \cdot h_{\tilde{y}} + \tilde{e}_{10} + \bar{B}_{\tilde{y},n-1})] \\ &- \frac{[(\alpha - \rho) p_{v_j} - L \cdot h_{v_j} - \bar{B}_{v_j,n-1} + \bar{B}_{s_1,n-1} v_{s_1 v_j} + (\bar{B}_{s_2,n-1} - 1) v_{s_2 v_j} + \bar{B}_{s_3,n-1} v_{s_3 v_j}] \phi_{v_j}}{1 - [(\alpha - \rho) p_{v_j} - L \cdot h_{v_j} - \bar{B}_{v_1,n-1} + \bar{B}_{s_1,n-1} v_{s_1 v_j} + (\bar{B}_{s_2,n-1} - 1) v_{s_2 v_j} + \bar{B}_{s_3,n-1} v_{s_3 v_j}] c_{v_j}} \\ &+ (\bar{B}_{s_1,n-1} v_{s_1 v_j} + (\bar{B}_{s_2,n-1} - 1) v_{s_2 v_j} + \bar{B}_{s_3,n-1} v_{s_3 v_j}) \phi_{v_j} \end{aligned}$$

with initial conditions $\bar{A}_0 = 0$, $\bar{B}_{\tilde{y},0} = \mathbf{0}$, and $\bar{B}_{v,0} = \mathbf{0}$, and where \otimes defines the Kronecker product, \odot the Hadamar product, $\tilde{\mathbf{I}}$ is the identity matrix, $\tilde{\mathbf{1}}$ is a column vector of ones, \tilde{e}_i ($i = 1, 2, \dots, 11$) and e_{v_i} ($i = 1, 2$) are coordinate vectors with all elements equal to zero except element $i = 1$, \bar{m} is defined in Equation (A.3), and the column vectors $\tilde{\mathbf{A}}$ and $\tilde{\mathbf{B}}_j$ are defined in Equation (B.3). It follows naturally that the term structure of risky LIBOR rates is given by:

$$\ell_t^n = n^{-1} \left(\bar{A}_n + \bar{B}_{\tilde{y},n}^\top \tilde{y}_t + \bar{B}_{v,n}^\top v_t \right).$$

B.5 Term structure of IRS rates

To price IRS rates, we take into account the convenience yield $s_{1,t}$, bank risk $s_{2,t}$, and cost of collateral $s_{3,t}$, with dynamics defined in Equation (3). The formula for an n -period IRS rate is given by

$$IRS_t^n = \left(\sum_{j=1}^{n/\Delta} (\tilde{\Psi}_{j,t}^\ell - \Psi_{j,t}^\ell) \right) \left(\sum_{j=1}^{n/\Delta} \Psi_{j,t}^\ell \right)^{-1},$$

where the one-month LIBOR rate is defined as $\ell_t = \tilde{y}_t + s_{1,t} + s_{2,t}$, Δ defines the time interval between two successive coupon periods, and where the expressions for $\tilde{\Psi}^\ell$ and Ψ^ℓ are defined as

$$\tilde{\Psi}_{n,t}^\ell = E_t \left[e^{m_t, t+n\Delta + s_{3,t+n\Delta}} e^{\Delta \cdot \ell_{t+(n-1)\Delta}^3} \right] \quad \text{and} \quad \Psi_{n,t}^\ell = E_t \left[e^{m_t, t+n+s_{3,t+n}} \right].$$

To derive closed-form solutions for the term structure of IRS rates, we conjecture that the expressions for $\tilde{\Psi}^\ell$ and Ψ^ℓ are exponentially affine in the extended state vector $\tilde{x}_t = [y_t^\top, s^\top, v_t^\top]^\top = [\tilde{y}_t^\top, v_t^\top]^\top$:

$$\tilde{\Psi}_{n,t}^\ell = e^{\tilde{A}_n^\ell + \tilde{B}_{\tilde{y},n}^{\ell\top} \tilde{y}_t + \tilde{B}_{v,n}^{\ell\top} v_t} \quad \text{and} \quad \Psi_{n,t}^\ell = e^{A_n^\ell + B_{\tilde{y},n}^{\ell\top} \tilde{y}_t + B_{v,n}^{\ell\top} v_t}.$$

It can be shown that for all n , the scalars \tilde{A}_n^ℓ and A_n^ℓ , and the components of the column vectors $\tilde{B}_{\tilde{y},n}^\ell$ and $B_{\tilde{y},n}^\ell$ for $j = 1, 2, \dots, 11$, and $\tilde{B}_{v,n}^\ell$ $B_{v,n}^\ell$ for $j = 1, 2$, follow the same recursion and are given by

$$\begin{aligned} A_n^\ell &= A_{n-1}^\ell + \bar{m} - \left[\tilde{e}_2 - B_{\tilde{y},n-1}^\ell - \tilde{e}_{11} \right]^\top \tilde{\mu}_{\tilde{y}} - \sum_{j=1}^2 v_{v_j} \log \left(1 - \left[(\alpha - \rho) p_{v_j} + B_{v_j,n-1}^\ell \right. \right. \\ &\quad \left. \left. + B_{s_1,n-1}^\ell v_{s_1 v_j} + B_{s_2,n-1}^\ell v_{s_2 v_j} + \left(B_{s_3,n-1}^\ell + 1 \right) v_{s_3 v_j} \right] c_{v_j} \right) \\ &\quad + \frac{1}{2} \left[(\rho - 1) \tilde{e}_1 + (\alpha - \rho) (P_{\tilde{y}} + \tilde{e}_1) - \left[\tilde{e}_2 - B_{\tilde{y},n-1}^\ell - \tilde{e}_{11} \right] \right]^\top \tilde{\Sigma}_{\tilde{y}} \left[\tilde{\mathbf{I}} \odot \left(\tilde{\mathbf{I}}^\top \otimes \tilde{\mathbf{A}} \right) \right] \\ &\quad \times \tilde{\Sigma}_{\tilde{y}}^\top \left[(\rho - 1) \tilde{e}_1 + (\alpha - \rho) (P_{\tilde{y}} + \tilde{e}_1) - \left[\tilde{e}_2 - B_{\tilde{y},n-1}^\ell - \tilde{e}_{11} \right] \right] \\ &\quad - \sum_{j=1}^2 \left(B_{s_1,n-1}^\ell v_{s_1 v_j} + B_{s_2,n-1}^\ell v_{s_2 v_j} + \left(B_{s_3,n-1}^\ell + 1 \right) v_{s_3 v_j} \right) v_{v_j} c_{v_j} \\ B_{\tilde{y},n}^\ell &= \left[(\rho - 1) \tilde{e}_1 - \left[\tilde{e}_2 - B_{\tilde{y},n-1}^\ell - \tilde{e}_{11} \right] \right]^\top \tilde{\Phi}_{\tilde{y}} \tilde{e}_j \\ B_{v_j,n}^\ell &= \left[(\rho - 1) \tilde{e}_1 - \left[\tilde{e}_2 - B_{\tilde{y},n-1}^\ell - \tilde{e}_{11} \right] \right]^\top \tilde{\Phi}_{\tilde{y}v} e_{v_j} \\ &\quad - \frac{(\alpha - \rho) p_{v_j} \phi_{v_j}}{1 - \alpha p_{v_j} c_{v_j}} - \frac{\alpha}{2} (\alpha - \rho) (P_{\tilde{y}} + \tilde{e}_1)^\top \tilde{\Sigma}_{\tilde{y}} \left[\tilde{\mathbf{I}} \odot \left(\tilde{\mathbf{I}}^\top \otimes \tilde{\mathbf{B}}_j \right) \right] \tilde{\Sigma}_{\tilde{y}}^\top (P_{\tilde{y}} + \tilde{e}_1) \\ &\quad + \frac{1}{2} \left[(\rho - 1) \tilde{e}_1 + (\alpha - \rho) (P_{\tilde{y}} + \tilde{e}_1) - \left[\tilde{e}_2 - B_{\tilde{y},n-1}^\ell - \tilde{e}_{11} \right] \right]^\top \tilde{\Sigma}_{\tilde{y}} \left[\tilde{\mathbf{I}} \odot \left(\tilde{\mathbf{I}}^\top \otimes \tilde{\mathbf{B}}_j \right) \right] \\ &\quad \times \tilde{\Sigma}_{\tilde{y}}^\top \left[(\rho - 1) \tilde{e}_1 + (\alpha - \rho) (P_{\tilde{y}} + \tilde{e}_1) - \left[\tilde{e}_2 - B_{\tilde{y},n-1}^\ell - \tilde{e}_{11} \right] \right] \\ &\quad + \frac{\left[(\alpha - \rho) p_{v_j} + B_{v_j,n-1}^\ell + B_{s_1,n-1}^\ell v_{s_1 v_j} + B_{s_2,n-1}^\ell v_{s_2 v_j} + \left(B_{s_3,n-1}^\ell + 1 \right) v_{s_3 v_j} \right] \phi_{v_j}}{1 - \left[(\alpha - \rho) p_{v_j} + B_{v_j,n-1}^\ell + B_{s_1,n-1}^\ell v_{s_1 v_j} + B_{s_2,n-1}^\ell v_{s_2 v_j} + \left(B_{s_3,n-1}^\ell + 1 \right) v_{s_3 v_j} \right] c_{v_j}} \\ &\quad - \left(B_{s_1,n-1}^\ell v_{s_1 v_j} + B_{s_2,n-1}^\ell v_{s_2 v_j} + \left(B_{s_3,n-1}^\ell + 1 \right) v_{s_3 v_j} \right) \phi_{v_j}, \end{aligned}$$

where \otimes defines the Kronecker product, \odot the Hadamar product, $\tilde{\mathbf{I}}$ is the identity matrix, $\tilde{\mathbf{1}}$ is a column vector of ones, \tilde{e}_i ($i = 1, 2, \dots, 11$) and e_{v_i} ($i = 1, 2$) are coordinate vectors with all elements equal to zero except element $i = 1$, \bar{m} is defined in Equation (A.3), and the column vectors $\tilde{\mathbf{A}}$ and $\tilde{\mathbf{B}}_j$ are defined in Equation (B.3).

While the expressions $\tilde{\Psi}^\ell$ and Ψ^ℓ have the same recursions, they have different starting conditions. For $\Psi_{n,t}^\ell$, the recursion starts at 0, with initial condition given by $A_0^\ell = 0$, and all elements of $B_{\tilde{y},0}^\ell = 0$ and $B_{v,0}^\ell = 0$, except for $B_{s_3,0}^\ell = 1$. For $\tilde{\Psi}_{n,t}^\ell$, the recursion starts at $n = \Delta$ (i.e., $\Delta = 3$ for quarterly coupon payments), with starting condition given by:

$$\tilde{\Psi}_{\Delta,t}^\ell = e^{\Delta \cdot \ell_t^3} E_t [e^{m_{t,t+\Delta+s_3,t+\Delta}}].$$

Since $\log E_t [e^{m_{t,t+\Delta+s_3,t+\Delta}}] = A_\Delta^\ell + B_{\tilde{y},\Delta}^{\ell\top} \tilde{y}_t + B_{v,\Delta}^{\ell\top} v_t$, and $\ell_t^3 = \frac{1}{3} (\bar{A}_3 + \bar{B}_{\tilde{y},3}^\top \tilde{y}_t + \bar{B}_{v,3}^\top v_t)$, the initial condition for $\tilde{\Psi}_{n,t}^\ell$ is given by:

$$\tilde{\Psi}_{\Delta,t}^\ell = e^{\frac{\Delta}{3} \bar{A}_3 + \frac{\Delta}{3} \bar{B}_{\tilde{y},3}^\top \tilde{y}_t + \frac{\Delta}{3} \bar{B}_{v,3}^\top v_t + A_\Delta^\ell + B_{\tilde{y},\Delta}^{\ell\top} \tilde{y}_t + B_{v,\Delta}^{\ell\top} v_t} = e^{A_\Delta^{\ell_{init}} + (B_{\tilde{y},\Delta}^{\ell_{init}})^\top \tilde{y}_t + (B_{v,\Delta}^{\ell_{init}})^\top v_t},$$

where the constant $A_\Delta^{\ell_{init}}$ and the elements of the column vectors $B_{\tilde{y},\Delta}^{\ell_{init}}$ for $j = 1, 2, \dots, 11$ and $B_{v,\Delta}^{\ell_{init}}$ for $j = 1, 2$ are given by:

$$\begin{aligned} A_\Delta^{\ell_{init}} &= \frac{\Delta}{3} \bar{A}_3 + A_\Delta^\ell \\ B_{\tilde{y},\Delta}^{\ell_{init}} &= \frac{\Delta}{3} \bar{B}_{\tilde{y},3} + B_{\tilde{y},\Delta}^\ell \\ B_{v,\Delta}^{\ell_{init}} &= \frac{\Delta}{3} \bar{B}_{v,3} + B_{v,\Delta}^\ell. \end{aligned}$$

B.6 Term structure of OIS rates

To price OIS rates, we take into account the convenience yield $s_{1,t}$ and cost of collateral $s_{3,t}$, with dynamics defined in Equation (3). The formula for an n -period OIS rate is given by

$$OIS_t^n = \left(\sum_{j=1}^{n/\Delta} (\tilde{\Psi}_{j,t}^o - \Psi_{j,t}^o) \right) \left(\sum_{j=1}^{n/\Delta} \Psi_{j,t}^o \right)^{-1},$$

where the one-month OIS rate is defined as $o_t = \tilde{y}_t^1 + s_{1,t}$, Δ defines the time interval between two successive coupon periods, and where the expressions for $\tilde{\Psi}^o$ and Ψ^o are defined as

$$\tilde{\Psi}_{n,t}^o = E_t \left[e^{m_{t,t+n+s_3,t+n}} \exp \left(\sum_{j=1}^{\Delta} o_{t+n\Delta-j} \right) \right] \quad \text{and} \quad \Psi_{n,t}^o = E_t [e^{m_{t,t+n+s_3,t+n}}].$$

To derive closed-form solutions for the term structure of OIS rates, we conjecture that the expressions for $\tilde{\Psi}^o$ and Ψ^o are exponentially affine in the extended state vector $\tilde{x}_t = [y_t^\top, s_t^\top, v_t^\top]^\top = [\tilde{y}_t^\top, v_t^\top]^\top$:

$$\tilde{\Psi}_{n,t}^o = e^{\tilde{A}_n^o + \tilde{B}_{\tilde{y},n}^{o\top} \tilde{y}_t + \tilde{B}_{v,n}^{o\top} v_t} \quad \text{and} \quad \Psi_{n,t}^o = e^{A_n^o + B_{\tilde{y},n}^{o\top} \tilde{y}_t + B_{v,n}^{o\top} v_t}.$$

It can be shown that for all n , the scalars \tilde{A}_n^o and A_n^o , and the components of the column vectors $\tilde{B}_{\tilde{y},n}^{o\top}$ and $B_{\tilde{y},n}^{o\top}$ for $j = 1, 2, \dots, 11$, and $\tilde{B}_{v,n}^{o\top}$ $B_{v,n}^{o\top}$ for $j = 1, 2$, follow the same recursion and are given by

$$\begin{aligned} A_n^o &= A_{n-1}^o + \bar{m} - [\tilde{e}_2 - B_{\tilde{y},n-1}^o - \tilde{e}_{11}]^\top \tilde{\mu}_{\tilde{y}} - \sum_{j=1}^2 v_{v_j} \log \left(1 - [(\alpha - \rho) p_{v_j} + B_{v_j,n-1}^o \right. \\ &\quad \left. + B_{s_1,n-1}^o v_{s_1 v_j} + B_{s_2,n-1}^o v_{s_2 v_j} + (B_{s_3,n-1}^o + 1) v_{s_3 v_j}] c_{v_j} \right) \\ &\quad + \frac{1}{2} [(\rho - 1) \tilde{e}_1 + (\alpha - \rho) (P_{\tilde{y}}^o + \tilde{e}_1) - [\tilde{e}_2 - B_{\tilde{y},n-1}^o - \tilde{e}_{11}]]^\top \tilde{\Sigma}_{\tilde{y}} [\tilde{\mathbf{I}} \odot (\tilde{\mathbf{I}}^\top \otimes \tilde{\mathbf{A}})] \\ &\quad \times \tilde{\Sigma}_{\tilde{y}}^\top [(\rho - 1) \tilde{e}_1 + (\alpha - \rho) (P_{\tilde{y}}^o + \tilde{e}_1) - [\tilde{e}_2 - B_{\tilde{y},n-1}^o - \tilde{e}_{11}]] \end{aligned}$$

$$\begin{aligned}
& - \sum_{j=1}^2 (B_{s_1, n-1}^o v_{s_1 v_j} + B_{s_2, n-1}^o v_{s_2 v_j} + (B_{s_3, n-1}^o + 1) v_{s_3 v_j}) v_{v_j} c_{v_j} \\
B_{\tilde{y}_j, n}^o &= [(\rho - 1) \tilde{e}_1 - [\tilde{e}_2 - B_{\tilde{y}, n-1}^o - \tilde{e}_{11}]]^\top \tilde{\Phi}_{\tilde{y}} \tilde{e}_j \\
B_{v_j, n}^o &= [(\rho - 1) \tilde{e}_1 - [\tilde{e}_2 - B_{\tilde{y}, n-1}^o - \tilde{e}_{11}]]^\top \tilde{\Phi}_{\tilde{y}v} e_{v_j} \\
& - \frac{(\alpha - \rho) p_{v_j} \phi_{v_j}}{1 - \alpha p_{v_j} c_{v_j}} - \frac{\alpha}{2} (\alpha - \rho) (P_{\tilde{y}} + \tilde{e}_1)^\top \tilde{\Sigma}_{\tilde{y}} \left[\tilde{\mathbf{I}} \odot \left(\tilde{\mathbf{I}}^\top \otimes \mathbf{B}_j \right) \right] \tilde{\Sigma}_{\tilde{y}}^\top (P_{\tilde{y}} + \tilde{e}_1) \\
& + \frac{1}{2} [(\rho - 1) \tilde{e}_1 + (\alpha - \rho) (P_{\tilde{y}} + \tilde{e}_1) - [\tilde{e}_2 - B_{\tilde{y}, n-1}^o - \tilde{e}_{11}]]^\top \tilde{\Sigma}_{\tilde{y}} \left[\tilde{\mathbf{I}} \odot \left(\tilde{\mathbf{I}}^\top \otimes \mathbf{B}_j \right) \right] \\
& \times \tilde{\Sigma}_{\tilde{y}}^\top [(\rho - 1) \tilde{e}_1 + (\alpha - \rho) (P_{\tilde{y}} + \tilde{e}_1) - [\tilde{e}_2 - B_{\tilde{y}, n-1}^o - \tilde{e}_{11}]] \\
& + \frac{[(\alpha - \rho) p_{v_j} + B_{v_j, n-1}^o + B_{s_1, n-1}^o v_{s_1 v_j} + B_{s_2, n-1}^o v_{s_2 v_j} + (B_{s_3, n-1}^o + 1) v_{s_3 v_j}] \phi_{v_j}}{1 - [(\alpha - \rho) p_{v_j} + B_{v_j, n-1}^o + B_{s_1, n-1}^o v_{s_1 v_j} + B_{s_2, n-1}^o v_{s_2 v_j} + (B_{s_3, n-1}^o + 1) v_{s_3 v_j}] c_{v_j}} \\
& - (B_{s_1, n-1}^o v_{s_1 v_j} + B_{s_2, n-1}^o v_{s_2 v_j} + (B_{s_3, n-1}^o + 1) v_{s_3 v_j}) \phi_{v_j}
\end{aligned}$$

where \otimes defines the Kronecker product, \odot the Hadamar product, $\tilde{\mathbf{I}}$ is the identity matrix, $\tilde{\mathbf{1}}$ is a column vector of ones, \tilde{e}_i ($i = 1, 2, \dots, 11$) and e_{v_i} ($i = 1, 2$) are coordinate vectors with all elements equal to zero except element $i = 1$, \tilde{m} is defined in Equation (A.3), and the column vectors $\tilde{\mathbf{A}}$ and $\tilde{\mathbf{B}}_j$ are defined in Equation (B.3).

While the expressions $\tilde{\Psi}^o$ and Ψ^o have the same recursions, they have different starting conditions. For $\Psi_{n,t}^o$, the recursion starts at 0, with initial condition given by $A_0^o = 0$, and all elements of $B_{\tilde{y}, 0}^o = 0$ and $B_{v, 0}^o = 0$, except for $B_{s_3, 0}^o = 1$. For $\tilde{\Psi}_{n,t}^o$, the recursion starts at $n = \Delta$ (i.e., $\Delta = 3$ for quarterly coupon payments), with starting condition given by:

$$\tilde{\Psi}_{\Delta, t}^o = E_t \left[e^{m_{t, t+\Delta} + s_{3, t+\Delta} + \sum_{j=1}^{\Delta} o_{t+\Delta-j}} \right] = e^{\tilde{A}_{\Delta}^o + \tilde{B}_{\tilde{y}, \Delta}^{o\top} \tilde{y}_t + \tilde{B}_{v, \Delta}^{o\top} v_t},$$

where the expressions for \tilde{A}_{Δ}^o , $\tilde{B}_{\tilde{y}, \Delta}^o$, and $\tilde{B}_{v, \Delta}^o$ are obtained recursively. Observe that

$$\tilde{\Psi}_{\Delta, t}^o = e^{o_t} E_t \left[e^{m_{t, t+1} + s_{3, t+1}} e^{o_{t+1}} E_{t+1} \left[e^{m_{t+1, t+2} + s_{3, t+2}} \dots e^{o_{t+\Delta-1}} E_{t+\Delta-1} \left[e^{m_{t+\Delta-1, t+\Delta} + s_{3, t+\Delta}} \right] \right] \right],$$

and define $\tilde{\Psi}_{n,t}^o$ to be equal to $\tilde{\Psi}_{n,t}^{o_{init}}$ characterized as

$$\tilde{\Psi}_{n,t}^{o_{init}} = E_t \left[e^{o_t + m_{t, t+1} + s_{3, t+1}} \tilde{\Psi}_{n-1, t+1}^{o_{init}} \right],$$

It can be shown that for all $n = 1, 2, 3, \dots, \Delta$

$$\tilde{\Psi}_{n,t}^{o_{init}} = e^{A_n^{o_{init}} + B_{\tilde{y}, n}^{o_{init}\top} \tilde{y}_t + B_{v, n}^{o_{init}\top} v_t}, \tag{B.5}$$

where the scalar $A_n^{o_{init}}$ and components of the column vectors $B_{\tilde{y}, n}^{o_{init}}$ for $j = 1, 2, \dots, 11$ (except for $B_{s_1, n}^{o_{init}}$) and $B_{v_j, n}^{o_{init}}$ are given by:

$$\begin{aligned}
A_n^{o_{init}} &= \tilde{A}_1 + A_{n-1}^{o_{init}} + \tilde{m} - [\tilde{e}_2 - B_{\tilde{y}, n-1}^{o_{init}} - \tilde{e}_{11}]^\top \tilde{\mu}_{\tilde{y}} - \sum_{j=1}^2 v_{v_j} \log \left(1 - [(\alpha - \rho) p_{v_j} + B_{v_j, n-1}^{o_{init}} \right. \\
& \quad \left. + B_{s_1, n-1}^{o_{init}} v_{s_1 v_j} + B_{s_2, n-1}^{o_{init}} v_{s_2 v_j} + (B_{s_3, n-1}^{o_{init}} + 1) v_{s_3 v_j}] c_{v_j} \right) \\
& + \frac{1}{2} [(\rho - 1) \tilde{e}_1 + (\alpha - \rho) (P_{\tilde{y}} + \tilde{e}_1) - [\tilde{e}_2 - B_{\tilde{y}, n-1}^{o_{init}} - \tilde{e}_{11}]]^\top \tilde{\Sigma}_{\tilde{y}} \left[\tilde{\mathbf{I}} \odot \left(\tilde{\mathbf{I}}^\top \otimes \tilde{\mathbf{A}} \right) \right] \\
& \times \tilde{\Sigma}_{\tilde{y}}^\top [(\rho - 1) \tilde{e}_1 + (\alpha - \rho) (P_{\tilde{y}} + \tilde{e}_1) - [\tilde{e}_2 - B_{\tilde{y}, n-1}^{o_{init}} - \tilde{e}_{11}]]
\end{aligned}$$

$$\begin{aligned}
& - \sum_{j=1}^2 (B_{s_1, n-1}^{o_{init}} v_{s_1 v_j} + B_{s_2, n-1}^{o_{init}} v_{s_2 v_j} + (B_{s_3, n-1}^{o_{init}} + 1) v_{s_3 v_j}) v_{v_j} c_{v_j} \\
B_{\tilde{y}_j, n}^{o_{init}} &= \left[(\rho - 1) \tilde{e}_1 - \left[\tilde{e}_2 - B_{\tilde{y}, n-1}^{o_{init}} - \tilde{e}_{11} \right] \right]^\top \tilde{\Phi}_{\tilde{y}} \tilde{e}_1 + \tilde{B}_{\tilde{y}_j, 1} \\
B_{s_1, n}^{o_{init}} &= \left[(\rho - 1) \tilde{e}_1 - \left[\tilde{e}_2 - B_{\tilde{y}, n-1}^{o_{init}} - \tilde{e}_{11} \right] \right]^\top \tilde{\Phi}_{\tilde{y}} \tilde{e}_9 + \tilde{B}_{s_1, 1} + 1 \\
B_{v_j, n}^{o_{init}} &= \left[(\rho - 1) \tilde{e}_1 - \left[\tilde{e}_2 - B_{\tilde{y}, n-1}^{o_{init}} - \tilde{e}_{11} \right] \right]^\top \tilde{\Phi}_{\tilde{y}v} e_{v_j} + \tilde{B}_{v_j, 1} \\
& - \frac{(\alpha - \rho) p_{v_j} \phi_{v_j}}{1 - \alpha p_{v_j} c_{v_j}} - \frac{\alpha}{2} (\alpha - \rho) (P_{\tilde{y}} + \tilde{e}_1)^\top \tilde{\Sigma}_{\tilde{y}} \left[\tilde{\mathbf{I}} \odot \left(\tilde{\mathbf{1}}^\top \otimes \mathbf{B}_j \right) \right] \tilde{\Sigma}_{\tilde{y}}^\top (P_{\tilde{y}} + \tilde{e}_1) \\
& + \frac{1}{2} \left[(\rho - 1) \tilde{e}_1 + (\alpha - \rho) (P_{\tilde{y}} + \tilde{e}_1) - \left[\tilde{e}_2 - B_{\tilde{y}, n-1}^{o_{init}} - \tilde{e}_{11} \right] \right]^\top \tilde{\Sigma}_{\tilde{y}} \left[\tilde{\mathbf{I}} \odot \left(\tilde{\mathbf{1}}^\top \otimes \mathbf{B}_j \right) \right] \\
& \times \tilde{\Sigma}_{\tilde{y}}^\top \left[(\rho - 1) \tilde{e}_1 + (\alpha - \rho) (P_{\tilde{y}} + \tilde{e}_1) - \left[\tilde{e}_2 - B_{\tilde{y}, n-1}^{o_{init}} - \tilde{e}_{11} \right] \right] \\
& + \frac{\left[(\alpha - \rho) p_{v_j} + B_{v_j, j-1}^{o_{init}} + B_{s_1, n-1}^{o_{init}} v_{s_1 v_j} + B_{s_2, n-1}^{o_{init}} v_{s_2 v_j} + (B_{s_3, n-1}^{o_{init}} + 1) v_{s_3 v_j} \right] \phi_{v_j}}{1 - \left[(\alpha - \rho) p_{v_j} + B_{v_j, n-1}^{o_{init}} + B_{s_1, n-1}^{o_{init}} v_{s_1 v_j} + B_{s_2, n-1}^{o_{init}} v_{s_2 v_j} + (B_{s_3, n-1}^{o_{init}} + 1) v_{s_3 v_j} \right] c_{v_j}} \\
& - (B_{s_1, n-1}^o v_{s_1 v_j} + B_{s_2, n-1}^o v_{s_2 v_j} + (B_{s_3, n-1}^o + 1) v_{s_3 v_j}) \phi_{v_j},
\end{aligned}$$

with starting condition $\tilde{\Psi}_{1,t}^{o_{init}} = e^{o_t} E_t [e^{m_t, t+1+s_3, t+1}]$. Since $E_t [e^{m_t, t+1+s_3, t+1}] = \Psi_{1,t}^o = e^{A_1^o + B_1^o \tilde{x}_t}$, $o_t = \tilde{y}_t^1 + s_{1,t}$, with $\tilde{y}_t^1 = \tilde{A}_1 + \tilde{B}_1^\top \tilde{x}_t$, we have that:

$$\begin{aligned}
\tilde{\Psi}_{1,t}^{o_{init}} &= e^{o_t} E_t [e^{m_t, t+1+s_3, t+1}] e^{\tilde{A}_1 + A_1^o + (\tilde{B}_{\tilde{y}, 1} + B_{\tilde{y}, 1}^o + \tilde{e}_9)^\top \tilde{y}_t + (\tilde{B}_{v, 1} + B_{v, 1}^o)^\top v_t} \\
&= e^{A_1^{o_{init}} + (B_{\tilde{y}, 1}^{o_{init}})^\top \tilde{x}_t + (B_{v, 1}^{o_{init}})^\top v_t},
\end{aligned}$$

where the constant $A_1^{o_{init}}$ and the elements of the column vectors $B_{\tilde{y}_j, 1}^{o_{init}}$ for $j = 1, 2, \dots, 11$ (except for $B_{s_1, 1}^{o_{init}}$) and $B_{v_j, 1}^{o_{init}}$ for $j = 1, 2$ are given by:

$$\begin{aligned}
A_1^{o_{init}} &= \tilde{A}_1 + A_1^o \\
B_{\tilde{y}_j, 1}^{o_{init}} &= \tilde{B}_{\tilde{y}_j, 1} + B_{\tilde{y}_j, 1}^o \\
B_{s_1, 1}^{o_{init}} &= \tilde{B}_{s_1, 1} + B_{s_1, 1}^o + 1 \\
B_{v_j, 1}^{o_{init}} &= \tilde{B}_{v_j, 1} + B_{v_j, 1}^o.
\end{aligned}$$

B.7 Term structure of CDS premiums

To price CDS premiums, we take into account the cost of collateral $s_{3,t}$, with dynamics defined in Equation (3), the hazard rate defined in Equation (B.1), and the corresponding survival probabilities defined in Equation (B.2). The formula for an n -period CDS premium is given by

$$CDS_t^n = L \cdot \left(\sum_{j=1}^n (\tilde{\Psi}_{j,t}^c - \Psi_{j,t}^c) \right) \left(\sum_{j=1}^{n/\Delta} \Psi_{j\Delta, t}^c + \sum_{j=1}^n \left(\frac{j}{\Delta} - \lfloor \frac{j}{\Delta} \rfloor \right) (\tilde{\Psi}_{j,t}^c - \Psi_{j,t}^c) \right)^{-1},$$

where the floor function $\lfloor \cdot \rfloor$ rounds to the nearest lower integer, Δ defines the time interval between two successive coupon periods, and where the expressions for $\tilde{\Psi}^c$ and Ψ^c are defined as

$$\tilde{\Psi}_{n,t}^c = E_t \left[e^{m_t, t+n+s_3, t+n} \frac{\mathcal{S}_{t+n-1}}{\mathcal{S}_t} \right] \quad \text{and} \quad \Psi_{n,t}^c = E_t \left[e^{m_t, t+n+s_3, t+n} \frac{\mathcal{S}_{t+n}}{\mathcal{S}_t} \right].$$

The law of iterated expectations implies that $\tilde{\Psi}_{j,t}^c$ and $\Psi_{j,t}^c$ satisfy the recursions

$$\tilde{\Psi}_{n,t}^c = E_t \left[e^{m_{t,t+1} + s_{3,t+1}} (1 - \mathcal{H}_{t+1}) \tilde{\Psi}_{n-1,t+1}^c \right], \quad \Psi_{n,t}^c = E_t \left[e^{m_{t,t+1} + s_{3,t+1}} (1 - \mathcal{H}_{t+1}) \Psi_{n-1,t+1}^c \right],$$

starting at $n = 1$ for $\tilde{\Psi}_{n,t}^c$ and at $n = 0$ for $\Psi_{n,t}^c$. To evaluate the expressions for $\tilde{\Psi}^c$ and Ψ^c , we conjecture that they are exponentially affine functions of the extended state vector \tilde{x}_t :

$$\tilde{\Psi}_{n,t}^c = e^{\tilde{A}_n^c + (\tilde{B}_{\tilde{y},n}^c)^\top \tilde{y}_t + (\tilde{B}_{v,n}^c)^\top v_t} \quad \text{and} \quad \Psi_{n,t}^c = e^{A_n^c + (B_{\tilde{y},n}^c)^\top \tilde{y}_t + (B_{v,n}^c)^\top v_t}.$$

It can be shown that for all n , the scalars \tilde{A}_n^c and A_n^c , and the components of the column vectors $\tilde{B}_{\tilde{y},n}^c$ and $B_{\tilde{y},n}^c$ for $j = 1, 2, \dots, 11$, and $\tilde{B}_{v,n}^c$ for $j = 1, 2$, follow the same recursion and are given by

$$\begin{aligned} \tilde{A}_n^c &= \tilde{A}_{n-1}^c - h + \bar{m} - \left[\tilde{e}_2 + h_{\tilde{y}} - \tilde{B}_{\tilde{y},n-1}^c - \tilde{e}_{11} \right]^\top \tilde{\mu}_{\tilde{y}} \\ &- \sum_{j=1}^2 v_{v_j} \log \left(1 - \left[(\alpha - \rho) p_{v_j} - h_{v_j} + \tilde{B}_{v_j,n-1}^c \right. \right. \\ &\quad \left. \left. + \tilde{B}_{s_1,n-1}^c v_{s_1 v_j} + \tilde{B}_{s_2,n-1}^c v_{s_2 v_j} + \left(\tilde{B}_{s_3,n-1}^c + 1 \right) v_{s_3 v_j} \right] c_{v_j} \right) \\ &+ \frac{1}{2} \left[(\rho - 1) \tilde{e}_1 + (\alpha - \rho) (P_{\tilde{y}} + \tilde{e}_1) - \left(\tilde{e}_2 + h_{\tilde{y}} - \tilde{B}_{\tilde{y},n-1}^c - \tilde{e}_{11} \right) \right]^\top \tilde{\Sigma}_{\tilde{y}} \left[\tilde{\mathbf{I}} \odot \left(\tilde{\mathbf{I}}^\top \otimes \tilde{\mathbf{A}} \right) \right] \\ &\times \tilde{\Sigma}_{\tilde{y}}^\top \left[(\rho - 1) \tilde{e}_1 + (\alpha - \rho) (P_{\tilde{y}} + \tilde{e}_1) - \left(\tilde{e}_2 + h_{\tilde{y}} - \tilde{B}_{\tilde{y},n-1}^c - \tilde{e}_{11} \right) \right] \\ &- \sum_{j=1}^2 \left(\tilde{B}_{s_1,n-1}^c v_{s_1 v_j} + \tilde{B}_{s_2,n-1}^c v_{s_2 v_j} + \left(\tilde{B}_{s_3,n-1}^c + 1 \right) v_{s_3 v_j} \right) v_{v_j} c_{v_j} \\ \tilde{B}_{\tilde{y},n}^c &= \left[(\rho - 1) \tilde{e}_1 - \left(\tilde{e}_2 + h_{\tilde{y}} - \tilde{B}_{\tilde{y},n-1}^c - \tilde{e}_{11} \right) \right]^\top \tilde{\Phi}_{\tilde{y}} \tilde{e}_j \\ \tilde{B}_{v_j,n}^c &= \left[(\rho - 1) \tilde{e}_1 - \left(\tilde{e}_2 + h_{\tilde{y}} - \tilde{B}_{\tilde{y},n-1}^c - \tilde{e}_{11} \right) \right]^\top \tilde{\Phi}_{\tilde{y}v} e_{v_j} \\ &- \frac{(\alpha - \rho) p_{v_j} \phi_{v_j}}{1 - \alpha p_{v_j} c_{v_j}} - \frac{\alpha}{2} (\alpha - \rho) (P_{\tilde{y}} + \tilde{e}_1)^\top \tilde{\Sigma}_{\tilde{y}} \left[\tilde{\mathbf{I}} \odot \left(\tilde{\mathbf{I}}^\top \otimes \tilde{\mathbf{B}}_j \right) \right] \tilde{\Sigma}_{\tilde{y}}^\top (P_{\tilde{y}} + \tilde{e}_1) \\ &+ \frac{1}{2} \left[(\rho - 1) \tilde{e}_1 + (\alpha - \rho) (P_{\tilde{y}} + \tilde{e}_1) - \left(\tilde{e}_2 + h_{\tilde{y}} - \tilde{B}_{\tilde{y},n-1}^c - \tilde{e}_{11} \right) \right]^\top \tilde{\Sigma}_{\tilde{y}} \left[\tilde{\mathbf{I}} \odot \left(\tilde{\mathbf{I}}^\top \otimes \tilde{\mathbf{B}}_j \right) \right] \\ &\times \tilde{\Sigma}_{\tilde{y}}^\top \left[(\rho - 1) \tilde{e}_1 + (\alpha - \rho) (P_{\tilde{y}} + \tilde{e}_1) - \left(\tilde{e}_2 + h_{\tilde{y}} - \tilde{B}_{\tilde{y},n-1}^c - \tilde{e}_{11} \right) \right] \\ &+ \frac{\left[(\alpha - \rho) p_{v_j} - h_{v_j} + \tilde{B}_{v_j,n-1}^c + \tilde{B}_{s_1,n-1}^c v_{s_1 v_j} + \tilde{B}_{s_2,n-1}^c v_{s_2 v_j} + \left(\tilde{B}_{s_3,n-1}^c + 1 \right) v_{s_3 v_j} \right] \phi_{v_j}}{1 - \left[(\alpha - \rho) p_{v_j} - h_{v_j} + \tilde{B}_{v_j,n-1}^c + \tilde{B}_{s_1,n-1}^c v_{s_1 v_j} + \tilde{B}_{s_2,n-1}^c v_{s_2 v_j} + \left(\tilde{B}_{s_3,n-1}^c + 1 \right) v_{s_3 v_j} \right] c_{v_j}} \\ &- \left(\tilde{B}_{s_1,n-1}^c v_{s_1 v_j} + \tilde{B}_{s_2,n-1}^c v_{s_2 v_j} + \left(\tilde{B}_{s_3,n-1}^c + 1 \right) v_{s_3 v_j} \right) \phi_{v_j}, \end{aligned}$$

where \otimes defines the Kronecker product, \odot the Hadamar product, $\tilde{\mathbf{I}}$ is the identity matrix, $\tilde{\mathbf{1}}$ is a column vector of ones, \tilde{e}_i ($i = 1, 2, \dots, 11$) and e_{v_i} ($i = 1, 2$) are coordinate vectors with all elements equal to zero except element $i = 1$, \bar{m} is defined in Equation (A.3), and the column vectors $\tilde{\mathbf{A}}$ and $\tilde{\mathbf{B}}_j$ are defined in Equation (B.3).

Even though the expressions for $\tilde{\Psi}^c$ and Ψ^c follow the same recursion, they have different initial conditions. The initial condition for Ψ^c is given by $\log \Psi_{0,t}^c = A_0^c + B_{\tilde{y},0}^{c\top} \tilde{y}_t + B_{v,0}^{c\top} v_t$, where the scalar $A_0^c = 0$ and the elements of the column vectors $B_{\tilde{y},0}^c = 0$ for $j = 1, 2, \dots, 11$, and $B_{v,0}^c = 0$ for $j = 1, 2$, except for $B_{s_3,0}^c = 1$. The initial condition for $\tilde{\Psi}^c$ is given by:

$$\tilde{\Psi}_{1,t}^c = E_t \left[e^{m_{t,t+1} + s_{3,t+1}} \right] = e^{\tilde{A}_1^c + \tilde{B}_{\tilde{y},1}^{c\top} \tilde{y}_t + \tilde{B}_{v,1}^{c\top} v_t},$$

where the scalar \tilde{A}_1^c and components of the column vectors $\tilde{B}_{y_j,1}^c$ for $j = 1, 2, \dots, 11$ and $\tilde{B}_{v_j,1}^c$ for $j = 1, 2$ are given by:

$$\begin{aligned}
\tilde{A}_1^c &= \bar{m} + [\tilde{e}_{11} - \tilde{e}_2]^\top \tilde{\mu}_Y - \sum_{j=1}^2 v_{v_j} \log(1 - [(\alpha - \rho) p_{v_j} + v_{s_3 v_j}] c_{v_j}) - \sum_{j=1}^2 v_{s_3 v_j} v_{v_j} c_{v_j} \\
&+ \frac{1}{2} [(\rho - 1) \tilde{e}_1 + (\alpha - \rho) (P_{\tilde{y}} + \tilde{e}_1) + \tilde{e}_{11} - \tilde{e}_2]^\top \tilde{\Sigma}_{\tilde{y}} [\tilde{\mathbf{I}} \odot (\tilde{\mathbf{I}}^\top \otimes \tilde{\mathbf{A}})] \\
&\times \tilde{\Sigma}_{\tilde{y}}^\top [(\rho - 1) \tilde{e}_1 + (\alpha - \rho) (P_{\tilde{y}} + \tilde{e}_1) + \tilde{e}_{11} - \tilde{e}_2] \\
\tilde{B}_{y_j,1}^c &= [(\rho - 1) \tilde{e}_1 + \tilde{e}_{11} - \tilde{e}_2]^\top \tilde{\Phi}_{\tilde{y}} \tilde{e}_j \\
\tilde{B}_{v_j,1}^c &= [(\rho - 1) \tilde{e}_1 + \tilde{e}_{11} - \tilde{e}_2]^\top \tilde{\Phi}_{\tilde{y}v} e_{v_j} \\
&- \frac{(\alpha - \rho) p_{v_j} \phi_{v_j}}{1 - \alpha p_{v_j} c_{v_j}} - \frac{\alpha}{2} (\alpha - \rho) (P_{\tilde{y}} + \tilde{e}_1)^\top \tilde{\Sigma}_{\tilde{y}} [\tilde{\mathbf{I}} \odot (\tilde{\mathbf{I}}^\top \otimes \tilde{\mathbf{B}}_j)] \tilde{\Sigma}_{\tilde{y}}^\top (P_{\tilde{y}} + \tilde{e}_1) \\
&+ \frac{1}{2} [(\rho - 1) \tilde{e}_1 + (\alpha - \rho) (P_{\tilde{y}} + \tilde{e}_1) + \tilde{e}_{11} - \tilde{e}_2]^\top \tilde{\Sigma}_{\tilde{y}} [\tilde{\mathbf{I}} \odot (\tilde{\mathbf{I}}^\top \otimes \tilde{\mathbf{B}}_j)] \\
&\times \tilde{\Sigma}_{\tilde{y}}^\top [(\rho - 1) \tilde{e}_1 + (\alpha - \rho) (P_{\tilde{y}} + \tilde{e}_1) + \tilde{e}_{11} - \tilde{e}_2] + \frac{[(\alpha - \rho) p_{v_j} + v_{s_3 v_j}] \phi_{v_j}}{1 - [(\alpha - \rho) p_{v_j} + v_{s_3 v_j}] c_{v_j}} - v_{s_3 v_j} \phi_{v_j}.
\end{aligned}$$

C Estimation

We provide two different state-space representations. The first one, shown in Section C.1, is used when macroeconomic fundamentals are only used in the estimation. The second one, shown in Section C.2, is an extended state-space representation for which we can (potentially) jointly use macroeconomic fundamentals and asset data.

C.1 State-space representation

The underlying state transition dynamics run at a monthly frequency. We first provide the case in which all observables are available at the monthly frequency. The corresponding state-transition dynamics are shown in Section C.1.1 and the measurement equation is presented in Section C.1.2. In the presence of mixed-frequency observables, i.e., some observables are available at the quarterly frequency, we explain how to adjust the state space in Section C.1.3 with an illustrative example. Finally, in Section C.1.4, we explain the availability of data and provide our state-space representation that we estimate.

C.1.1 State transition dynamics

Define $x_t = [z_t^\top, w_t^\top, v_t^\top]^\top$. We describe the joint dynamics of x_t below

$$\begin{aligned}
 \underbrace{\begin{bmatrix} z_{1,t+1} \\ z_{2,t+1} \\ z_{3,t+1} \\ z_{4,t+1} \\ w_{1,t+1} \\ w_{2,t+1} \\ w_{3,t+1} \\ w_{4,t+1} \\ v_{1,t+1} \\ v_{2,t+1} \end{bmatrix}}_{x_{t+1}} &= \underbrace{\begin{bmatrix} \mu_{z1} \\ \mu_{z2} \\ \mu_{z3} \\ \mu_{z4} \\ 0 \\ 0 \\ 0 \\ 0 \\ \nu_{v1} c_{v1} \\ \nu_{v2} c_{v2} \end{bmatrix}}_{\mu} + \underbrace{\begin{bmatrix} \phi_{z11} & \phi_{z12} & \phi_{z13} & \phi_{z14} & 1 & 0 & 0 & 0 & \phi_{zv11} & \phi_{zv12} \\ \phi_{z21} & \phi_{z22} & \phi_{z23} & \phi_{z24} & 0 & 1 & 0 & 0 & \phi_{zv21} & \phi_{zv22} \\ \phi_{z31} & \phi_{z32} & \phi_{z33} & \phi_{z34} & 0 & 0 & 1 & 0 & \phi_{zv31} & \phi_{zv32} \\ \phi_{z41} & \phi_{z42} & \phi_{z43} & \phi_{z44} & 0 & 0 & 0 & 1 & \phi_{zv41} & \phi_{zv42} \\ 0 & 0 & 0 & 0 & 0 & 0 & 0 & 0 & 0 & 0 \\ 0 & 0 & 0 & 0 & 0 & 0 & 0 & 0 & 0 & 0 \\ 0 & 0 & 0 & 0 & 0 & 0 & 0 & 0 & 0 & 0 \\ 0 & 0 & 0 & 0 & 0 & 0 & 0 & 0 & 0 & 0 \\ 0 & 0 & 0 & 0 & 0 & 0 & 0 & 0 & \phi_{v1} & 0 \\ 0 & 0 & 0 & 0 & 0 & 0 & 0 & 0 & 0 & \phi_{v2} \end{bmatrix}}_{\Phi} \underbrace{\begin{bmatrix} z_{1,t} \\ z_{2,t} \\ z_{3,t} \\ z_{4,t} \\ w_{1,t} \\ w_{2,t} \\ w_{3,t} \\ w_{4,t} \\ v_{1,t} \\ v_{2,t} \end{bmatrix}}_{x_t} \\
+ \underbrace{\begin{bmatrix} 1 & 0 & 0 & 0 & 0 & 0 & 0 & 0 & 0 & 0 \\ 0 & 1 & 0 & 0 & 0 & 0 & 0 & 0 & 0 & 0 \\ 0 & 0 & 1 & 0 & 0 & 0 & 0 & 0 & 0 & 0 \\ 0 & 0 & 0 & 1 & 0 & 0 & 0 & 0 & 0 & 0 \\ \theta_{w11} & \theta_{w12} & \theta_{w13} & \theta_{w14} & 0 & 0 & 0 & 0 & 0 & 0 \\ \theta_{w21} & \theta_{w22} & \theta_{w23} & \theta_{w24} & 0 & 0 & 0 & 0 & 0 & 0 \\ \theta_{w31} & \theta_{w32} & \theta_{w33} & \theta_{w34} & 0 & 0 & 0 & 0 & 0 & 0 \\ \theta_{w41} & \theta_{w42} & \theta_{w43} & \theta_{w44} & 0 & 0 & 0 & 0 & 0 & 0 \\ 0 & 0 & 0 & 0 & 0 & 0 & 0 & 0 & 1 & 0 \\ 0 & 0 & 0 & 0 & 0 & 0 & 0 & 0 & 0 & 1 \end{bmatrix}}_{\Sigma_A} \times \underbrace{\begin{bmatrix} \nu_{11} & 0 & 0 & 0 & 0 & 0 & 0 & 0 & 0 & 0 \\ \nu_{21} & \nu_{22} & 0 & 0 & 0 & 0 & 0 & 0 & 0 & 0 \\ \nu_{31} & \nu_{32} & \nu_{33} & 0 & 0 & 0 & 0 & 0 & 0 & 0 \\ \nu_{41} & \nu_{42} & \nu_{43} & \nu_{44} & 0 & 0 & 0 & 0 & 0 & 0 \\ 0 & 0 & 0 & 0 & 0 & 0 & 0 & 0 & 0 & 0 \\ 0 & 0 & 0 & 0 & 0 & 0 & 0 & 0 & 0 & 0 \\ 0 & 0 & 0 & 0 & 0 & 0 & 0 & 0 & 0 & 0 \\ 0 & 0 & 0 & 0 & 0 & 0 & 0 & 0 & 0 & 0 \\ 0 & 0 & 0 & 0 & 0 & 0 & 0 & 0 & 0 & 1 \\ 0 & 0 & 0 & 0 & 0 & 0 & 0 & 0 & 0 & 1 \end{bmatrix}}_{\Sigma_B} \\
\times \left(\underbrace{\begin{bmatrix} V_{1,t} & 0 & 0 & 0 & 0 & 0 & 0 & 0 & 0 & 0 \\ 0 & V_{2,t} & 0 & 0 & 0 & 0 & 0 & 0 & 0 & 0 \\ 0 & 0 & V_{3,t} & 0 & 0 & 0 & 0 & 0 & 0 & 0 \\ 0 & 0 & 0 & V_{4,t} & 0 & 0 & 0 & 0 & 0 & 0 \\ 0 & 0 & 0 & 0 & 0 & 0 & 0 & 0 & 0 & 0 \\ 0 & 0 & 0 & 0 & 0 & 0 & 0 & 0 & 0 & 0 \\ 0 & 0 & 0 & 0 & 0 & 0 & 0 & 0 & 0 & 0 \\ 0 & 0 & 0 & 0 & 0 & 0 & 0 & 0 & 0 & 0 \\ 0 & 0 & 0 & 0 & 0 & 0 & 0 & 0 & \omega_{v1,t} & 0 \\ 0 & 0 & 0 & 0 & 0 & 0 & 0 & 0 & 0 & \omega_{v2,t} \end{bmatrix}}_{V_t} \right)^{1/2} \underbrace{\begin{bmatrix} \varepsilon_{z1,t+1} \\ \varepsilon_{z2,t+1} \\ \varepsilon_{z3,t+1} \\ \varepsilon_{z4,t+1} \\ 0 \\ 0 \\ 0 \\ 0 \\ \eta_{v1,t+1} \\ \eta_{v2,t+1} \end{bmatrix}}_{\eta_{t+1}},
 \end{aligned}$$

for $i \in \{1, 2, 3, 4\}$ and $j \in \{1, 2\}$,

$$V_{i,t} = a_i + b_{i1}v_{1,t} + b_{i2}v_{2,t}, \quad \omega_{v_j,t} = \nu_{v_j}c_{v_j}^2 + 2c_{v_j}\phi_{v_j}v_{j,t}$$

with $\varepsilon_{z_i,t+1} \sim \mathcal{N}(0, 1)$ and $\eta_{v_j,t+1}$ being a zero mean unit variance shock. In vector notations, we express the state space by

$$\underbrace{\begin{bmatrix} z_{t+1} \\ w_{t+1} \\ v_{t+1} \end{bmatrix}}_{x_{t+1}} = \underbrace{\begin{bmatrix} \mu_z \\ \mathbf{0} \\ \nu_v \odot c_v \end{bmatrix}}_{\mu} + \underbrace{\begin{bmatrix} \Phi_{z4 \times 4} & \mathbf{I}_{4 \times 4} & \Phi_{zv4 \times 2} \\ \mathbf{0}_{4 \times 4} & \mathbf{0}_{4 \times 4} & \mathbf{0}_{4 \times 2} \\ \mathbf{0}_{2 \times 4} & \mathbf{0}_{2 \times 4} & \Phi_{v2 \times 2} \end{bmatrix}}_{\Phi} \underbrace{\begin{bmatrix} z_t \\ w_t \\ v_t \end{bmatrix}}_{x_t} + \underbrace{\begin{bmatrix} \mathbf{I}_{4 \times 4} & \mathbf{0}_{4 \times 4} & \mathbf{0}_{4 \times 2} \\ \Theta_{w4 \times 4} & \mathbf{0}_{4 \times 4} & \mathbf{0}_{4 \times 2} \\ \mathbf{0}_{2 \times 4} & \mathbf{0}_{2 \times 4} & \mathbf{I}_{2 \times 2} \end{bmatrix}}_{\Sigma_A} \quad (\text{C.1})$$

$$\times \underbrace{\begin{bmatrix} \nu_{z,4 \times 4} & \mathbf{0}_{4 \times 4} & \mathbf{0}_{4 \times 2} \\ \mathbf{0}_{4 \times 4} & \mathbf{0}_{4 \times 4} & \mathbf{0}_{4 \times 2} \\ \mathbf{0}_{2 \times 4} & \mathbf{0}_{2 \times 4} & \mathbf{I}_{2 \times 2} \end{bmatrix}}_{\Sigma_B} \times \left(\underbrace{\begin{bmatrix} V_{z,t,4 \times 4} & \mathbf{0}_{4 \times 4} & \mathbf{0}_{4 \times 2} \\ \mathbf{0}_{4 \times 4} & \mathbf{0}_{4 \times 4} & \mathbf{0}_{4 \times 2} \\ \mathbf{0}_{2 \times 4} & \mathbf{0}_{2 \times 4} & \omega_{v,t,2 \times 2} \end{bmatrix}}_{V_t} \right)^{1/2} \times \underbrace{\begin{bmatrix} \varepsilon_{z,t+1} \\ \mathbf{0} \\ \eta_{v,t+1} \end{bmatrix}}_{\eta_{t+1}}.$$

C.1.2 Measurement equation

For ease of illustration, assume that the observables are available at a monthly frequency. Define $o_t = [\Delta c_t, d_t, g_t, \pi_t]^\top$. Then, the measurement equation becomes

$$o_t = \beta^\top x_t + u_t, \quad u_t \sim N(0, \Sigma_u) \quad (\text{C.2})$$

where $\beta = [1, 1, 1, 1, 0, 0, 0, 0, 0, 0]^\top$ and Σ_u is a measurement error (diagonal) variance-covariance matrix.

C.1.3 Dealing with the mixed-frequency issue

When some observables are available at a quarterly frequency, we need to adjust both measurement and transition equations to deal with the mixed-frequency issue. We provide an example whereby the dimension of z_t , w_t , and v_t are reduced to half for ease of illustration. We assume that the first observable is available at a quarterly while the second observable is available at a monthly frequency. We introduce the superscript q to indicate if the observable is available at the quarterly frequency. Thus, $o_t = [z_{1,t}^q, z_{2,t}]'$. Also for simplicity, we do not allow for measurement errors. There are two cases to consider.

1. If $z_{1,t}^q$ is expressed in growth rates, adjust the measurement loading β and state vector to

$$\beta = \begin{bmatrix} \frac{1}{3} & \frac{2}{3} & 1 & \frac{2}{3} & \frac{1}{3} & 0 & 0 & 0 & 0 & 0 & 0 \\ 0 & 0 & 0 & 0 & 0 & 1 & 0 & 0 & 0 & 0 & 0 \end{bmatrix}, \quad x_t = \begin{bmatrix} z_{1,t} \\ z_{1,t-1} \\ z_{1,t-2} \\ z_{1,t-3} \\ z_{1,t-4} \\ z_{2,t} \\ z_{2,t-1} \\ z_{2,t-2} \\ z_{2,t-3} \\ z_{2,t-4} \\ w_{1,t} \\ w_{2,t} \\ v_{1,t} \end{bmatrix}. \quad (\text{C.3})$$

We can relate the mixed-frequency observables to the state vector by

$$o_t = \begin{bmatrix} z_{1,t}^q \\ z_{2,t} \end{bmatrix} = \begin{bmatrix} \frac{z_{1,t} + 2z_{1,t-1} + 3z_{1,t-2} + 2z_{1,t-3} + z_{1,t-4}}{3} \\ z_{2,t} \end{bmatrix} = \beta^\top x_t. \quad (\text{C.4})$$

2. If $z_{1,t}^q$ is expressed in levels, adjust the measurement loading β and state vector to

$$\beta = \begin{bmatrix} \frac{1}{3} & \frac{1}{3} & \frac{1}{3} & 0 & 0 & 0 & 0 & 0 & 0 & 0 & 0 \\ 0 & 0 & 0 & 0 & 0 & 1 & 0 & 0 & 0 & 0 & 0 \end{bmatrix}, \quad x_t = \begin{bmatrix} z_{1,t} \\ z_{1,t-1} \\ z_{1,t-2} \\ z_{1,t-3} \\ z_{1,t-4} \\ z_{2,t} \\ z_{2,t-1} \\ z_{2,t-2} \\ z_{2,t-3} \\ z_{2,t-4} \\ w_{1,t} \\ w_{2,t} \\ v_{1,t} \end{bmatrix}. \quad (\text{C.5})$$

We can relate the mixed-frequency observables to the state vector by

$$o_t = \begin{bmatrix} z_{1,t}^q \\ z_{2,t} \end{bmatrix} = \begin{bmatrix} \frac{z_{1,t} + z_{1,t-1} + z_{1,t-2}}{3} \\ z_{2,t} \end{bmatrix} = \beta^\top x_t. \quad (\text{C.6})$$

C.1.4 Implementation

We use quarterly consumption growth (Δc_t^q), output growth (d_t^q), and log government expenditure-to-output ratio (g_t^q), and monthly inflation (π_t) in the estimation. Except for consumption growth data, we are using the highest available frequency. Our choice of using quarterly consumption growth avoids modeling measurement errors in monthly consumption growth (see [Schorfheide, Song, and Yaron \(2018\)](#) for a detailed discussion), which significantly reduces the dimension of the state vector leading to a much more tractable estimation problem. Note that Δc_t^q and d_t^q are expressed in growth rates, but π_t and g_t^q are expressed in levels. Following the idea described in Section [C.1.3](#), we modify the measurement equation loading β and state vector X_t to equate the observables to our state variables

$$o_t = \begin{bmatrix} \Delta c_t^q \\ d_t^q \\ g_t^q \\ \pi_t \end{bmatrix} = \begin{bmatrix} \frac{z_{1,t} + 2z_{1,t-1} + 3z_{1,t-2} + 2z_{1,t-3} + z_{1,t-4}}{3} \\ \frac{z_{2,t} + 2z_{2,t-1} + 3z_{2,t-2} + 2z_{2,t-3} + z_{2,t-4}}{3} \\ \frac{z_{3,t} + z_{3,t-1} + z_{3,t-2}}{3} \\ z_{4,t} \end{bmatrix}. \quad (\text{C.7})$$

The most efficient characterization of the state vector is

$$x_t = \begin{bmatrix} z_{1,t}, z_{1,t-1}, z_{1,t-2}, z_{1,t-3}, z_{1,t-4}, z_{2,t}, z_{2,t-1}, z_{2,t-2}, z_{2,t-3}, z_{2,t-4}, \\ z_{3,t}, z_{3,t-1}, z_{3,t-2}, z_{4,t}, w_{1,t}, w_{2,t}, w_{3,t}, w_{4,t}, v_{1,t}, v_{2,t} \end{bmatrix}^\top. \quad (\text{C.8})$$

The coefficient matrices in [\(C.1\)](#) are adjusted accordingly to match the dimension of [\(C.8\)](#). It is easy to deduce the form of β from [\(C.7\)](#) and [\(C.8\)](#).

Because of the conditionally linear structure of our state-space form, we can directly apply the Rao-Blackwellization particle filter as in [Schorfheide, Song, and Yaron \(2018\)](#). The details are omitted for brevity.

C.2 State-space representation: Extended form

We now introduce an extended state-space representation in which we additionally introduce s factors which are crucial elements for asset prices. We allow the s factors to depend on the lagged values of z and ν factors to model inter-dependence.

C.2.1 State transition dynamics

$$\begin{bmatrix} z_{1,t+1} \\ z_{2,t+1} \\ z_{3,t+1} \\ z_{4,t+1} \\ w_{1,t+1} \\ w_{2,t+1} \\ w_{3,t+1} \\ w_{4,t+1} \\ s_{1,t+1} \\ s_{2,t+1} \\ s_{3,t+1} \\ v_{1,t+1} \\ v_{2,t+1} \end{bmatrix} = \begin{bmatrix} \mu_1 \\ \mu_2 \\ \mu_3 \\ \mu_4 \\ 0 \\ 0 \\ 0 \\ 0 \\ \mu_{s_1} \\ \mu_{s_2} \\ \mu_{s_3} \\ \nu_{v_1} c_{v_1} \\ \nu_{v_2} c_{v_2} \end{bmatrix} + \begin{bmatrix} \phi_{z11} & \phi_{z12} & \phi_{z13} & \phi_{z14} & 1 & 0 & 0 & 0 & 0 & 0 & 0 & \phi_{zv11} & \phi_{zv12} \\ \phi_{z21} & \phi_{z22} & \phi_{z23} & \phi_{z24} & 0 & 1 & 0 & 0 & 0 & 0 & 0 & \phi_{zv21} & \phi_{zv22} \\ \phi_{z31} & \phi_{z32} & \phi_{z33} & \phi_{z34} & 0 & 0 & 1 & 0 & 0 & 0 & 0 & \phi_{zv31} & \phi_{zv32} \\ \phi_{z41} & \phi_{z42} & \phi_{z43} & \phi_{z44} & 0 & 0 & 0 & 1 & 0 & 0 & 0 & \phi_{zv41} & \phi_{zv42} \\ 0 & 0 & 0 & 0 & 0 & 0 & 0 & 0 & 0 & 0 & 0 & 0 & 0 \\ 0 & 0 & 0 & 0 & 0 & 0 & 0 & 0 & 0 & 0 & 0 & 0 & 0 \\ 0 & 0 & 0 & 0 & 0 & 0 & 0 & 0 & 0 & 0 & 0 & 0 & 0 \\ 0 & 0 & 0 & 0 & 0 & 0 & 0 & 0 & 0 & 0 & 0 & 0 & 0 \\ \phi_{sz11} & \phi_{sz12} & \phi_{sz13} & \phi_{sz14} & 0 & 0 & 0 & 0 & \phi_{s11} & \phi_{s12} & \phi_{s13} & \phi_{sv11} & \phi_{sv12} \\ \phi_{sz21} & \phi_{sz22} & \phi_{sz23} & \phi_{sz24} & 0 & 0 & 0 & 0 & \phi_{s21} & \phi_{s22} & \phi_{s23} & \phi_{sv21} & \phi_{sv22} \\ \phi_{sz31} & \phi_{sz32} & \phi_{sz33} & \phi_{sz34} & 0 & 0 & 0 & 0 & \phi_{s31} & \phi_{s32} & \phi_{s33} & \phi_{sv31} & \phi_{sv32} \\ 0 & 0 & 0 & 0 & 0 & 0 & 0 & 0 & 0 & 0 & 0 & \phi_{v1} & 0 \\ 0 & 0 & 0 & 0 & 0 & 0 & 0 & 0 & 0 & 0 & 0 & 0 & \phi_{v2} \end{bmatrix} \begin{bmatrix} z_{1,t} \\ z_{2,t} \\ z_{3,t} \\ z_{4,t} \\ w_{1,t} \\ w_{2,t} \\ w_{3,t} \\ w_{4,t} \\ s_{1,t} \\ s_{2,t} \\ s_{3,t} \\ v_{1,t} \\ v_{2,t} \end{bmatrix}$$

$$+ \begin{bmatrix} 1 & 0 & 0 & 0 & 0 & 0 & 0 & 0 & 0 & 0 & 0 & 0 & 0 & 0 \\ 0 & 1 & 0 & 0 & 0 & 0 & 0 & 0 & 0 & 0 & 0 & 0 & 0 & 0 \\ 0 & 0 & 1 & 0 & 0 & 0 & 0 & 0 & 0 & 0 & 0 & 0 & 0 & 0 \\ 0 & 0 & 0 & 1 & 0 & 0 & 0 & 0 & 0 & 0 & 0 & 0 & 0 & 0 \\ \theta_{w11} & \theta_{w12} & \theta_{w13} & \theta_{w14} & 0 & 0 & 0 & 0 & 0 & 0 & 0 & 0 & 0 & 0 \\ \theta_{w21} & \theta_{w22} & \theta_{w23} & \theta_{w24} & 0 & 0 & 0 & 0 & 0 & 0 & 0 & 0 & 0 & 0 \\ \theta_{w31} & \theta_{w32} & \theta_{w33} & \theta_{w34} & 0 & 0 & 0 & 0 & 0 & 0 & 0 & 0 & 0 & 0 \\ \theta_{w41} & \theta_{w42} & \theta_{w43} & \theta_{w44} & 0 & 0 & 0 & 0 & 0 & 0 & 0 & 0 & 0 & 0 \\ 1 & 1 & 1 & 1 & 1 & 1 & 1 & 1 & 1 & 0 & 0 & 1 & 1 & 1 \\ 1 & 1 & 1 & 1 & 1 & 1 & 1 & 1 & 1 & 0 & 1 & 0 & 1 & 1 \\ 1 & 1 & 1 & 1 & 1 & 1 & 1 & 1 & 0 & 0 & 1 & 1 & 1 & 1 \\ 0 & 0 & 0 & 0 & 0 & 0 & 0 & 0 & 0 & 0 & 0 & 1 & 1 & 0 \\ 0 & 0 & 0 & 0 & 0 & 0 & 0 & 0 & 0 & 0 & 0 & 0 & 0 & 1 \end{bmatrix}$$

$$\times \begin{bmatrix} \nu_{11} & 0 & 0 & 0 & 0 & \mathbf{0}_{1 \times 4} & \mathbf{0}_{1 \times 3} & 0 & 0 \\ \nu_{21} & \nu_{22} & 0 & 0 & 0 & \mathbf{0}_{1 \times 4} & \mathbf{0}_{1 \times 3} & 0 & 0 \\ \nu_{31} & \nu_{32} & \nu_{33} & 0 & 0 & \mathbf{0}_{1 \times 4} & \mathbf{0}_{1 \times 3} & 0 & 0 \\ \nu_{41} & \nu_{42} & \nu_{43} & \nu_{44} & 0 & \mathbf{0}_{1 \times 4} & \mathbf{0}_{1 \times 3} & 0 & 0 \\ 0 & 0 & 0 & 0 & 0 & \mathbf{0}_{1 \times 4} & \mathbf{0}_{1 \times 3} & 0 & 0 \\ 0 & 0 & 0 & 0 & 0 & \mathbf{0}_{1 \times 4} & \mathbf{0}_{1 \times 3} & 0 & 0 \\ 0 & 0 & 0 & 0 & 0 & \mathbf{0}_{1 \times 4} & \mathbf{0}_{1 \times 3} & 0 & 0 \\ 0 & 0 & 0 & 0 & 0 & \mathbf{0}_{1 \times 4} & \mathbf{0}_{1 \times 3} & 0 & 0 \\ -(\nu_{11} + \nu_{21} + \nu_{31} + \nu_{41}) + \nu_{sz11} & -(\nu_{22} + \nu_{32} + \nu_{42}) + \nu_{sz12} & -(\nu_{33} + \nu_{43}) + \nu_{sz13} & -\nu_{44} + \nu_{sz14} & \mathbf{0}_{1 \times 4} & [\nu_{s1}, 0, 0] & -1 + \nu_{sv11} & -1 + \nu_{sv12} \\ -(\nu_{11} + \nu_{21} + \nu_{31} + \nu_{41}) + \nu_{sz21} & -(\nu_{22} + \nu_{32} + \nu_{42}) + \nu_{sz22} & -(\nu_{33} + \nu_{43}) + \nu_{sz23} & -\nu_{44} + \nu_{sz24} & \mathbf{0}_{1 \times 4} & [0, \nu_{s2}, 0] & -1 + \nu_{sv21} & -1 + \nu_{sv22} \\ -(\nu_{11} + \nu_{21} + \nu_{31} + \nu_{41}) + \nu_{sz31} & -(\nu_{22} + \nu_{32} + \nu_{42}) + \nu_{sz32} & -(\nu_{33} + \nu_{43}) + \nu_{sz33} & -\nu_{44} + \nu_{sz34} & \mathbf{0}_{1 \times 4} & [0, 0, \nu_{s3}] & -1 + \nu_{sv31} & -1 + \nu_{sv32} \\ 0 & 0 & 0 & 0 & 0 & \mathbf{0}_{1 \times 4} & \mathbf{0}_{1 \times 3} & 1 & 0 \\ 0 & 0 & 0 & 0 & 0 & \mathbf{0}_{1 \times 4} & \mathbf{0}_{1 \times 3} & 0 & 1 \end{bmatrix}$$

$$\times \left(\begin{bmatrix} V_{1,t} & 0 & 0 & 0 & 0 & 0 & 0 & 0 & 0 & 0 & 0 & 0 & 0 & 0 \\ 0 & V_{2,t} & 0 & 0 & 0 & 0 & 0 & 0 & 0 & 0 & 0 & 0 & 0 & 0 \\ 0 & 0 & V_{3,t} & 0 & 0 & 0 & 0 & 0 & 0 & 0 & 0 & 0 & 0 & 0 \\ 0 & 0 & 0 & V_{4,t} & 0 & 0 & 0 & 0 & 0 & 0 & 0 & 0 & 0 & 0 \\ 0 & 0 & 0 & 0 & 0 & 0 & 0 & 0 & 0 & 0 & 0 & 0 & 0 & 0 \\ 0 & 0 & 0 & 0 & 0 & 0 & 0 & 0 & 0 & 0 & 0 & 0 & 0 & 0 \\ 0 & 0 & 0 & 0 & 0 & 0 & 0 & 0 & 1 & 0 & 0 & 0 & 0 & 0 \\ 0 & 0 & 0 & 0 & 0 & 0 & 0 & 0 & 0 & 1 & 0 & 0 & 0 & 0 \\ 0 & 0 & 0 & 0 & 0 & 0 & 0 & 0 & 0 & 0 & 1 & 0 & 0 & 0 \\ 0 & 0 & 0 & 0 & 0 & 0 & 0 & 0 & 0 & 0 & 0 & \omega_{v1,t} & 0 & 0 \\ 0 & 0 & 0 & 0 & 0 & 0 & 0 & 0 & 0 & 0 & 0 & 0 & \omega_{v2,t} & 0 \end{bmatrix} \right)^{1/2} \begin{bmatrix} \varepsilon_{z1,t+1} \\ \varepsilon_{z2,t+1} \\ \varepsilon_{z3,t+1} \\ \varepsilon_{z4,t+1} \\ 0 \\ 0 \\ 0 \\ 0 \\ 0 \\ \varepsilon_{s1,t+1} \\ \varepsilon_{s2,t+1} \\ \varepsilon_{s3,t+1} \\ \eta_{v1,t+1} \\ \eta_{v2,t+1} \end{bmatrix},$$

for $i \in \{1, 2, 3, 4\}$, $l \in \{1, 2, 3\}$ and $j \in \{1, 2\}$,

$$V_{i,t} = a_i + b_{i1}v_{1,t} + b_{i2}v_{2,t}, \quad \omega_{v_j,t} = \nu_{v_j} c_{v_j}^2 + 2c_{v_j} \phi_{v_j} v_{j,t}$$

with $\varepsilon_{z_i,t+1} \sim \mathcal{N}(0, 1)$, $\varepsilon_{s_l,t+1} \sim \mathcal{N}(0, 1)$, and $\eta_{v_j,t+1}$ being a zero mean unit variance shock.

In vector notations, we express the state space by

$$\underbrace{\begin{bmatrix} z_{t+1} \\ w_{t+1} \\ s_{t+1} \\ v_{t+1} \end{bmatrix}}_{\tilde{x}_{t+1}} = \underbrace{\begin{bmatrix} \mu_z \\ \mathbf{0} \\ \mu_s \\ \nu_v \odot c_v \end{bmatrix}}_{\tilde{\mu}} + \underbrace{\begin{bmatrix} \Phi_{z4 \times 4} & \mathbf{I}_{4 \times 4} & \mathbf{0}_{4 \times 3} & \Phi_{zv4 \times 2} \\ \mathbf{0}_{4 \times 4} & \mathbf{0}_{4 \times 4} & \mathbf{0}_{4 \times 3} & \mathbf{0}_{4 \times 2} \\ \Phi_{sz3 \times 4} & \mathbf{0}_{3 \times 4} & \Phi_{s3 \times 3} & \Phi_{sv3 \times 2} \\ \mathbf{0}_{2 \times 4} & \mathbf{0}_{2 \times 4} & \mathbf{0}_{2 \times 3} & \Phi_{v2 \times 2} \end{bmatrix}}_{\tilde{\Phi}} \underbrace{\begin{bmatrix} z_t \\ w_t \\ s_t \\ v_t \end{bmatrix}}_{\tilde{x}_t} \quad (\text{C.9})$$

$$\begin{aligned}
& + \underbrace{\begin{bmatrix} \mathbf{I}_{4 \times 4} & \mathbf{0}_{4 \times 4} & \mathbf{0}_{4 \times 3} & \mathbf{0}_{4 \times 2} \\ \Theta_{w4 \times 4} & \mathbf{0}_{4 \times 4} & \mathbf{0}_{4 \times 3} & \mathbf{0}_{4 \times 2} \\ \mathbf{J}_{3 \times 4} & \mathbf{J}_{3 \times 4} & \mathbf{I}_{3 \times 3} & \mathbf{J}_{3 \times 2} \\ \mathbf{0}_{2 \times 4} & \mathbf{0}_{2 \times 4} & \mathbf{0}_{2 \times 3} & \mathbf{I}_{2 \times 2} \end{bmatrix}}_{\tilde{\Sigma}_A} \times \underbrace{\begin{bmatrix} \nu_{z4 \times 4} & \mathbf{0}_{4 \times 4} & \mathbf{0}_{4 \times 3} & \mathbf{0}_{4 \times 2} \\ \mathbf{0}_{4 \times 4} & \mathbf{0}_{4 \times 4} & \mathbf{0}_{4 \times 3} & \mathbf{0}_{4 \times 2} \\ -\mathbf{J}_{3 \times 4} \cdot \nu_{z4 \times 4} + \nu_{sz3 \times 4} & \mathbf{0}_{3 \times 4} & \nu_{s3 \times 3} & -\mathbf{J}_{3 \times 2} + \nu_{sv3 \times 2} \\ \mathbf{0}_{2 \times 4} & \mathbf{0}_{2 \times 4} & \mathbf{0}_{2 \times 3} & \mathbf{I}_{2 \times 2} \end{bmatrix}}_{\tilde{\Sigma}_B} \\
& \times \left(\underbrace{\begin{bmatrix} V_{z,t4 \times 4} & \mathbf{0}_{4 \times 4} & \mathbf{0}_{4 \times 3} & \mathbf{0}_{4 \times 2} \\ \mathbf{0}_{4 \times 4} & \mathbf{0}_{4 \times 4} & \mathbf{0}_{4 \times 3} & \mathbf{0}_{4 \times 2} \\ \mathbf{0}_{3 \times 4} & \mathbf{0}_{3 \times 4} & \mathbf{I}_{3 \times 3} & \mathbf{0}_{3 \times 2} \\ \mathbf{0}_{2 \times 4} & \mathbf{0}_{2 \times 4} & \mathbf{0}_{2 \times 3} & \omega_{v,t2 \times 2} \end{bmatrix}}_{\tilde{V}_t} \right)^{1/2} \times \underbrace{\begin{bmatrix} \varepsilon_{z,t+1} \\ \mathbf{0} \\ \varepsilon_{s,t+1} \\ \eta_{v,t+1} \end{bmatrix}}_{\tilde{\eta}_{t+1}}.
\end{aligned}$$

C.2.2 Measurement equation

Consider various different maturities of the risky Treasury zero-coupon yields (T), interest rate swap premiums (I), CDS premiums (C), and OIS spreads (O). We introduce new notations to relate the observed rates to our state variables, given our solution coefficients. Define

$$\begin{aligned}
y_{m,t}^T &= \Xi^T(A_m^T, B_m^T, \tilde{A}_m^T, \tilde{B}_m^T, \tilde{x}_t) = \Xi^T(\tilde{A}_m^T, \tilde{B}_m^T, \tilde{x}_t) \\
y_{m,t}^C &= \Xi^C(A_m^C, B_m^C, \tilde{A}_m^C, \tilde{B}_m^C, \tilde{x}_t) \\
y_{m,t}^I &= \Xi^I(A_m^I, B_m^I, \tilde{A}_m^I, \tilde{B}_m^I, \tilde{x}_t) \\
y_{m,t}^O &= \Xi^I(A_m^O, B_m^O, \tilde{A}_m^O, \tilde{B}_m^O, \tilde{x}_t)
\end{aligned} \tag{C.10}$$

to match the m -maturity rate of the observable to our state variables \tilde{x}_t . We provide the derivation of solution coefficients $A_m^j, B_m^j, \tilde{A}_m^j, \tilde{B}_m^j$ and an expression for $\Xi^j(\cdot)$ in Appendix B for $j \in \{T, I, C, O\}$. We select the maturities of 1y, 3y, 5y, 7y, 10y, and 15y in the estimation, which are collected in

$$y_t^j = \begin{bmatrix} y_{1,t}^j \\ \vdots \\ y_{m,t}^j \\ \vdots \\ y_{15,t}^j \end{bmatrix} = \begin{bmatrix} \Xi^j(A_1^j, B_1^j, \tilde{A}_1^j, \tilde{B}_1^j, \tilde{x}_t) \\ \vdots \\ \Xi^j(A_m^j, B_m^j, \tilde{A}_m^j, \tilde{B}_m^j, \tilde{x}_t) \\ \vdots \\ \Xi^j(A_{15}^j, B_{15}^j, \tilde{A}_{15}^j, \tilde{B}_{15}^j, \tilde{x}_t) \end{bmatrix}. \tag{C.11}$$

We consider y_t^T, y_t^C, y_t^I in the estimation and use y_t^O as out-of-sample validation. We have defined $s_{1,t}$ and $s_{2,t}$ as observables in the main body of our paper. Define vectors e_{s_1} and e_{s_2} that select $s_{1,t}$ and $s_{2,t}$ from \tilde{x}_t , respectively. Put together,

$$\begin{bmatrix} s_{1,t} \\ s_{2,t} \end{bmatrix} = \begin{bmatrix} e_{s_1}^\top \\ e_{s_2}^\top \end{bmatrix} \tilde{x}_t \tag{C.12}$$

disciplines the dynamics of the s factors. In sum, our state-space representation is comprised of state transition equations (C.9) and measurement equations (C.11) for $j \in \{T, C, I\}$ and (C.12). There are two ways in which we can proceed.

1. A joint estimation of macroeconomic observables and prices:

We augment our measurement equations with (C.7) and adjust the state transition equation (C.9) to deal with mixed-frequency observations as explained in Section C.1.3. While the joint estimation approach can be appealing, it is computationally challenging since we have to increase the dimension of our state vector substantially. More importantly, because the system no longer preserves the conditionally linear structure, e.g., (C.11), we cannot apply the solution proposed by [Schorfheide, Song, and Yaron \(2018\)](#), and thus the non-linear filtering algorithm can be highly inefficient.

2. Two-stage estimation in which macroeconomic observables and prices are separated:

For this, we treat the filtered estimates of \hat{z}_t and \hat{w}_t from the first stage estimation, which only involves macroeconomic data, as observables for the second stage estimation. Among our state vector \tilde{x}_t , we are assuming that $z_t, w_t, s_{1,t}, s_{2,t}$ are observed factors and treating $s_{3,t}, v_{1,t}, v_{2,t}$ as latent factors. We can then partition the state vector into

$$\tilde{x}_t = (\tilde{x}_t^{o,\top}, \tilde{x}_t^{l,\top})^\top \quad (\text{C.13})$$

where the superscript o and l indicate “observed” and “latent” respectively. The non-linear filtering technique only deals with \tilde{x}_t^l in the state transition equation (C.9), since the other variables are observed. In this case, the measurement equations are (C.11) for $j \in \{T, C, I\}$ and (C.12).

C.2.3 Particle filter

We use a particle-filter approximation of the likelihood function and embed this approximation into a fairly standard random walk Metropolis algorithm. In the subsequent exposition, we omit the dependence of all densities on the parameter vector Θ . In slight abuse of notations, we denote all observables with

$$y_t = [y_t^{C,\top}, y_t^{T,\top}, y_t^{I,\top}, s_{1,t}, s_{2,t}]^\top \quad (\text{C.14})$$

The particle filter approximates the sequence of distributions $\{p(\tilde{x}_t^l | y_{1:t})\}_{t=1}^T$ by a set of pairs $\{\tilde{x}_t^{l,(i)}, \pi_t^{(i)}\}_{i=1}^N$, where $\tilde{x}_t^{l,(i)}$ is the i th particle vector, $\pi_t^{(i)}$ is its weight, and N is the number of particles. As a by-product, the filter produces a sequence of likelihood approximations $\hat{p}(y_t | y_{1:t-1})$, $t = 1, \dots, T$.

- Initialization: We generate the particle values $\tilde{x}_0^{l,(i)}$ from the unconditional distribution. We set $\pi_0^{(i)} = 1/N$ for each i .
- Propagation of particles: We simulate (C.9) forward to generate $\tilde{x}_t^{l,(i)}$ conditional on $\tilde{x}_{t-1}^{l,(i)}$ and observed \tilde{x}_{t-1}^o . We use $q(\tilde{x}_t^{l,(i)} | \tilde{x}_{t-1}^{l,(i)}, \tilde{x}_{t-1}^o, y_t)$ to represent the distribution from which we draw $\tilde{x}_t^{l,(i)}$.
- Correction of particle weights: Define the unnormalized particle weights for period t as

$$\tilde{\pi}_t^{(i)} = \pi_{t-1}^{(i)} \times \frac{p(y_t | \tilde{x}_t^{l,(i)}, \tilde{x}_t^o) p(\tilde{x}_t^{l,(i)} | \tilde{x}_{t-1}^{l,(i)}, \tilde{x}_{t-1}^o)}{q(\tilde{x}_t^{l,(i)} | \tilde{x}_{t-1}^{l,(i)}, \tilde{x}_{t-1}^o, y_t)}.$$

The term $\pi_{t-1}^{(i)}$ is the initial particle weight and the ratio $\frac{p(y_t | \tilde{x}_t^{l,(i)}, \tilde{x}_t^o) p(\tilde{x}_t^{l,(i)} | \tilde{x}_{t-1}^{l,(i)}, \tilde{x}_{t-1}^o)}{q(\tilde{x}_t^{l,(i)} | \tilde{x}_{t-1}^{l,(i)}, \tilde{x}_{t-1}^o, y_t)}$ is the importance weight of the particle.

The approximation of the log likelihood function is given by

$$\log \hat{p}(y_t | y_{1:t-1}) = \log \hat{p}(y_{t-1} | y_{1:t-2}) + \log \left(\sum_{i=1}^N \tilde{\pi}_t^{(i)} \right).$$

- Resampling: Define the normalized weights

$$\pi_t^{(i)} = \frac{\tilde{\pi}_t^{(i)}}{\sum_{j=1}^N \tilde{\pi}_t^{(j)}}$$

and generate N draws from the distribution $\{\tilde{x}_t^{l,(i)}, \pi_t^{(i)}\}_{i=1}^N$ using multinomial resampling. In slight abuse of notation, we denote the resampled particles and their weights also by $\tilde{x}_t^{l,(i)}$ and $\pi_t^{(i)}$, where $\pi_t^{(i)} = 1/N$.